Quaternary Science Reviews 110 (2015) 72–91

Contents lists available at ScienceDirect

Quaternary Science Reviews

journal homepage: www.elsevier.com/locate/quascirev

Late Quaternary chronostratigraphic framework of terraces and alluvium along the lower Ohio River, southwestern Indiana and western Kentucky, USA

Ronald C. Counts [a, b, *], Madhav K. Murari [a], Lewis A. Owen [a], Shannon A. Mahan [c], Michele Greenan [d]

[a] Department of Geology, University of Cincinnati, Cincinnati, OH 45221, USA
[b] U.S. Geological Survey, National Center MS-926A, Reston, VA 20192, USA
[c] U.S. Geological Survey, Box 25046 MS-974, Denver, CO 80225, USA
[d] Indiana State Museum, Indianapolis, IN 46204, USA

ARTICLE INFO

Article history:
Received 2 May 2014
Received in revised form
19 November 2014
Accepted 25 November 2014
Available online

Keywords:
Lower Ohio River
Geomorphology
Fluvial terraces
Optically-stimulated luminescence
Holocene climate

ABSTRACT

The lower Ohio River valley is a terraced fluvial landscape that has been profoundly influenced by Quaternary climate change and glaciation. A modern Quaternary chronostratigraphic framework was developed for the lower Ohio River valley using optically stimulated luminescence (OSL) dating and allostratigraphic mapping to gain insights into the nature of fluvial responses to glacial–interglacial/stadial–interstadial transitions and Holocene climate change. River deposits, T0 (youngest) to T7 (oldest), were mapped along a 75 km reach of the lower Ohio River and were dated using 46 OSL and 5 radiocarbon samples. The examination of cores combined with OSL and radiocarbon dating shows that fluvial sediments older than marine oxygen isotope stage (MIS) 2 are present only in the subsurface. Aggradation during MIS 6 (Illinoian glaciation) filled the valley to within ~7 m of the modern floodplain, and by ~114 ka (MIS 5e/Sangamon interglacial) the Ohio River had scoured the MIS 6 sediments to ~22 m below the modern floodplain surface. There were no fluvial sediments in the valley with ages between MIS 5e and the middle of MIS 3. The MIS 3 ages (~39 ka) and stratigraphic position of T5 deposits suggest the Ohio River aggraded 8–14 m during MIS 4 or MIS 3. Near the end of MIS 3, the Ohio River incised the mid Last Glacial (mid-Wisconsinan) deposits ~10 m and began aggrading again by ~30 ka. Aggradation continued into MIS 2, with maximum MIS 2 aggradation occurring before ~21 ka, which is coincident with the global Last Glacial Maximum (LGM). As the Ohio River adjusted to changing fluxes in sediment load and discharge following the LGM, it formed a sequence of fill-cut terraces in the MIS 2 outwash that get progressively younger with decreasing elevation, ranging in age from ~21 ka to ~13 ka. From ~14 ka to ~13 ka the Ohio River rapidly incised ~3 m to form a new terrace, and by ~12 ka at the onset of the Holocene, the Ohio River established a meandering channel pattern. The river formed a broad floodplain surface from ~12 ka to ~6 ka, and then incised ~1 m and formed a fill-cut terrace from ~6 ka to ~5 ka. After ~5 ka, likely in response to mid-Holocene drought in North America, the Ohio River incised ~5 m, and by ~4 ka the river began aggrading again. The Ohio River has aggraded ~4 m since aggradation began at ~4 ka. The chronostratigraphic framework and reconstructed history developed here suggest that the lower Ohio River is highly sensitive to glacial–interglacial transitions and abrupt Holocene climate change and responds rapidly to these allogenic forcings.

Published by Elsevier Ltd.

1. Introduction and background

Rivers are dynamic systems that continuously adjust to their environmental conditions, making them very sensitive to variables such as crustal deformation, changes in base level, and sediment load and runoff volume changes caused by climate oscillations (e.g.

* Corresponding author. U.S. Geological Survey, National Center MS-926A, Reston, VA 20192, USA.
E-mail address: rcounts@usgs.gov (R.C. Counts).

http://dx.doi.org/10.1016/j.quascirev.2014.11.011
0277-3791/Published by Elsevier Ltd.

Leopold et al., 1964; Schumm, 1977: Schumm et al., 1987; Bull, 1991; Maddy et al., 2000, 2001; Blum, 2007). Fluvial terraces and deposits, therefore, represent useful archives for the study of paleoenvironmental change and landscape development.

The landforms and sediments of major rivers that drain the midwestern United States provide an important record of Quaternary paleoenvironmental change and landscape development for the mid-continent. Yet there are few studies that use modern techniques, particularly numerical dating, to study these system. Of particular note, however, is the work of Rittenour et al. (2003, 2005, 2007) and Shen et al. (2012) on the lower Mississippi valley that presents detailed and robust chronologies for terrace formation based on optically stimulated luminescence (OSL) dating. These studies are shedding light on the timing and nature of environmental changes that influenced rivers in the central continental United States during the late Quaternary.

The Ohio River is the largest river in the eastern United States, traversing much of the glaciated northeast through the physiographic provinces of the Appalachian highlands of Pennsylvania, the glaciated Central Lowlands of Ohio, the Interior Low Plateaus of Kentucky and Indiana, and onto the Coastal Plain at its confluence with the Mississippi River (Fenneman, 1928, Fig. 1). During the Tertiary and early Pleistocene, the master drainage of the northeastern United States was the Teays–Mahomet River system; the headwaters of the Ohio River were in south-central Indiana and it was a relatively small 2nd or 3rd order tributary of the Cumberland River (Fowke, 1925; Wayne, 1952; Ray, 1974; Melhorn and Kempton, 1991). The repeated advance and retreat of Pleistocene ice sheets disrupted and reorganized the Teays–Mahomet system (Tight, 1903; Ver Steeg, 1946; Ray, 1974; Melhorn and Kempton, 1991), and by ~1.5 Ma the Teays drainage system was permanently captured by the Ohio River (Granger et al., 2001).

Diamict interpreted as MIS-6 (Illinoian) glacial drift is present within the upper Ohio River valley between Louisville, Kentucky, and Cincinnati, Ohio, and pre-Illinoian diamict is present on upland areas south of the river, indicating the upper reaches have been glaciated by multiple pre-Last Glacial (pre-Wisconsinan) ice sheets (see Ray, 1974 and references therein). The upper valley is a narrow and constricted bedrock valley where river terraces and alluvium are typically discontinuous and are either the remnants of glacial outwash or narrow bands of Holocene floodplain deposits (e.g. Swadley, 1969, 1976; Luft, 1971; Gibbons, 1972), though a few reaches of the constricted valley widen and contain more extensive alluvium (e.g. Crittenden and Hose, 1965; Kepferle, 1974). In contrast, where the lower Ohio River flows through the physiographic province of the Illinois Basin (from Tell City, Indiana to the Wabash–Ohio River confluence), the river meanders across a broad valley and has thick and continuous alluvial-fill successions with multiple river terrace levels (Ray, 1965; Moore et al., 2007, 2009). The lower Ohio River terraces and fluvial deposits provide useful geomorphic proxies that record late Quaternary hydrologic and paleoenvironmental change for the Midwest, which were greatly influenced by advance and retreat of the Laurentide ice sheet in the eastern United States. However, little modern research has been undertaken on the Quaternary fluvial record of the Ohio River. To help address this lack of knowledge, we describe the alluvium and terraces in the lower Ohio River valley and use OSL and radiocarbon dating to develop a chronology of deposition and incision for the past ~100 ka. We then compare the reconstructed fluvial responses of the lower Ohio River to that of the Mississippi River. The chronostratigraphic framework developed for the lower Ohio River will benefit future research investigating fluvial responses to Quaternary paleoenvironmental change in the American Midwest.

Owen (1859) undertook the first research on Quaternary sediments in the lower Ohio River valley, which included interpreting the loess deposits as water-lain in origin. This was followed much later by the work of Fuller and Ashley (1902) and Fuller and Clapp (1904), which resulted in two U.S. Geological Survey (USGS) folios for the region immediately northeast of the Ohio–Wabash River confluence. This work included the recognition of pre-Last Glacial (pre-Wisconsinan) glacial deposits and 1:125,000 scale surficial geologic mapping. Theis (1922) recognized multiple bedrock and alluvial terraces in Henderson County, Kentucky, and used gastropod assemblages to conclude that loess was an eolian deposit. Other research in the lower Ohio valley in the 1960s–70s included geologic mapping at a 7.5-min quadrangle scale by the USGS. However, this mapping was based on the early 20th century paradigm of four continental glaciations in North America (e.g. Walker, 1957; Ray, 1965, 1974) and the fluvial deposits were primarily mapped as a single undifferentiated unit (e.g. Johnson, 1972, 1973a, 1973b, 1974; Johnson and Norris, 1974).

Alexander and Prior (1971), Alexander and Nelson (1972), and Alexander (1974) used radiocarbon dating to study the timing of floodplain formation in southern Illinois, and determined there were three changes in vertical aggradation rates during the Holocene. Fraser (1986) drilled cores and concluded the mid-channel islands in the Ohio River were not depositional landforms of the modern flow regime but were relict braid bars that were obstructions to flow. Fraser and Fishbaugh (1986) drilled a core transect across part of the lower Ohio Valley and identified Holocene, Last Glacial (MIS 2), and pre-Last Glacial (pre-Wisconsinan) alluvium. Later, Eggert and Woodfield (1996) and Woodfield (1998) used auger cuttings, gamma logs, and several radiocarbon ages to propose that megafloods down the Wabash River were responsible for much of the tributary valley fill in the Little Pigeon basin in Vanderburgh County, Indiana. Most recently, the USGS (Moore et al., 2007, 2009) completed 1:24,000 and 1:50,000 scale surficial geologic maps, with supporting geochronology, for seven contiguous quadrangles that include parts of Vanderburgh and Warrick Counties in Indiana, and Henderson County, Kentucky.

There has been no critical evaluation of the high-level terraces on the Ohio River. High-energy fluvial environments like the braided late Pleistocene Ohio River often lack sufficient organic material for reliable radiocarbon dating. Dateable carbon (wood and charcoal) is commonly destroyed in these high-energy settings, and where carbon is preserved it is virtually impossible to tell if it was reworked from older deposits. Therefore, multiple samples from the same deposit are required to establish a reliable age for any particular unit, which is difficult given the scarcity of organic material and the associated expense of the dating. Fluvial sediments such as those present in the Ohio River, however, were transported far from glacial source areas and had ample exposure to sunlight, making them well suited for OSL dating (Duller, 1996; Stokes, 1999; Wallinga, 2002; Rittenour et al., 2003; Wintle, 2008).

2. Study area

The study area encompasses a ~75 km reach of the lower Ohio River valley along the border of southwestern Indiana and western Kentucky, immediately upstream of the confluence of the Ohio and Wabash Rivers (Fig. 1). This reach of the valley lies within the southern half of the Illinois Basin (or Eastern Interior Basin of Fenneman, 1928) and is bounded to the south by the Rough Creek graben, a Precambrian aulacogen which is the eastern extension of the New Madrid rift complex (Johnson and Schwalb, 2010), and to the west by the Wabash Valley seismic zone (Nuttli, 1979; Obermeier et al., 1991). The Green River is the only major

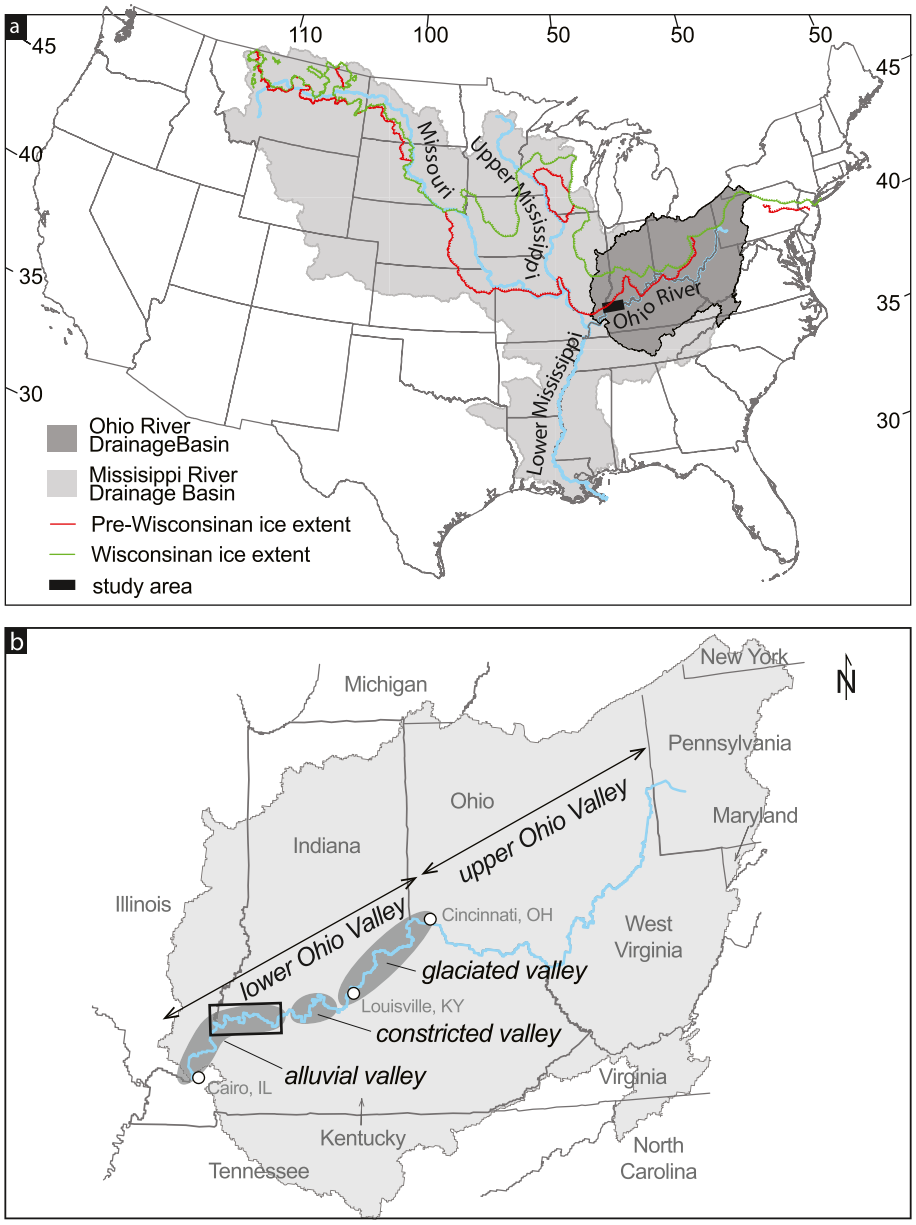

Fig. 1. (a) Map showing the extent of glaciation in the Ohio River and Mississippi River drainage basins in the northeastern United States. The black rectangle represents the study area. (b) The lower Ohio River valley begins at Cincinnati, Ohio, and ends at Cairo, Illinois, where the Ohio joins the Mississippi. The three primary geomorphic subdivisions of the lower Ohio valley, from upstream to downstream, include a glaciated, a constricted, and an alluvial section (adapted from Ray, 1974). The rectangular box outlines the study area.

tributary that joins the Ohio River in the study area, flowing northward from unglaciated regions of Kentucky.

2.1. Bedrock geology

The Ohio River valley transitions from a narrow, constricted valley in Mississippian limestone to a broad and expansive valley as it enters the Illinois Basin. Pennsylvanian rocks (McDowell, 1986) comprise cyclic sequences of sandstone, mudstone, shale, coal, and limestone that gently dip north towards the center of the basin (Rice et al., 1979; Nelson, 1991). The Ohio River has laterally eroded these relatively soft rocks and formed a very broad and deep bedrock valley with no bedrock constrictions. This large accommodation space has preserved thick alluvial fill successions and multiple terrace levels, which represent one of the most complete alluvial records in the valley and is arguably one of the best locations to study the glaciofluvial stratigraphy of the Ohio River. The Wabash Valley fault system, a Paleozoic fault system that has been reactivated during the Quaternary, defines the border of the western end of the study area (Nelson, 1991; Bodziak, 1999; Rutledge, 2004; Woolery, 2005; Smith, 2007).

2.2. Quaternary paleoclimate and paleoenvironments

The presence of the Laurentide ice sheet in the northern part of the Ohio River drainage basin caused rapid aggradation in the main valley (e.g. Leverett, 1902; Wayne, 1952; Ray, 1965, 1974; Straw, 1968; Fraser, 1994). Tributaries had much smaller sediment loads and did not aggrade in phase with the main valley, so outwash dammed the mouths of the tributaries and created an extensive network of lakes (Shaw, 1911, 1915; Frye et al., 1972; Fraser, 1994). Sediments deposited in tributary valleys are primarily composed of

fine silt and clay from the main Ohio River valley, with coarser outwash prograding up the tributaries as fluvio-deltaic successions deposited during large flood events (Fraser, 1994; Kvale and Archer, 2007).

Locally within the study area, more than 10 m of Peoria Loess accumulated on upland areas south of the Ohio River during the latter part of the Last Glacial. The thick loess contains alternating, faint bands of light and dark layers that represents multiple incipient soil (A) horizons and also contains several discernible weakly developed soils (Hayward and Lowell, 1993; Counts et al., 2008). Similar banding and paleosols are present in thick Peoria Loess in Illinois (Wang et al., 2003, 2009). The Peoria Loess is very calcareous, has large prismatic carbonate concretions, and is rich in terrestrial gastropod shells. The Roxana Silt, a mid-Wisconsinan (MIS 3) loess, underlies the Peoria Loess throughout the study area and is 0.3–~1.0 m thick (Johnson, 1965; Ray, 1957, 1960, 1963, 1965; Ruhe and Olson, 1978, 1980). Preliminary OSL dating indicates that the Peoria Loess was deposited between 23.5 ± 1.3 ka and 11.5 ± 0.7 ka in the lower Ohio River valley (Counts et al., 2008; Counts and Monaghan, 2014).

Boreal forest with spruce and pine dominated the forest vegetation from ~23 ka to ~20 ka during the global Last Glacial Maximum (LGM) (Wilkins et al., 1991; Jackson et al., 1997, 2000). During the Lateglacial (~15 ka to ~12 ka), boreal forest transitioned into taiga-boreal woodland dominated by pine (*Pinus*) and sedge (*Cyperaceae*) (Jackson et al., 1997, 2000), and deciduous woodlands replaced the taiga-boreal woodland during the Pleistocene–Holocene transition (~12 ka to ~9 ka) (Jackson et al., 1997; Williams, 2003).

Megafauna fossils are common within the Pleistocene deposits in the study area. The type specimen for the dire wolf (Canis dirus) was discovered on the banks of the Ohio River in 1854 near Evansville, Indiana (Leidy, 1856). Giant ground sloth (*Megalonyx jeffersonii*) bones were discovered in an exposure of a tributary paleochannel being eroded by the Ohio River near Henderson, Kentucky (Owen, 1861), and a complete mastodon (*Mammut americanum*) skeleton was discovered in Henderson County, Kentucky in 1953 (Armstrong, 1956). Operators of barges that mine sand and gravel from the Ohio River channel report that teeth, bone, and tusk fragments are commonly dredged from the channel.

2.3. Present climate and vegetation

Currently, the study area has a humid continental climate with large seasonal temperature fluctuations of hot and humid summers and cold to very cold winters (Kottek et al., 2006). The warmest month is July, averaging ~25.8 °C, and the coolest month is January, averaging ~1 °C (averaged for 1981–2010 AD; NOAA-NCDC, 2014). Prevailing winds are from the south to southwest, and precipitation is somewhat evenly distributed throughout the year. Topography in the study area is characterized by flat-lying fluvial landscapes and upland regions. Terraces, floodplains, oxbow lakes, sloughs, and low-gradient streams with sand and silt bedloads compose the fluvial landscapes, which are bordered to the north and south by rolling hills that range from 125 to 165 m above sea level (asl). Native vegetation (pre-European settlement) of the flat bottomlands included mixed hardwood forests dominated by oak (*Quercus*) and hickory (*Carya*), marshes populated with cord grass (*Spartina*) and bulrush (*Scirpus*), and bald cypress (*Taxodium distichum*) swamps. Discontinuous prairies and beech–maple–oak-hickory (*Fagus–Acer–Quercus–Carya*) forests were native to the upland hills (Woods et al., 1998). Today, much of the forested areas on flat-topped upland hills and flat bottomlands have been removed for agriculture, and most forested areas exist in small patches on flatlands and on steeper upland slopes.

3. Methods

3.1. Field methods

Most of the Quaternary surficial mapping was undertaken for the USGS and the Kentucky Geological Survey during the years 2004–2010 by combining geomorphic and surficial geologic mapping to develop a Quaternary allostratigraphic framework for the study area. Geologic mapping involved field traverses across the valley, interpretation of aerial photographs and digital elevation models (DEMs), description of field exposures and sediment cores, surface soil descriptions and pedogenic development, and the identification of geomorphic relationships between landforms. The landscape position, sedimentology, elevation above the modern floodplain, OSL and radiocarbon geochronology, and bounding surfaces such as paleosols, sediment discontinuities, and the bedrock surface were used to classify terraces and deposits into the chronostratigraphic units defined here as T7 (oldest) to T0 (youngest) (Fig. 2). Units T7, T6, and T5 are only present in the subsurface and are buried; these older deposits are not shown on Fig. 2.

Three allostratigraphic units representing Holocene, Last Glacial (Wisconsinan), and pre-Last Glacial (pre-Wisconsinan) sediments were identified in the study area. Wisconsinan sediments were primarily stacked sequences of massive and cross-bedded, pebbly coarse sand, and no unconformities or paleosols were observed; so correlations of Last Glacial (Wisconsinan) sediments were based upon their stratigraphic positions and OSL age control.

More than 30 sediment cores were drilled at key sites to develop our Quaternary stratigraphic framework for the fluvial sedimentary record. Cores were obtained using a variety of methods, including the use of a Central Mining Equipment (CME 75) wireline rotary drill rig, an AMS Inc. Powerprobe, Giddings and Geoprobe direct-push soil probes, and hand auguring and coring. Wireline natural gamma logs were collected for deep core boreholes, field descriptions were done on all cores in unique locations, and the deep cores were split, photographed, and described in more detail. Forty-one OSL samples were processed and analyzed at the Luminescence Dating Laboratory at the University of Cincinnati, and five were processed and analyzed at the USGS Luminescence Geochronology Laboratory in Denver.

3.2. Sampling for OSL dating

There were few natural exposures in the study area that were suitable for the collection of OSL samples, so most were taken from cores. To ensure that bioturbation or pedogenesis did not expose sediments to sunlight after burial, all samples were collected from non-weathered sand at depths immediately below the modern soil profile or deeper (field descriptions for most cores are shown in Table S1 in the Supplementary data). Multiple OSL ages were obtained for each fluvial unit except for T6 alluvium; T6 was identified at depths >20 m below the modern floodplain, and only one OSL sample was available for this alluvium.

Six samples were collected from backhoe trenches, basement excavations, and soil pits by hammering stainless steel tubes into the freshly cleaned faces of the excavations. The remaining samples were collected from subsurface cores. Deep subsurface samples (>20 m) were collected from standard, wireline drill core barrels by hammering opaque tubes into the bottom of the core barrels. Two shallow samples (<4 m) were acquired with a Geoprobe using plastic core barrel liners that were wrapped with opaque foil tape. The remaining subsurface samples (<8 m) were acquired using a Giddings soil probe equipped with dual-tube coring system. A customized 30 cm core barrel with stainless steel liners was used to collect the OSL samples. After

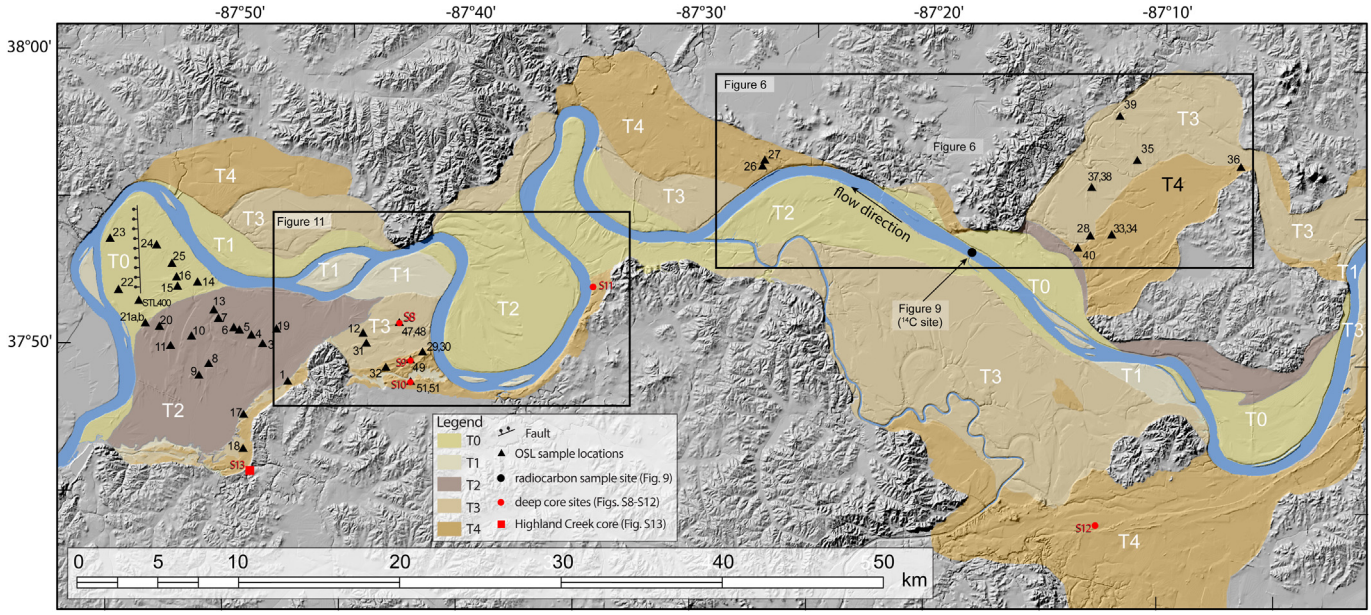

Fig. 2. Map of the study area (box on Fig. 1) showing terraces, OSL sample sites, and geomorphic relationships in the lower Ohio valley. Terrace numbers are from youngest (T0) to oldest (T4). Boxes show the locations of Fig. 6 and 11.

coring the desired interval, the core barrel was placed under a black cloth where the sample tubes were extracted from the core barrel and the ends of the tubes were covered with foil, sealed with water-tight caps, and then placed in opaque bags. If the sample tubes were not completely filled with sediment, foam or plastic spacers were added to the ends of the tube until the tubes were filled to prevent exposed sediment at the ends of the tubes from mixing with shielded sediments in the center of the tubes. A total of 52 samples were collected for luminescence dating, and after processing 46 samples contained enough quartz for OSL analysis.

3.3. Sampling for radiocarbon dating

Charcoal suitable for radiocarbon dating is rare in high-energy outwash deposits such as those in the deposits of the lower Ohio River, but is relatively abundant in overbank floodplain sediments and in areas that were occupied by indigenous peoples. Four samples of charred wood and one nutshell were collected from an exposure of T0 deposits in a cutbank of the Ohio River floodplain at an archeological site near Newburgh, Indiana. The samples were sent to the Illinois State Geological Survey Geochronology Laboratory for AMS ^{14}C dating. The ^{14}C ages were converted to calendar years using the Oxcal version 4.1.7 package (Bronk Ramsey, 1995, 2008) with the INTCAL98 calibration (Stuiver et al., 1998).

3.4. Laboratory methods for OSL

The theory behind OSL (blue light stimulated luminescence – BLSL) and infrared stimulated luminescence (IRSL) dating is explained in detail in Aitken (1998). Samples for OSL dating must remain shielded from light until they are analyzed in darkroom laboratory conditions using sodium vapor lighting or some other red filtered or red wavelength light.

3.4.1. Sample preparation

Most OSL samples were processed and measured in the Geochronology Laboratories at the University of Cincinnati; samples LORV-47, 48, -49, -50 and -51 were processed and measured at the Luminescence Geochronology Laboratory at the U.S. Geological Survey in Denver. In the laboratory, at least 5 cm of sediment was removed from the ends of each OSL tube, the sediment was weighed, oven dried at 40 °C, and weighed again to determine the field moisture content for each sample. The sediment was then disaggregated and sent to the USGS TRIGA Reactor facility in Denver, Colorado, for instrumental neutron activation analysis (INAA), following the procedures described in Snyder and Duval (2003). INAA was used to measure the U, Th, and K concentrations (Tables 1 and 2) for dose rate (D_R) determinations (following conversion factors specified by Aitken, 1998, his Appendix A). Sediment from the center of each of the tubes was used for the age analyses and was pretreated with 10% HCl and then with 10% H_2O_2 to remove carbonates and organic matter, respectively. The pretreated samples were rinsed in deionized water, decanted to remove clay and fine silt, dried, and sieved through 90–250 μm screens. This particle-size fraction was then treated with concentrated (44%) HF acid for 80 min (with frequent stirring) to etch the quartz grains and dissolve feldspar grains that may be present. Next the HF was decanted and the sample rinsed with deionized water, and was then treated with concentrated HCl for ~30 min. After decanting the HCl and rinsing with deionized water, the sample was dried and sieved to obtain the 90–150 μm particle size fraction (if there was insufficient sample after the HF digestion, the 150–250 micron fraction was used). Heavy minerals were removed from the 90–150 μm fraction by passing the sample through a variable magnetic field using a LFC Model-2 (low-field controlled) Frantz isodynamic magnetic separator, with forward and side slope angles each set at 10° (Porat, 2006). The magnetic separation was performed three times to ensure the sample only contained quartz.

3.4.2. OSL dating of quartz grains

An automated Risø TL-DA-20 OSL reader was used for OSL measurements and irradiation. Aliquots containing several hundred grains were mounted onto ~10 mm-diameter stainless steel discs as a small central circle approximately 3 mm across. Aliquots for each sample were first checked for feldspar contamination

Table 1
Radioisotope, water content, cosmic dose data, and the calculated dose rate for samples. Water content was measured in the lab, and cosmic dose rate was calculated using Prescott and Hutton (1994) formulation. Dose rate conversion factor was followed by using Adamiec and Aitken (1998). Complete dose rate calculated using software by Grün (2009).

Sample ID	SiteName	U (ppm)	Th (ppm)	K%	Water content %	Cosmic μGy/a)	Dose Rate(Gy/ka)
STL400	T0 terrace	1.70 ± 0.17	4.80 ± 0.05	0.90 ± 0.01	10.0 ± 2.00	104 ± 21	1.52 ± 0.01
LORV-01	T3u terrace	1.12 ± 0.11	2.95 ± 0.30	0.78 ± 0.04	4.8 ± 0.96	133 ± 27	1.28 ± 0.07
LORV-03	T2 terrace	1.29 ± 0.13	3.38 ± 0.34	0.71 ± 0.04	8.9 ± 1.79	163 ± 33	1.25 ± 0.08
LORV-05	T2 terrace	1.42 ± 0.14	4.05 ± 0.41	0.79 ± 0.04	10.3 ± 2.05	139 ± 28	1.35 ± 0.08
LORV-06	T2 terrace	1.36 ± 0.14	3.98 ± 0.40	0.76 ± 0.04	5.1 ± 1.03	109 ± 22	1.35 ± 0.08
LORV-07	T2 terrace	0.62 ± 0.06	1.75 ± 0.18	0.49 ± 0.02	1.4 ± 0.29	139 ± 28	0.87 ± 0.05
LORV-08	T2 terrace	1.92 ± 0.19	5.76 ± 0.58	0.90 ± 0.05	9.4 ± 1.89	139 ± 28	1.66 ± 0.10
LORV-09	T2 terrace	1.71 ± 0.17	4.91 ± 0.49	0.81 ± 0.04	12.3 ± 2.47	95 ± 19	1.39 ± 0.16
LORV-10	T2 terrace	1.70 ± 0.17	5.29 ± 0.53	0.89 ± 0.04	2.5 ± 0.49	139 ± 28	1.71 ± 0.09
LORV-11	T3L alluvium	1.23 ± 0.12	3.31 ± 0.33	0.74 ± 0.04	2.4 ± 0.49	139 ± 28	1.33 ± 0.07
LORV-12	T2 terrace	1.85 ± 0.19	5.52 ± 0.55	0.90 ± 0.05	12.6 ± 2.52	147 ± 29	1.58 ± 0.10
LORV-13	T0 terrace	2.07 ± 0.21	5.82 ± 0.58	0.98 ± 0.05	8.6 ± 1.72	104 ± 21	1.74 ± 0.11
LORV-14	T1 terrace	1.45 ± 0.15	4.16 ± 0.42	0.80 ± 0.04	12.9 ± 2.59	120 ± 24	1.30 ± 0.08
LORV-15	T0 terrace	1.31 ± 0.13	3.50 ± 0.35	0.88 ± 0.04	0.8 ± 0.16	126 ± 25	1.51 ± 0.09
LORV-16	T3L alluvium	1.78 ± 0.18	4.15 ± 0.42	0.92 ± 0.05	6.9 ± 1.38	155 ± 31	1.61 ± 0.08
LORV-17	T3U terrace	2.47 ± 0.25	6.02 ± 0.60	1.38 ± 0.07	8.9 ± 1.77	109 ± 22	2.19 ± 0.13
LORV-18	T3L terrace	0.93 ± 0.09	2.55 ± 0.26	0.70 ± 0.04	1.8 ± 0.36	109 ± 22	1.16 ± 0.06
LORV-19	T2 terrace	0.98 ± 0.10	2.83 ± 0.28	0.80 ± 0.04	9.7 ± 1.93	147 ± 29	1.21 ± 0.07
LORV-20	T2 terrace	0.75 ± 0.07	2.38 ± 0.24	0.57 ± 0.03	1.3 ± 0.27	147 ± 29	1.02 ± 0.06
LORV-21A	T1 terrace	2.06 ± 0.21	5.85 ± 0.59	0.91 ± 0.05	3.5 ± 0.69	102 ± 20	1.83 ± 0.09
LORV-21B	T1 terrace	1.55 ± 0.16	3.94 ± 0.39	0.65 ± 0.03	1.6 ± 0.32	132 ± 26	1.40 ± 0.07
LORV-22	T0 terrace	2.06 ± 0.21	6.01 ± 0.60	0.90 ± 0.05	4.7 ± 0.94	147 ± 29	1.85 ± 0.10
LORV-23	T0 terrace	2.84 ± 0.28	8.97 ± 0.90	1.31 ± 0.07	6.7 ± 1.33	91 ± 18	2.49 ± 0.13
LORV-24	T0 terrace	1.00 ± 0.10	2.21 ± 0.22	0.72 ± 0.04	1.0 ± 0.20	139 ± 28	1.23 ± 0.06
LORV-25	T0 terrace	3.33 ± 0.33	10.60 ± 1.06	1.52 ± 0.08	6.1 ± 1.22	91 ± 18	2.92 ± 0.15
LORV-26	T4 alluvium	2.05 ± 0.21	5.00 ± 0.50	1.00 ± 0.05	4.8 ± 0.96	100 ± 20	1.82 ± 0.09
LORV-27	T4 terrace	1.50 ± 0.15	3.01 ± 0.30	0.87 ± 0.04	1.8 ± 0.35	99 ± 20	1.50 ± 0.07
LORV-28	T4 terrace	1.72 ± 0.17	3.58 ± 0.36	0.91 ± 0.05	3.0 ± 0.61	150 ± 30	1.65 ± 0.08
LORV-29	T4 dune	1.68 ± 0.17	3.83 ± 0.38	0.93 ± 0.05	0.9 ± 0.17	135 ± 27	1.71 ± 0.08
LORV-30	T4 dune	1.66 ± 0.17	3.70 ± 0.37	0.84 ± 0.04	3.4 ± 0.67	88 ± 18	1.51 ± 0.07
LORV-31	T3L terrace	1.70 ± 0.17	4.52 ± 0.45	0.89 ± 0.04	7.6 ± 1.53	121 ± 24	1.58 ± 0.08
LORV-32	T3L terrace	2.60 ± 0.26	6.74 ± 0.67	1.07 ± 0.05	4.1 ± 0.81	96 ± 19	2.14 ± 0.11
LORV-33	T4 terrace	1.50 ± 0.15	2.70 ± 0.27	0.88 ± 0.04	8.4 ± 1.67	111 ± 22	1.39 ± 0.03
LORV-34	T4 dune	1.84 ± 0.18	4.36 ± 0.44	0.86 ± 0.04	2.7 ± 0.55	152 ± 30	1.70 ± 0.08
LORV-35	T3U terrace	1.99 ± 0.20	6.32 ± 0.63	1.15 ± 0.06	6.0 ± 1.19	156 ± 31	2.07 ± 0.10
LORV-36	T3L terrace	2.01 ± 0.20	6.21 ± 0.62	1.11 ± 0.06	4.8 ± 0.96	169 ± 34	2.07 ± 0.10
LORV-37	T4 alluvium	1.63 ± 0.16	4.95 ± 0.50	1.00 ± 0.05	8.5 ± 1.69	96 ± 19	1.65 ± 0.08
LORV-38	T4 terrace	1.67 ± 0.17	2.95 ± 0.30	0.84 ± 0.04	7.2 ± 1.45	161 ± 32	1.47 ± 0.07
LORV-39	T3U terrace	1.77 ± 0.18	4.65 ± 0.47	0.94 ± 0.05	8.8 ± 1.77	156 ± 31	1.66 ± 0.09
LORV-41	T2 terrace	2.71 ± 0.27	9.48 ± 0.95	1.50 ± 0.08	3.9 ± 0.80	148 ± 30	2.82 ± 0.14
LORV-42	T3L terrace	2.37 ± 0.24	6.21 ± 0.62	1.08 ± 0.05	2.8 ± 0.60	62 ± 12	2.06 ± 0.10
LORV-47	T4 alluvium	0.67 ± 0.05	1.81 ± 0.17	0.68 ± 0.02	0.0 ± 0.00	46 ± 9	0.94 ± 0.06
LORV-48	T4 alluvium	0.62 ± 0.05	1.78 ± 0.16	0.66 ± 0.02	9.9 ± 2.00	45 ± 9	0.89 ± 0.06
LORV-49	T5 alluvium	1.24 ± 0.08	2.43 ± 0.16	0.89 ± 0.02	5.2 ± 1.00	24 ± 5	1.29 ± 0.07
LORV-50	T5 alluvium	4.02 ± 0.08	12.00 ± 1.13	2.04 ± 0.12	24.7 ± 5.00	22 ± 4	2.50 ± 0.11
LORV-51	T6 alluvium	3.96 ± 0.08	11.40 ± 1.28	2.02 ± 0.11	34.2 ± 6.80	18 ± 4	2.93 ± 0.12

using room-temperature IRSL before the main OSL measurements were undertaken (Jain and Singhvi, 2001). Samples that did not pass the IRSL test were etched for a second time in 44% HF for an additional 30 min to remove feldspar, followed by HCl treatment and sieving again. Samples that passed the IRSL test were used for OSL dating. The single aliquot regeneration (SAR) method of Murray and Wintle (2000) was used to determine the equivalent dose (D_E) for age estimation. Aliquots of samples were illuminated with blue light emitting diodes stimulating at a wavelength of 470 nm. The detection optics consist of Hoya U-340 and Schott BG-39 color glass filters coupled to an EMI 9235 QA photomultiplier tube. The samples were irradiated using a $^{90}Y/^{90}Sr$ beta source, regenerated using four cycles of measurement, and in each case the OSL signal was recorded for 40 s at 125 °C.

Standard OSL tests as suggested by Duller (2008) for recycling, recuperation, preheat, and dose recovery were performed. We accepted recycling ratios and recuperation between 0.90 and 1.1. Only aliquots that satisfied the recycling and recuperation range of 10% or better were used in determining D_E. The preheat tests indicated that acceptable preheats between 200 °C and 260 °C could be used; we chose to consistently use 240 °C. OSL sensitivity of the samples had a high signal to noise ratio. Dose recovery tests (Wintle and Murray, 2006) indicate that a laboratory dose could be recovered to within 2% by the SAR protocol (Fig. 3a), and shine-down curves show a sharp decay in all samples (Fig. 3b), indicating the OSL signal is fast-component dominated and thus acceptable for measurements using the SAR protocol.

To prevent cross-talk contamination to adjacent disc positions, 24 aliquots were loaded into alternating positions on the carousel (i.e. 2, 4, 6, 8, and so on) for each sample. Although probability plots of D_E for many of the samples had multiple peaks in their distributions, most aliquots plotted under large,narrow peaks with few outliers (Fig. 4), indicating partial bleaching was minimal and 24 aliquots were sufficient for age determinations. We used weighted mean ages to interpret our data, as the weighted mean age gives less significance to outliers (Bevington and Robinson, 2002) and produces more robust data sets when the given sets of measurements are below 30–50 aliquots per sample (Duller, 2008; Rodnight, 2008). D_R and D_E estimation data are summarized in Table 1. The D_E data were normally distributed with few significant

Table 2
Equivalent dose and ages estimated using single aliquot regenerative (SAR) method. The age for each sample was calculated using Grün software (2009).

Sample ID	Landform/ Deposit	Discs[a]	Surface Elev (m)	Sample depth (m)	Lat. (N)	Lon. (E)	DE (Gy) Wt_mean	Dose rate (Gy/ka)	Wt mean (Ka)
LORV-23	T0 Terrace	24 (24)	107.6	5.0	37.89656	−87.91759	1.84 ± 0.01	2.49 ± 0.13	0.7 ± 0.1
LORV-22	T0 Terrace	22 (24)	106.7	2.0	37.86748	−87.91082	1.69 ± 0.01	1.85 ± 0.10	0.9 ± 0.1
LORV-25	T0 Terrace	23 (24)	107.9	5.0	37.88289	−87.87263	8.16 ± 0.03	2.92 ± 0.15	2.8 ± 0.2
LORV-24	T0 Terrace	19 (24)	108.2	2.3	37.89330	−87.88419	3.91 ± 0.04	1.23 ± 0.06	3.2 ± 0.2
LORV-13	T0 Terrace	21 (24)	109.4	4.1	37.85713	−87.84204	7.00 ± 0.02	1.74 ± 0.11	4.0 ± 0.2
LORV-15	T0 Terrace	21 (24)	109.7	2.9	37.87016	−87.86827	6.45 ± 0.03	1.51 ± 0.09	4.3 ± 0.2
STL400	T1 Terrace	21 (24)	102.0	4.0	37.85943	−87.94230	7.10 ± 0.03	1.52 ± 0.01	4.7 ± 0.0
LORV-21A	T1 Terrace	24 (24)	109.7	2.6	37.84614	−87.89034	9.12 ± 0.02	1.83 ± 0.09	5.0 ± 0.3
LORV-21B	T1 Terrace	20 (24)	109.7	2.6	37.84614	−87.89034	7.99 ± 0.02	1.4 ± 0.07	5.7 ± 0.3
LORV-14	T1 Terrace	23 (24)	109.1	3.2	37.87272	−87.85404	7.51 ± 0.02	1.3 ± 0.08	5.8 ± 0.4
LORV-10	T2 Terrace	24 (24)	110.3	2.3	37.84197	−87.85768	10.56 ± 0.03	1.71 ± 0.09	6.2 ± 0.3
LORV-09	T2 Terrace	24 (24)	108.8	4.7	37.81990	−87.85162	9.77 ± 0.03	1.39 ± 0.16	7.0 ± 0.8
LORV-20	T2 Terrace	23 (24)	110.0	4.3	37.84725	−87.88061	7.64 ± 0.04	1.02 ± 0.06	7.5 ± 0.4
LORV-19	T2 Terrace	24 (24)	109.7	2.0	37.84714	−87.79695	9.62 ± 0.03	1.21 ± 0.07	8.0 ± 0.5
LORV-05	T2 Terrace	23 (24)	109.7	2.3	37.84614	−87.82356	11.05 ± 0.06	1.35 ± 0.08	8.2 ± 0.5
LORV-12	T2 Terrace	24 (24)	109.7	2.0	37.84575	−87.73501	14.05 ± 0.03	1.58 ± 0.10	8.9 ± 0.6
LORV-41	T2 Terrace	17 (24)	117.4	2.0	37.90162	−87.22407	26.17 ± 0.23	2.82 ± 0.14	9.3 ± 0.5
LORV-06	T2 Terrace	22 (24)	109.1	3.8	37.84722	−87.82751	12.68 ± 0.05	1.35 ± 0.08	9.4 ± 0.5
LORV-03	T2 Terrace	24 (24)	109.7	1.4	37.83887	−87.80649	12.03 ± 0.02	1.25 ± 0.08	9.6 ± 0.6
LORV-08	T2 Terrace	24 (24)	107.3	2.3	37.82660	−87.84471	16.32 ± 0.03	1.66 ± 0.10	9.8 ± 0.6
LORV-07	T2 Terrace	24 (24)	109.4	2.3	37.85248	−87.83850	9.15 ± 0.03	0.87 ± 0.05	11.5 ± 0.6
LORV-42	T3L Terrace	20 (24)	119.2	7.9	37.82678	−87.71803	26.17 ± 0.21	2.06 ± 0.1	12.7 ± 0.6
LORV-36	T3L Terrace	20 (24)	118.5	1.2	37.94873	−87.10818	27.66 ± 0.27	2.07 ± 0.1	13.4 ± 0.7
LORV-16	T3L Terrace	20 (24)	109.7	1.7	37.87526	−87.86931	21.67 ± 0.12	1.61 ± 0.08	13.5 ± 0.8
LORV-18	T3L Terrace	23 (24)	114.6	3.8	37.77917	−87.81894	15.63 ± 0.05	1.16 ± 0.06	13.5 ± 0.7
LORV-32	T3L Terrace	22 (24)	119.2	4.7	37.82678	−87.71803	31.15 ± 0.23	2.14 ± 0.11	14.5 ± 0.7
LORV-31	T3L Terrace	24 (24)	112.8	3.2	37.84017	−87.73222	23.32 ± 0.14	1.58 ± 0.08	14.8 ± 0.7
LORV-11	T3 alluvium	23 (24)	110.0	2.3	37.83655	−87.87255	19.90 ± 0.08	1.33 ± 0.07	14.9 ± 0.8
LORV-39	T3U Terrace	23 (24)	117.7	1.7	37.97670	−87.19546	25.20 ± 0.20	1.66 ± 0.09	15.2 ± 2.8
LORV-35	T3U Terrace	20 (24)	117.7	1.7	37.95167	−87.18250	31.84 ± 0.25	2.07 ± 0.1	15.4 ± 0.8
LORV-01	T3U Terrace	24 (24)	113.4	2.6	37.81774	−87.78790	20.44 ± 0.05	1.28 ± 0.07	15.9 ± 0.9
LORV-17	T3U Terrace	24 (24)	110.6	3.8	37.79840	−87.81916	36.52 ± 0.17	2.19 ± 0.13	16.7 ± 1.0
LORV-38	T4 Terrace	17 (24)	117.7	1.5	37.93610	−87.21492	25.86 ± 0.27	1.47 ± 0.07	17.6 ± 0.9
LORV-26	T4 Terrace	22 (24)	117.0	4.4	37.94503	−87.45107	32.49 ± 0.24	1.82 ± 0.09	17.8 ± 0.9
LORV-34	T4 Terrace	21 (24)	119.8	1.8	37.90935	−87.20000	31.47 ± 0.27	1.7 ± 0.08	18.6 ± 0.9
LORV-28	T4 Terrace	21 (24)	118.9	1.9	37.90854	−87.21547	30.84 ± 0.18	1.65 ± 0.08	18.7 ± 0.9
LORV-29	T4 Dune	23 (24)	128.3	2.5	37.83590	−87.69182	32.29 ± 0.26	1.71 ± 0.08	18.9 ± 0.9
LORV-37	T4 alluvium	23 (24)	117.7	4.7	37.93610	−87.21492	31.26 ± 0.18	1.65 ± 0.08	18.9 ± 1.0
LORV-33	T4 Terrace	20 (24)	119.8	3.7	37.90935	−87.20000	27.72 ± 0.27	1.39 ± 0.03	20.0 ± 1.0
LORV-27	T4 Terrace	19 (22)	122.8	4.5	37.94835	−87.44941	31.69 ± 0.25	1.5 ± 0.07	21.2 ± 1.0
LORV-30	T4 Dune	17 (24)	127.1	5.3	37.83583	−87.69191	32.43 ± 0.26	1.51 ± 0.07	21.4 ± 1.0
LORV-47	T4 alluvium	10 (20)	112.5	13.7	37.85507	−87.69799	32.49 ± 0.24	0.94 ± 0.06	18.9 ± 2.5
LORV-48	T4 alluvium	21 (22)	112.5	24.1	37.85507	−87.69799	22.00 ± 1.28	0.89 ± 0.06	29.9 ± 2.7
LORV-49	T5 alluvium	15 (30)	128.3	24.1	37.83173	−87.69697	42.60 ± 1.45	1.29 ± 0.07	38.8 ± 2.4
LORV-50	T5 alluvium	18 (20)	123.8	26.5	37.82075	−87.70747	96.00 ± 6.92	2.5 ± 0.11	38.4 ± 5.9
LORV-51	T6 alluvium	21 (24)	123.8	36.8	37.82075	−87.70747	334.00 ± 23.40	2.93 ± 0.12	114.0 ± 11.5

[a] The number of aliquots used for age calculations; total number of aliquots measured are shown in parentheses.

deviations. All histograms for D_E distributions are included in the Supplementary data (Figs. S1–S7).

4. Results

4.1. Fluvial landforms and associated sediments within the study area

Fluvial sediments and landforms in the study area include braided and meandering channel-belt deposits with multiple terrace levels formed upon them, and fine-grained floodbasin/backswamp deposits that compose much of the fill in the tributary basins. Tributary basin fill is characterized by stacked successions of fluvio-deltaic sediments, buried floodplain deposits, paleosols, lacustrine muds, and overbank deposits, all overlain by a broad, extremely flat lacustrine terrace that lies 10–15 m above the modern floodplain.

The alluvium in the valley is similar lithologically and can be difficult to differentiate based upon composition alone. Unit designations (summarized in Table 3) were based upon OSL ages, compaction, degree of weathering, pedogenesis, sedimentology, landscape position, and stratigraphic and geomorphic relationships. Terraces and alluvium were divided into seven units and named from the youngest, T0, to the oldest, T7.

4.1.1. T7 alluvium

T7 deposits are the oldest fluvial deposits identified in the study area and were only observed at the bottom of three deep cores. T7 deposits are highly compacted compared to the overlying Wisconsinan sediments (Fraser and Fishbaugh, 1986), and can be difficult to recover by coring. T7 alluvium is typically strong brown (7.5YR 4/6) to olive (5Y 4/3) in color and is well-rounded sandy cobble gravel primarily composed of chert, siltstone, sandstone, limestone, and quartzite clasts, with a smaller percentages of igneous and metamorphic lithologies derived from the Canadian Shield. Many clasts in the T7 alluvium were highly weathered and friable. T7 deposits are 1–5 m thick, underlain by Paleozoic bedrock (Fig. 5a), and were identified at elevations ranging from ~37 m to ~24 m below the modern floodplain. The oxidized brown colors of T7 alluvium are similar to pedogenic horizons at or near the

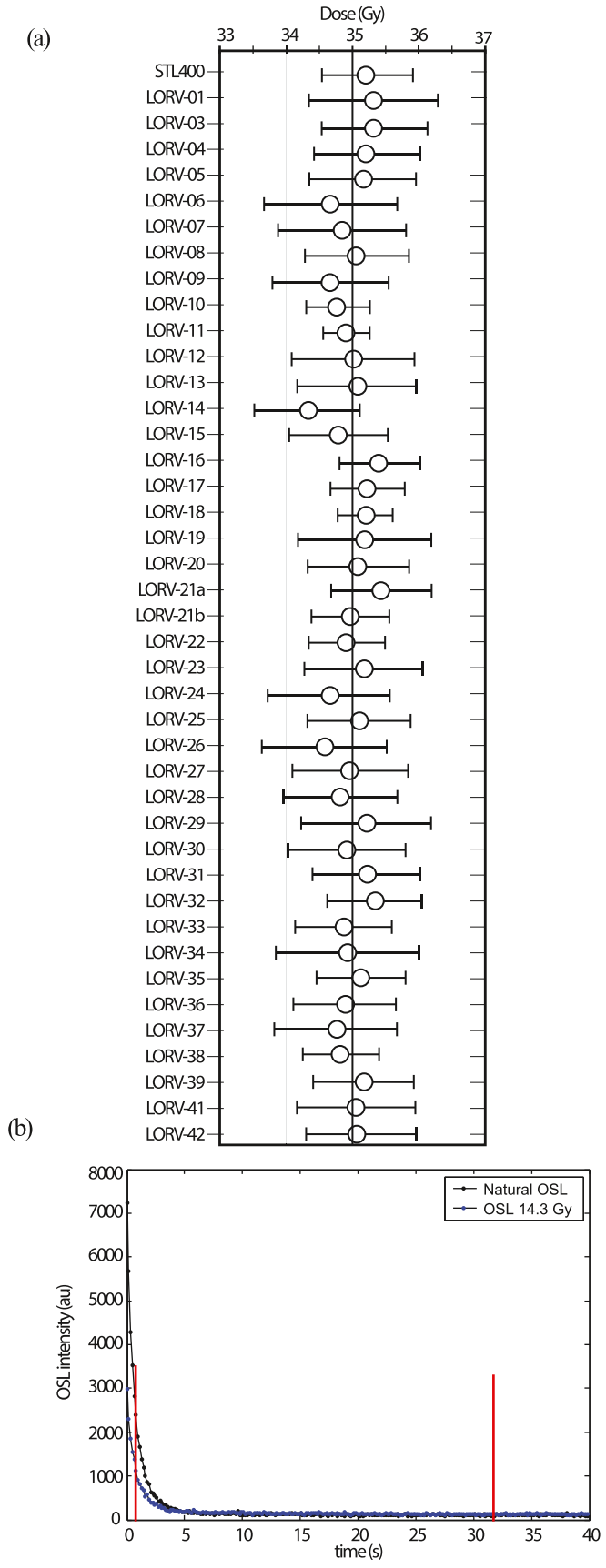

Fig. 3. (a) Dose recovery test for samples analyzed at the University of Cincinnati. A dose of 35 Gy was given to each sample and recovered using the single aliquot regenerative (SAR) method. The dose recovered for each sample is the mean of 5 aliquots and error bars are the standard deviation. This test shows the mean value for each recovered dose was within the range of 2–3% uncertainty. (b) Typical shine down curve for sample LORV26. Blue light stimulated luminescence (BLSL) for natural and artificial dose. The two line bars show the first 5 and last 50 channels of the background region.

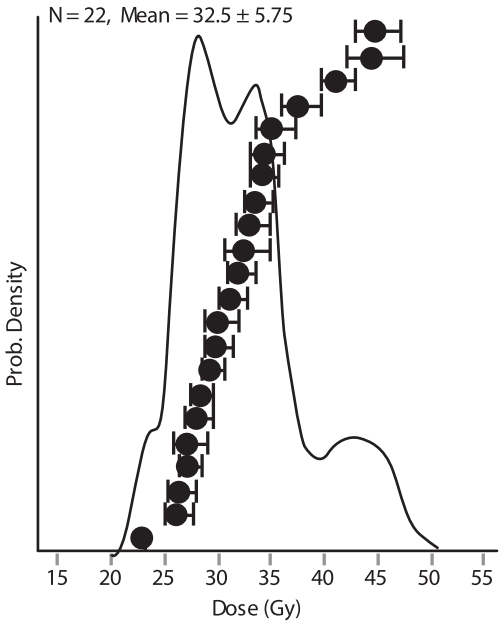

Fig. 4. Probability plot for sample LORV-26, which shows that there are four distributions of D_E. Most aliquots plot beneath the two large, narrow peaks in the middle of the distribution, and outliers plot beneath the smaller peaks. The first small peak is a low dose and includes 1 aliquot, and the other small peak is a high dose and includes 4 aliquots. The high dose peak may have a partially bleached component, which would produce and overestimation of age. To minimize the effects of outliers from the main population, sample ages were estimated using weighted mean statistics(D_E distributions for all samples are shown in the Supplementary data, Figs S1-S7).

surface, but there were no other indicators of pedogenic modification due to poor recovery. T7 alluvium could not be dated.

4.1.2. T6 alluvium

T6 deposits are moderately to poorly sorted, dark grayish brown (10YR 4/2) and olive gray (5Y4/2) coarse pebble sand; pebble clasts include chert, quartz, sandstone, limestone, and siltstone along with igneous and metamorphic lithologies from the Canadian Shield. T6 alluvium was identified in 3 cores ~20–~24 m below the modern floodplain and ranged from ~2 to 6 m thick where it was observed (Fig. 5a–b). No buried terraces or paleosols were positively identified in the T6 alluvium, and only one sample of T6 could be collected for OSL dating.

4.1.3. T5 alluvium

T5 deposits consist of dark grayish brown (10YR 4/2) and gray (10YR 5/1) moderately sorted medium to coarse sand and fine pebbles. Pebbles consist of quartz, chert, quartzite, sandstone, limestone, and granitoid rock fragments. T5 deposits were only identified in two cores ~10 m below the modern floodplain, and the maximum observed thickness of T5 alluvium was ~7 m (Fig. 5a–b). No surfaces or paleosols were identified in the T5 alluvium. Two samples of T5 alluvium were collected for OSL dating.

4.1.4. T4 terraces and alluvium

The T4 terraces stand ~13 m above the modern floodplain, ~120 m above sea level (asl), and are the highest fluvial landforms in the study area. There is an upper and lower T4 terrace (Fig. 6) and

Table 3
Summary of alluvial deposits and landforms in the lower Ohio River valley.

Deposit	Description	Munsell	Thickness (m)	Landscape position	Geomorphic/Sed. characteristics	Diagnostic features	Interpretation
T0 terrace and alluvium	Silt and silt loam	10YR 3/2 (v. dark grayish brown), 10YR 4/4 (dark yellowish brown)	~4 m	Grade	Active floodplain level	No soil development	Holocene climate
T1 terrace and alluvium	Silty clay loam and silty clay that is underlain by massive, moderately sorted medium and fine sand	10YR 4/3 (brown), 10YR 4/6 (dark yellowish brown)	4–8 m	~1 m above grade	Meandering river deposits	Very weak soil development (inceptisols)	Holocene climate
T2 terrace and alluvium	Silty clay loam underlain by moderately to well sorted medium and fine sand	10YR 4/3 (brown), 10YR 4/4 (dark yellowish brown)	4–8 m	1–2 m above grade	Meandering river deposits	Alfisols	Transition to Holocene optimum
T3 terraces and alluvium	Fill-cut terrace in T4 alluvium	10YR 3/3 (dark brown), 10YR 4/6 (dark yellowish brown)	n/a	3–5 m above grade	Braided (upper T3) to anabranching (lower T3) surface morphology	Distinct terrace risers between T4 and T3, low angle risers between upper and lower T3 terraces	Terraces represent hiatuses in incision into the T4 alluvium, lower T3 terrace corresponds to beginning of Bølling-Allerød interstadial
T4 terrace	Highest fill terrace in the Ohio Valley	n/a	n/a	12–13 m above grade	Braided surface	n/a	Maximum level of aggradation during the LGM
T4 alluvium (fine facies)	Loamy sand, silty clay to clay	5Y 4/3 (olive), 10YR 3/1 (very dark gray), and 5B 7/6 (light blue)	~1–5 m	~10–20 m below grade	Lens shaped geometries	Dark gray/reduced colors	Fines deposited in distributary channels, in pools, and on leeward side of bars during low flow
T4 alluvium (coarse)	Coarse pebble sand with lenses of pebble gravel; similar lithologies as T5	10YR 5/4 (yellowish brown)and 5Y 7/6 (yellow)	Up to 35 m	From ~22 m below grade to ~15 m above grade	Coarse, cross-bedded pebble sand	Unweathered	Braided MIS 2 outwash deposits
T5 alluvium	Medium and coarse sand and fine pebbles; composed of quartz, chert, quartzite, sandstone, limestone, and granitoid rock fragments	10YR 4/2 (dark grayish brown) and 10YR 5/1 (gray)	~5 m	~10 m below grade	Coarse, cross-bedded pebble sand	Unweathered, only identified as different than T4 alluvium by OSL dating	Aggradation/outwash deposited during MIS 3 ice advance
T6 alluvium	Pebble sand and gravel; clasts composed of quartz, chert, quartzite, sandstone, coal, limestone, and igneous and metamorphic rock fragments from Canadian Shield	10YR 4/2 (dark grayish brown) and 5Y 4/2 (olive gray)	~2–6 m	20–24 m below grade	Similar to T7 but sediment caliber is smaller and not weathered	Oxidized colors	MIS 6 outwash reworked at the end of MIS 5e or aggradation/ alluvium deposited at the beginning of MIS 5d
T7 alluvium	Coarse gravel and sandy gravel composed of chert, quartzite, sandstone, coal, limestone, and igneous and metamorphic rock fragments from Canadian Shield	7.5YR 4/6 (strong brown) to 5Y 4/3 (olive)	0–5 m	~30–37 m below grade	Coarse gravel and cobbles, highly compacted and severely weathered	Friable igneous clasts: oxidized colors	Outwash deposited during MIS 6 or earlier glaciation

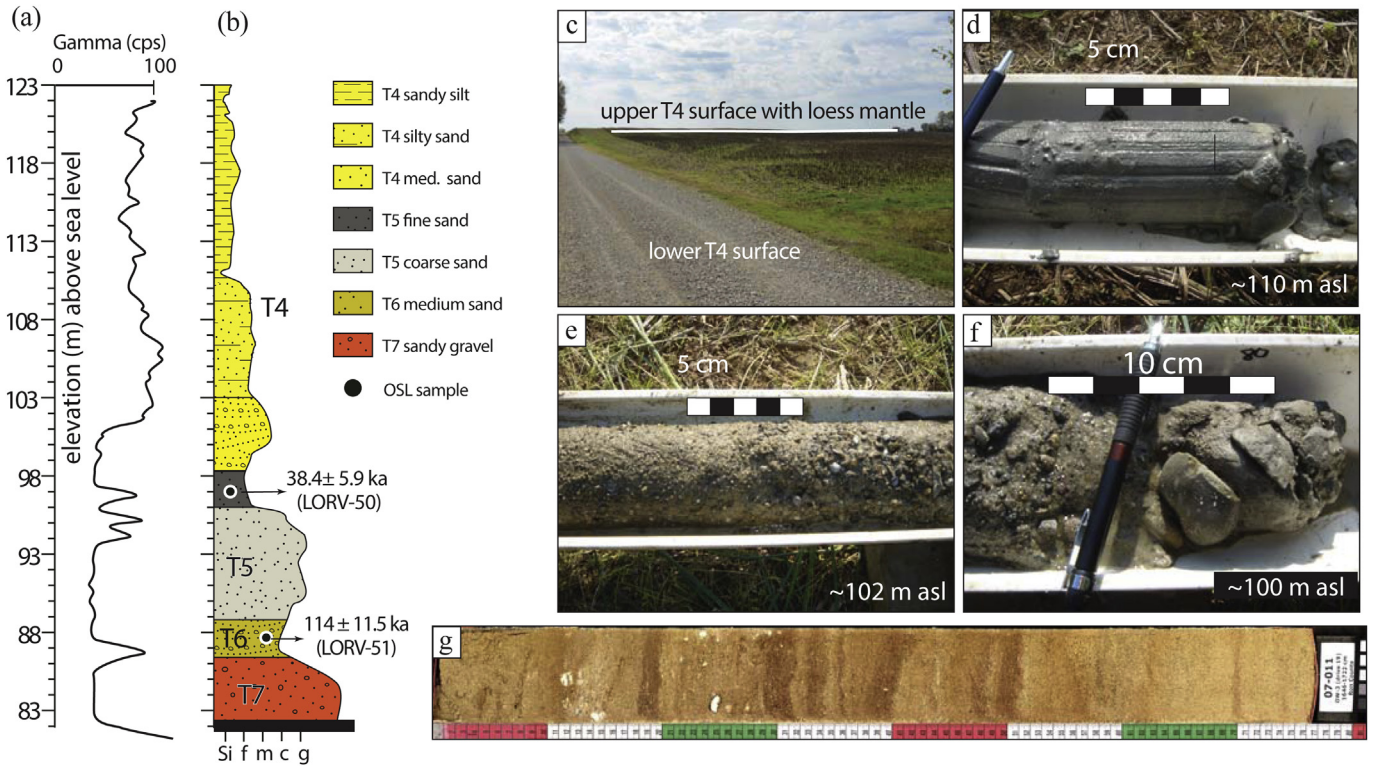

Fig. 5. (a) Natural gamma log and (b) graphic log of a sediment core drilled a T4 terrace down to bedrock, represented by the black bar. (c) A thin mantle of loess and dune sand is present in some locations, making the upper T4 terrace seem higher than it actually is. (d–f) Fine sandy to gravelly facies of the T4 fill deposit. (g) Digital line-scan of a T4 core ~16 m below the T4 terrace (Color scale alternates every 10 cm; Si, f,m,c, and g = silt, fine, medium, coarse sand, and gravel, respectively; gamma log units are counts per second (cps) of American Petroleum Industry units (API). (For interpretation of the references to color in this figure legend, the reader is referred to the web version of this article.)

their treads are usually separated by <2 m. The lower T4 terrace is inset in the upper terrace (Figs. 5c and 6), and the scarp that separates them is generally eroded and has a low slope angle; so it can be difficult to distinguish between them except in the few areas where they occur together.

T4 deposits are typically poorly to moderately sorted, yellowish brown (10YR 5/4) and yellow (5Y 7/6) coarse sand with lenses of pebble gravel. Pebbles include quartz, chert, quartzite, sandstone, coal, limestone, and igneous and metamorphic lithologies from the Canadian Shield. T4 deposits also include lenses of olive (5Y 4/3), dark gray (10YR 3/1) and light-blue (5B 7/6) silty clay and plastic clay (Fig. 5d–g and Figs S8–S12 in the supplementary data). T4 terrace deposits are stacked, braided channel-belt deposits up to 35 m thick. On the southern side of the Ohio River, T4 terraces can be covered with up to 7 m of dune sand (Ray, 1965); elsewhere, the T4 terraces can be covered with a relatively thin, 1–3 m mantle of loess. Older aerial photography reveals relict braid channels and braid bars on the surfaces of T4 terraces. T4 terraces were not inundated during the largest recorded flood, a 1000-year flood event on the Ohio River in AD 1937 (Grover and Mansfield, 1938), suggesting they have not been significantly aggraded or scoured since they formed.

4.1.5. T3 terraces and alluvium

T3 terraces are inset 3–4 m into T4 terraces and stand ~9 m above the modern floodplain. Like the T4 terraces, there are at least two T3 surfaces with <2.0 m of relief between them (Fig. 6). The lower T3 surface is inset in the upper surface, and they can only be distinguished in the field where they occur together, and even then it can be challenging (Fig. 7a). T3 deposits are predominantly dark brown (10YR 3/3) to dark yellowish brown (10YR 4/6) poorly sorted, fine to coarse sand and pebbly sand with minor gravel (Fig. 7c). Pebbles include quartz, chert, quartzite, sandstone, coal, limestone, and igneous and metamorphic lithologies from the Canadian Shield. T3 deposits also contain a second facies comprising local lenses of dark gray (2.5Y 4/1) to olive gray (5Y 4/2) clayey silt and clay that are 1–2 m to 5 m thick.

4.1.6. T2 terraces and alluvium

T2 terraces stand ~3 m above the modern floodplain. T2 deposits consist of brown (10YR 4/4) silty clay loam underlain by moderately to well sorted dark yellowish brown (10YR 4/4) medium and fine sand (Fig. 8a). Sand includes mineral grains of quartz, chert, quartzite, sandstone, coal, limestone, and igneous and metamorphic lithologies from the Canadian Shield. T2 deposits also contain lenses of olive brown (2.5Y 4/3) to dark gray (5Y 4/1) clay and clay loam that are up to 5 m thick; the maximum observed thickness of T2 deposits was ~9 m. T2 deposits are inset into T3 deposits, and the T2 terraces have ridge-and-swale scroll morphology. T2 terrace elevations are slightly higher than the bank full flood stage and are not inundated annually, but it is common for T2 terraces to flood every 5–10 years.

4.1.7. T1 terraces and alluvium

T1 terraces lay ~1.5–2 m above the modern floodplain and they are frequently inundated by floods. T1 deposits are typically 3–4 m-thick and comprise brown (10YR 4/3) to dark yellowish brown (10YR 4/6) silty clay loam and silty clay that is underlain by massive, moderately sorted fine and medium sand (Fig. 8b). T1 is

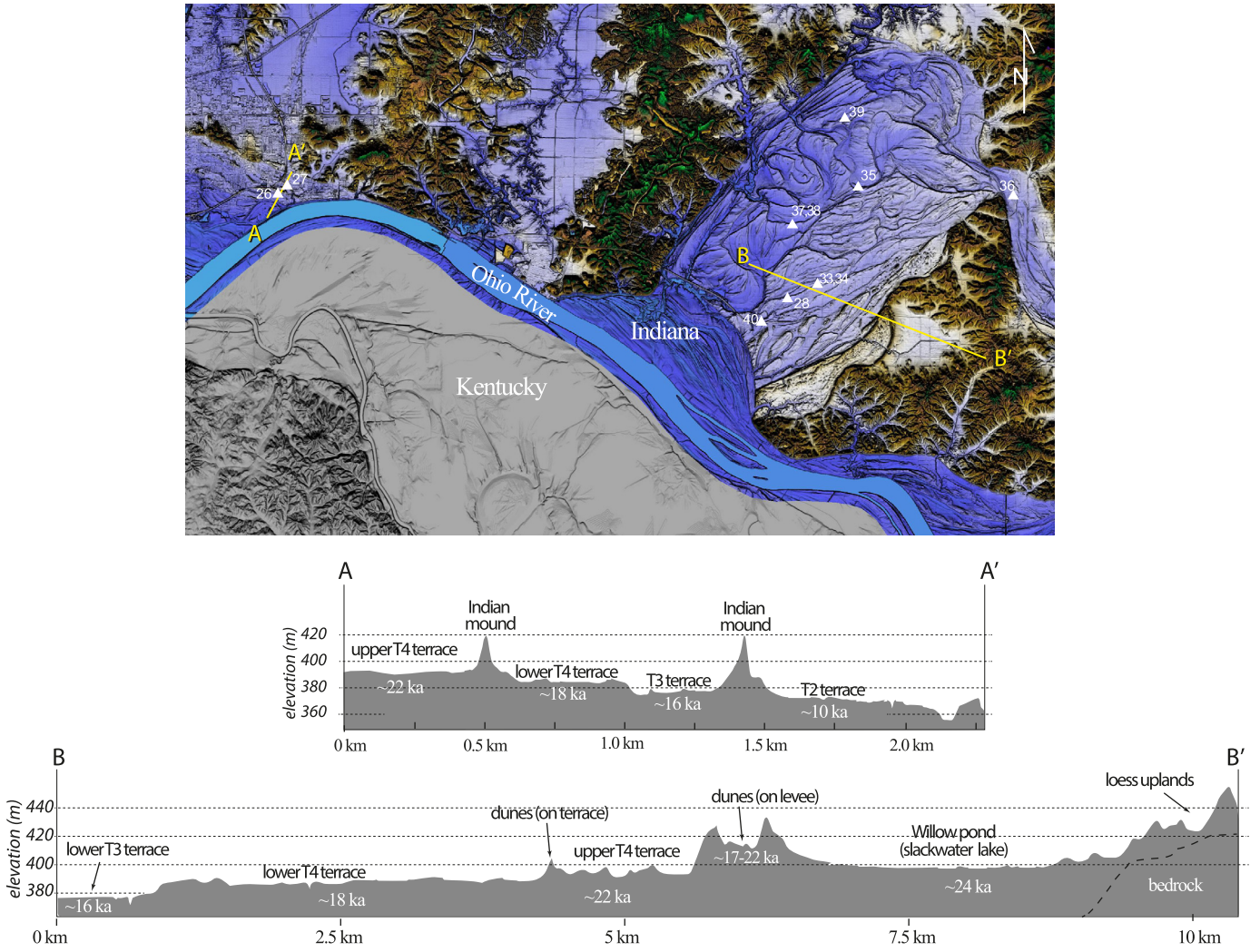

Fig. 6. Digital terrain model (DTM) and topographic profiles showing relationships between terraces and landforms in an eastern section of the study area (location shown on Fig. 2). The DTM for Indiana was created with 1.5 m/pixel IndianaMAP LiDAR data; the DTM for Kentucky was created with the USGS 10-m National Elevation Dataset.

incised into the T2 terrace, and flood-chute channels commonly dissect T1 surfaces.

4.1.8. T0 terraces and alluvium

The T0 surface is the active floodplain of the Ohio River. T0 deposits are very dark grayish brown (10YR 3/2) to dark yellowish brown (10YR 4/4) silt and silt loam with extremely weak to no soil development (Fig. 9a).

4.2. Dating results

4.2.1. OSL dating

D_R calculations and D_E data are summarized in Table 1. OSL ages of lower Ohio River sediments span from the MIS 5e to MIS 5d transition (~114 ka), MIS 3 (~38 ka), pre LGM (~28 ka), MIS 2/LGM (~22 ka), post LGM/Lateglacial (~18–16 ka), the MIS 2 to MIS 1 transition (~12 ka), and the Holocene (~11–1 ka) (Table 2).

4.2.2. Radiocarbon dating

The ^{14}C ages of the five samples sent to the Illinois State Geological Survey Geochronology Laboratory were converted to calendar years using the Oxcal version 4.1.7 package (Bronk Ramsey, 1995, 2008) with the INTCAL98 calibration (Stuiver et al., 1998) so they could be directly compared to the OSL ages. The ages are presented in Table 4.

4.2.3. Validity of geochronology

Where paired radiocarbon and OSL samples were collected, calibrated 2σ radiocarbon ages overlap with the 1σ OSL ages (Fig. 9b), and ages from each terrace level cluster and have little overlap with ages from other terraces (Fig. 10). In our dataset, only two of the 46 OSL ages were not in stratigraphic order. One of the anomalous ages was a sample taken 14 m below a T3 terrace (in T4 alluvium) and had an age that was virtually the same as T4 alluvium at the surface (Table 2, LORV-47); however, this sample location lies within a well-formed scour channel. Though uncommon, channel depths >10 m have been recorded on modern braided rivers (e.g. Sambrook Smith et al., 2006), so it is possible this age is correct and represents the age of a deeply scoured braid channel (Fig. 11). A second age anomaly is from two samples taken from the same core, 4.65 and 7.85 m below the surface of a T3 terrace. These ages are inverted; the deeper sample age is 12.7 ± 0.6 ka (LORV-42), and the shallow sample age is 14.5 ± 0.7 ka (LORV 32). When considering the uncertainty these ages nearly overlap; so there may have been minor subaqueous slumping or some other post-depositional disturbance that juxtaposed slightly older sediments over younger ones.

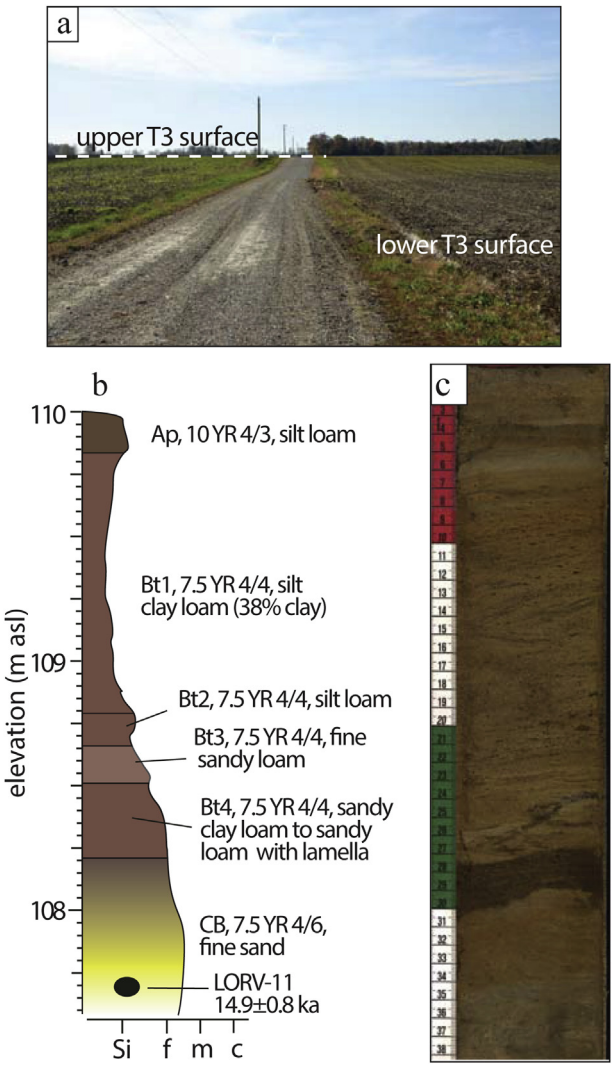

Fig. 7. (a) Photograph of the eroded, low-angle scarp separating the upper and lower T3 terraces. (b) Graphic sediment log of a core shallow core drilled on a T3 terrace (Si, f, m, and c = silt, fine, medium, and coarse sand, respectively). (c) Digital line-scan image of a T3 core; interval is 3.6–4.0 m below the land surface (color alternates every 10 cm in scale to the left).

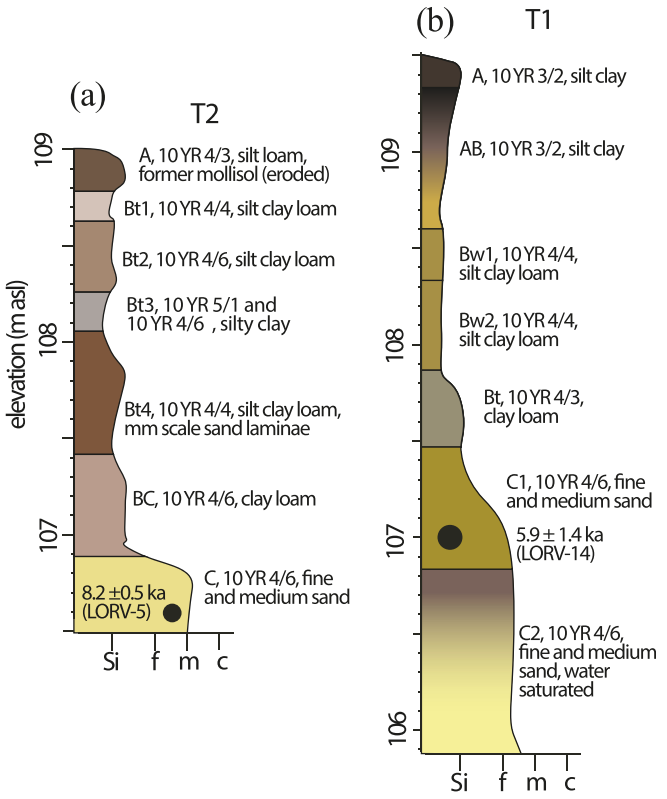

Fig. 8. (a) Graphic log showing stratigraphy and typical OSL sample depth (black circle) from a shallow core drilled on a T2 terrace (note that the T2 surface has been eroded). (b) Graphic log showing typical stratigraphy and OSL sample depth from a shallow core drilled on a T1 terrace (Si, f, m, and c = silt, fine, medium, coarse sand, respectively).

5. Discussion

5.1. OSL chronology and fluvial responses

The chronostratigraphic framework developed from OSL and radiocarbon dating identifies four major phases of aggradation and incision over the past ~110 ka (Fig. 12). Deposits and landforms from the LGM and younger are abundant in the lower Ohio valley, and most of our OSL ages are for these deposits. Older deposits (T7-T5) have been extensively eroded or are deeply buried, making them difficult to sample for OSL dating, with only ~10% of our samples representing these deposits.

5.1.1. Pre T7 history

Coring data from this study and from online databases at the Indiana and Kentucky Geological Surveys show that the study area has a flat bedrock floor with benches at 90 and 75 m asl that are overlain by up to 50 m of alluvium (Fig. 13a). The bedrock valley was deeply incised after the Ohio River captured the much larger Teays River, when early Pleistocene continental ice sheets blocked the Teays River valley and forced water into the headwaters of the Ohio River (Fowke, 1925; Melhorn and Kempton, 1991). Cosmogenic burial ages of sediments deposited in Mammoth Cave in Kentucky indicate that this capture occurred ~1.4 Ma, when the Green River, a tributary of the Ohio River, responded to the stream capture by rapidly incising ~15 m into bedrock (Granger et al., 2001).

5.1.2. T7 alluvium

Several properties of T7 alluvium indicate it is an MIS 6 (Illinoian) or older deposit. T7 alluvium was the deepest nonlithified unit in the fluvial stratigraphy, directly overlying bedrock. T7 alluvium includes much larger clasts than the younger overlying alluvium, suggesting it was deposited under higher energy conditions, its source area was closer, or both. The latter interpretation is supported by the presence of several misfit streams in the study area with headwaters near the MIS 6 ice margin (Counts and Monaghan, 2014), located ~30 km to the north (Fuller and Ashley, 1902; Fuller and Clapp, 1904), which indicates there was a source of outwash proximal to the study area during MIS 6. Additionally, T7 alluvium is severely weathered and highly compacted compared to MIS 2 alluvium (Fraser, 1986; Fraser and Fishbaugh, 1986; Moore et al., 2007), which also suggests it is older, pre-Wisconsinan alluvium (Fig. 11b). Whether T7 could be MIS 6 outwash or is older alluvium could not be determined (Fig. 13b). Regardless of its age, T7 alluvium is thin (1–5 m thick), which suggests there was significant erosion if it is alluvium that was deposited prior to or during MIS 6 (Fig. 13c).

5.1.3. T6 alluvium

The 114 ± 11.5 ka age of T6 alluvium, based on a single OSL age, spans from the end of MIS 6 to MIS 5d. The southern limit of ice

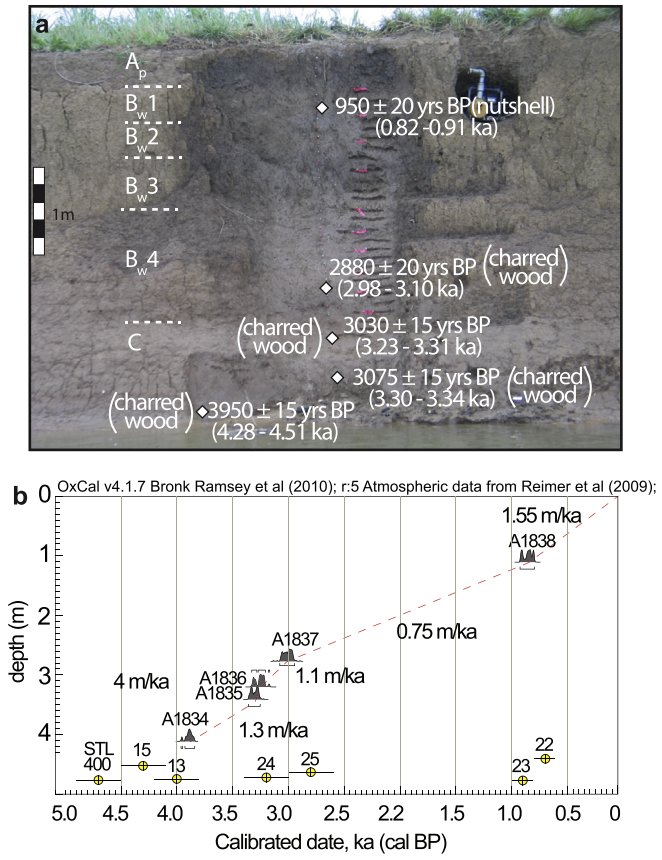

Fig. 9. (a) Natural exposure of T0 alluvium with ^{14}C ages (2 sigma) reported in radiocarbon years. Terrace has very weak soil development and is primarily silt loam and silt. (b) Aggradation rates at this site, calculated using calibrated radiocarbon ages, show rapid aggradation occurred between ~4 ka and 3 ka. OSL ages for T0 alluvium at other locations (yellow circles with LORV sample number above them) are consistent with calibrated radiocarbon ages. (For interpretation of the references to color in this figure legend, the reader is referred to the web version of this article.)

margins and marine oxygen isotope stratigraphy indicate that glaciation was more extensive during MIS 6 than during MIS 2 (Lisiecki and Raymo, 2005), so the original thickness of MIS 6 outwash should be comparable to that for MIS 2. However, the combined thickness of T6 and T7 alluvium was less than 10 m where observed, much thinner than the MIS 2 alluvium. The OSL age of T6 alluvium, the presence of clasts from the Canadian Shield, and the reduced thickness suggest that T6 alluvium represents MIS 6 outwash that was reworked at the beginning of the Last Interglacial.

Though much of the MIS 6 alluvium appears to be missing from borings in the main valley where preservation potential is low, the amount of MIS 6 aggradation can be estimated by examining sediments in tributary valleys adjacent to the main valley. The Last Interglacial (Sangamon) paleosol, a diagnostic marker horizon in the American Midwest that developed on MIS 6 deposits during MIS 5 (Ruhe et al., 1974), is preserved in many Ohio River tributary valleys (Counts and Martin, 2004a, 2004b; Counts, 2006, 2007, 2008a, 2008b) and can be used as a proxy of minimum MIS 6 aggradation. In cores the Sangamon (Last Interglacial) paleosol is typically characterized by bioturbated, yellowish brown (5Y hue), clay-rich, gleyed horizons with well-developed soil structure. In the Highland Creek tributary in Union County, Kentucky, at the edge of the main valley (Fig. 2), the Last Interglacial (Sangamon) paleosol was present ~8 m below the modern floodplain (~18 m above the T7 alluvium). This stratigraphic position suggests that at least 18 m of MIS 6 alluvium were eroded from the main valley before T6 alluvium was deposited/reworked at the end of MIS 5e (Fig. 13c).

There were no other MIS 5 aged sediments identified within the study area, suggesting these deposits were eroded or there was no deposition during MIS 5. Similarly, lacking any MIS 4 sediments or landforms, how the Ohio River responded to MIS 4 climate is unknown. Though the field area lies within one of the widest reaches of the Ohio River valley, it is relatively narrow compared to the Mississippi River valley, and the older sediments may have been scoured during extreme flood events, thus limiting the preservation of older and deeper sediments.

5.1.4. T5 alluvium

The stratigraphic position of T5 alluvium (10 m above T6 alluvium) and OSL ages of ~38 ka suggest there was a considerable period of aggradation before the beginning of the LGM (Fig. 13d). The T5 alluvium may be outwash deposited during an MIS 4 ice advance that was reworked during MIS 3, or could correspond to aggradation during an MIS 3 ice advance. The latter interpretation is supported by evidence from other studies. OSL dating of proglacial lake sediments in a cave in central Indiana suggests there was an MIS 3 ice margin near the cave (Wood et al., 2010), and at least two Ohio River tributary valleys within the study area experienced significant aggradation during MIS 3 (Woodfield, 1998; Counts and Monaghan, 2014). The interpretation of an MIS 3 ice advance is also supported by the ubiquitous presence of the Roxana Silt in the lower Ohio valley (Ray, 1957, 1963, 1965; Johnson, 1965; Ruhe and Olson, 1978, 1980), a time transgressive loess sheet deposited from ~60 to ~30 ka (Leigh and Knox, 1992; Rodbell et al., 1997; Markewich et al., 1998; Forman and Pierson, 2002), and by the presence of MIS 3-aged braided channel belts in the lower Mississippi River valley (Rittenour et al., 2005, 2007).

5.1.5. T4 alluvium

The oldest T4 alluvium (LORV-48) present in the study area (~29 ka), was ~12 m lower in the landscape than the older T5 alluvium (Figs. 1, 9 and 103e). This suggests there was a significant pulse of incision that removed T5 alluvium from the main valley at the end of MIS 3 and before the Laurentide ice sheet first advanced into the upper Ohio River basin (e.g. Clark et al., 1993; Szabo et al., 2011).

Table 4
Radiocarbon analyses for samples collected from a natural exposure of a T0 terrace.[a]

ISGS#	Sample#	Material	$\delta^{13}C$	Fraction of MC	±	D[a]4C	±	^{14}C yr BP[b]	±	Calibrated age ka[c]
A1834	858.203	Wood	−24.6	0.6397	0.0012	−360.3	1.2	3950	15	4278–4512
A1835	858.202	Wood	−24.2	0.6821	0.0012	−317.9	1.2	3075	15	3277–3340
A1836	858.201	Wood	−25.1	0.6856	0.0012	−314.4	1.2	3030	15	3227–3309
A1837	858.2	Wood	−25	0.6987	0.0015	−301.3	1.5	2880	20	2977–3050
A1838	858.062	Nutshell	−24.3	0.8885	0.1117	−111.5	1.7	950	20	824–912

[a] Profile Location: N 4194879.25 m, E 472897.35 m (UTM Zone 16, WGS 84 Datum).
[b] The half-life of 5730 is used for the age calculation, reported as years BP.
[c] Calibrated with OxCal v4.1.7, r5 (Bronk Ramsey et al., 2010). Atmospheric data from Reimer et al. (2009).

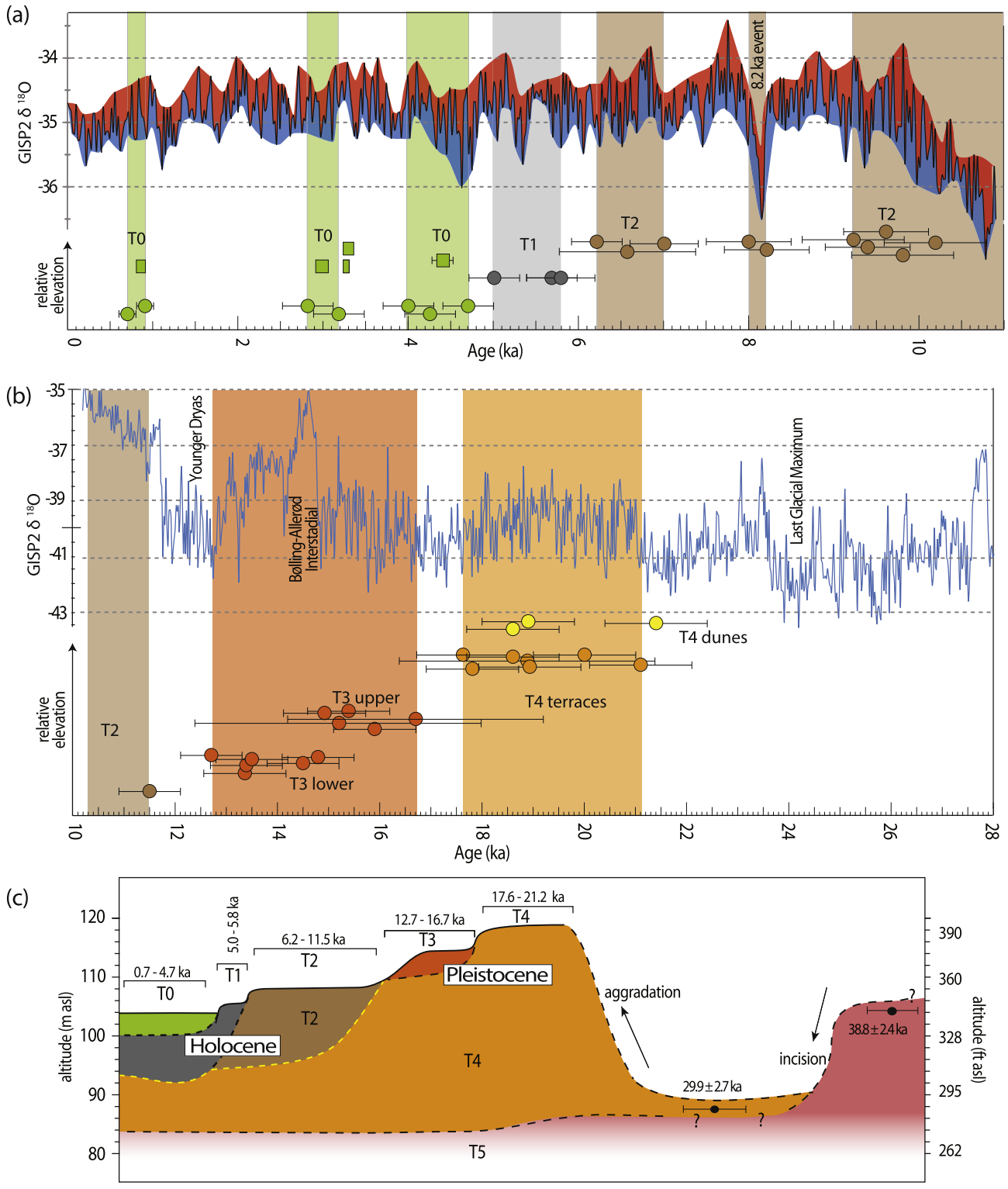

Fig. 10. (a) Distribution of OSL (circles) and radiocarbon (squares) ages for Holocene terraces compared to the GISP2 $\delta^{18}O$ ice core record (from Stuiver et al., 1997). (b) Distribution of OSL ages for late Pleistocene terraces compared to the GISP2 $\delta^{18}O$ ice core record (from Stuiver et al., 1997). The vertical colored bars in (a) and (b) show where terrace ages cluster for each terrace level. The apparent synchronicity between terrace ages and changes in climate suggests the lower Ohio River responds rapidly to both warming and cooling transitions. (c) Schematic diagram showing the aggradation and incision history of the lower Ohio River for the past ~40 ka, based upon the stratigraphic position and OSL ages of deposits and terraces.

5.1.6. T4 terraces

The timing of maximum advance of the Laurentide ice sheet into the Great Miami River valley (southwest Ohio), which is the nearest source of meltwater input to the study area, was defined by Lowell et al. (1990) at ~23.5 ka (19,670 ± 68 ^{14}C yrs BP). This is somewhat younger than the oldest T4 terrace age of 21.4 ± 1.0 ka (Fig. 13e). However, terrace ages are based on the age of sand-rich alluvium below the surface soil and are therefore minimum ages, so the

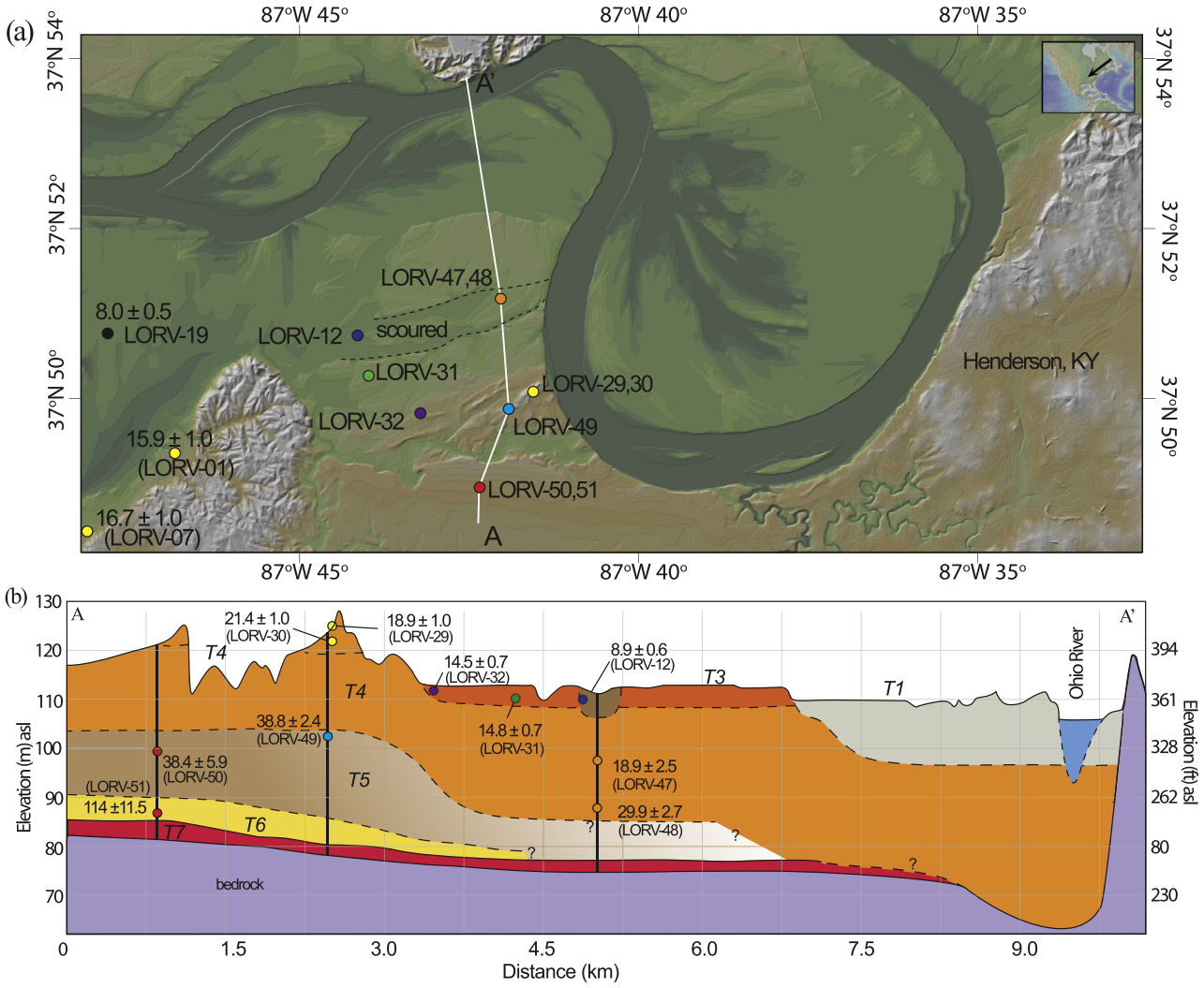

Fig. 11. (a) DEM of part of the lower Ohio River valley ~10 km west of Henderson, KY, showing sample sites, ages, and cross-section location (location shown on Fig. 2). (b) Cross-section showing chronostratigraphy of T4 to T2 terraces. Samples LORV 29-32 and 11 were projected onto the cross section.

formation of the T4 terrace appears to coincide with the LGM. There was as much as 35 m of fluvial aggradation in the valley in the period from ~30 ka up to the LGM (Fig. 13e).

5.1.7. T4 and T3 fill-cut terraces

The Ohio River incised the LGM outwash as the Laurentide ice retreated, likely in response to a variety of factors including larger discharges from melting ice and a reduction in sediment supply caused by recovering vegetative growth (e.g. Smith, 1976; Meade et al., 1990; Bull, 1991; Saucier, 1994). The incision was not continuous; a series of fill-cut terraces were formed in the LGM outwash (Fig. 13f). Fill-cut terrace ages are 21.2 ± 1.0 to 18.6 ± 0.9 ka for T4, 16.7 ± 1.0 to 14.5 ± 0.7 ka for the upper T3 terrace, and 13.5 ± 0.3 ka to 12.7 ± 0.6 ka for the lower T3 terrace (Fig. 10b). Relict braid-bar morphology is preserved on the surfaces of T4 and upper T3 terraces, though lower T3 terrace surfaces transition to an anastomosing pattern, suggesting there was a significant flow regime shift at ~14.5 ka. The timing of terrace formation generally corresponds to millennial-scale climate fluctuations shown in the Greenland Ice Sheet Project Two (GISP2) core record (Fig. 10a–b).

5.1.8. T2- T0 terraces

The terrace surface morphology changed to a meandering pattern for T2 terraces, showing a shift from an anastomosing to a meandering flow regime. This change, indicated by the 11.5 ± 0.6 ka age of the oldest T2 terrace, shows that the change in fluvial regime took place at the beginning of the Holocene. The sedimentology/geomorphology and OSL ages indicate meandering persisted until ~6.2 ± 0.3 ka (Fig. 13g). The Ohio River incised ~1 m into the T2 terrace after 6.2 ± 0.3 ka, forming the T1 terrace (Fig. 13h). After the T1 terrace formed (5.8 ± 0.4 to 5.0 ± 0.3 ka), the Ohio River incised at least 4 m into the T1 terrace. The timing of this incision corresponds to a major shift in climate during the mid-Holocene (e.g. Dorale et al., 1998; Steig, 1999; Mayewski et al., 2004). This climatic shift has also been recognized in the dune deposits/landforms on the Great Plains (Dean et al., 1996; Forman et al., 2001; Miao et al., 2007), in major changes in the pollen record reflecting vegetation changes in the eastern United States (Jackson et al., 2000; Foster et al., 2006), and in foreland basins of the Appalachian Mountains, recorded by abrupt shifts in $\delta^{13}C$ in soil organic matter (Driese et al., 2008) and rapid shifts in floodplain sedimentation rates (Driese et al., 2005, 2008).

Aggradation began in the study area ~1 ka after the T1 terrace was incised (Fig. 13i). Aggradation also began at about this time downstream (Alexander and Prior, 1971) and upstream (De Rego, 2012) of the study area, suggesting the aggradation was an allogenic response to changing climate and not autogenic processes. The timing of this aggradation, ~4 ka, may reflect drought in the

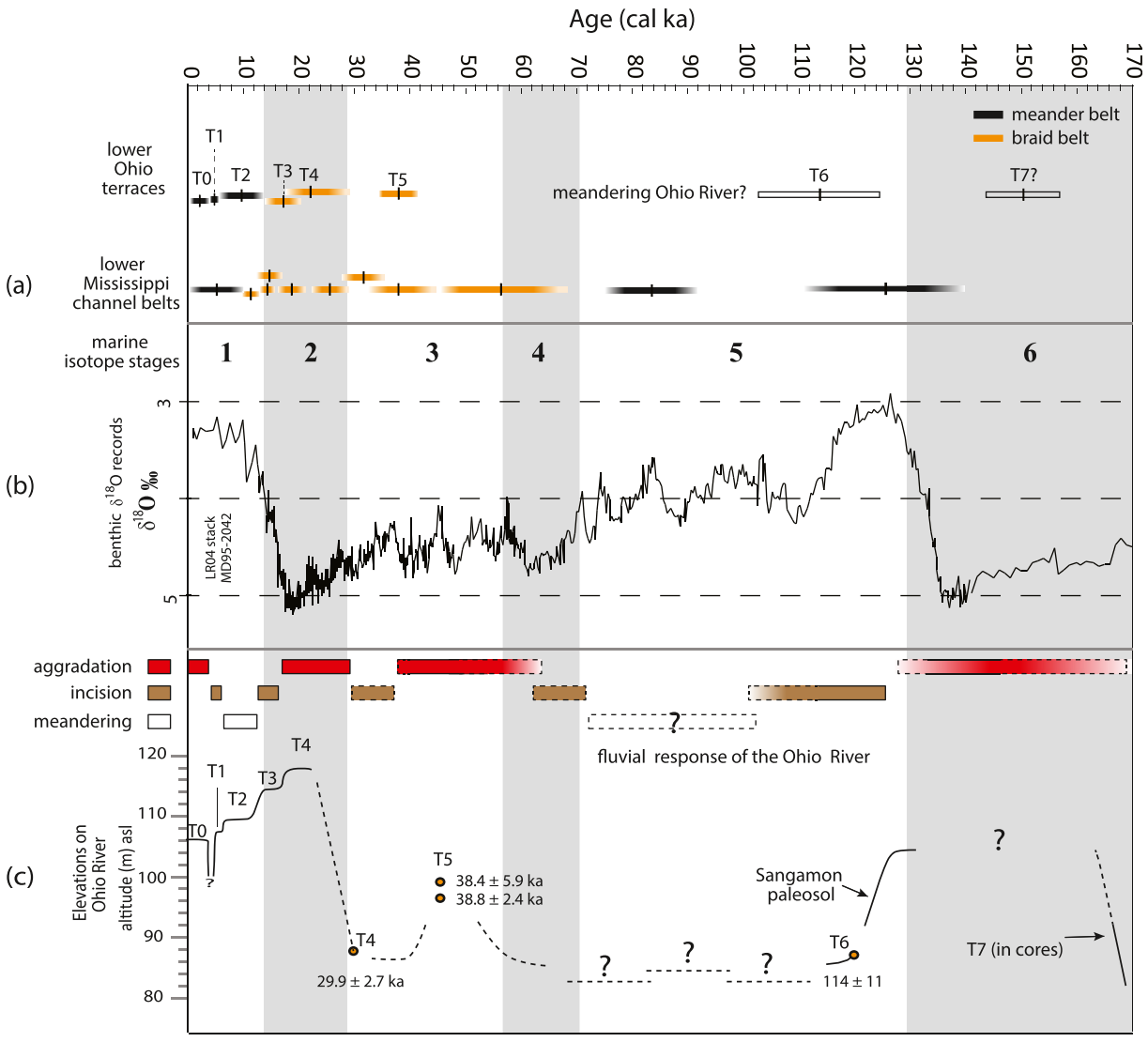

Fig. 12. Comparison of Ohio River terrace chronology to the Mississippi fluvial system and to marine and terrestrial proxy records of climate change. (a) The channel belt chronology of the Mississippi River (from Rittenour et al., 2007; Shen et al., 2012). (b) Benthic $\delta^{18}O$ foram record (Lisiecki and Raymo, 2005). (c) A fluvial response model for the lower Ohio River valley. Our chronostratigraphic framework, developed from cores and OSL dating, indicates phases of aggradation and incision are climatically modulated.

midcontinental United States (e.g. Booth et al., 2005) or possibly global cooling that initiated the expansion of many mountain glaciers during the Neoglaciation (e.g. Wanner et al., 2008). Since ~4 ka, there has been 4 m of vertical aggradation in the study area, with aggradation rates ranging from 0.75 m/ka to 4 m/ka over this time interval (Fig. 9b).

5.2. Comparisons of the Ohio River and the lower Mississippi River valley

The timing and nature of fluvial adjustments of the Mississippi and Ohio Rivers are similar but not identical (Fig. 12a). Pre-MIS 6 and Last Interglacial OSL ages (MIS7, MIS5e, and MIS5a) of multiple meander belt packages preserved along the margins of the Mississippi valley, known as the Prairie Complex, indicate the Mississippi River was a meandering system during the last two interglacial periods (Rittenour et al., 2007; Shen et al., 2012). The only Last Interglacial age from the lower Ohio River valley (MIS 5e) was deeply buried, but it is reasonable to assume the Ohio River also meandered during interglacials. Aggradation began in the Mississippi River valley near the end of MIS 4 in response to ice advancement into the Mississippi basin (Rittenour et al., 2007), but no evidence of aggradation during MIS 4 was found within the Ohio River valley. Aggradation continued in the Mississippi valley through the middle of MIS 3, and the Melville Ridge braid belts (42 ± 3 to 35 ± 3 ka) in the Mississippi valley are similar in age to Ohio River T6 alluvium (38.8 ± 2.4 ka) and implies the rivers were responding synchronously to environmental conditions by the middle of MIS 3.

The oldest T4 alluvium in the Ohio Valley, deposited at the end of MIS 3 (29.9 ± 2.7 ka) is contemporaneous with the Ash Hill braid belt in the Mississippi valley (27 ± 2 ka to 25 ± 2 ka). Following MIS 3, the fluvial responses in the Mississippi and Ohio valleys were largely synchronous. The T4 terraces (20.0 ± 1.0 to 17.6 ± 0.9 ka), upper T3 terraces (16.7 ± 1.0 to 15.4 ± 0.8 ka), and lower T3 terraces (14.8 ± 0.7 to 12.7 ± 0.6 ka) of the Ohio River are contemporaneous with the Sikeston braid belt (19.7 ± 1.6 to 17.8 ± 1.3 ka), the Kennett braid belt (16.1 ± 1.2 to 14.4 ± 1.1 ka), and the Brownfield and Blodgett braid belts (14.1 ± 1.0 to 13.0 ± 0.9 ka) of the Mississippi River (Rittenour et al., 2007). The Ohio and Mississippi Rivers also

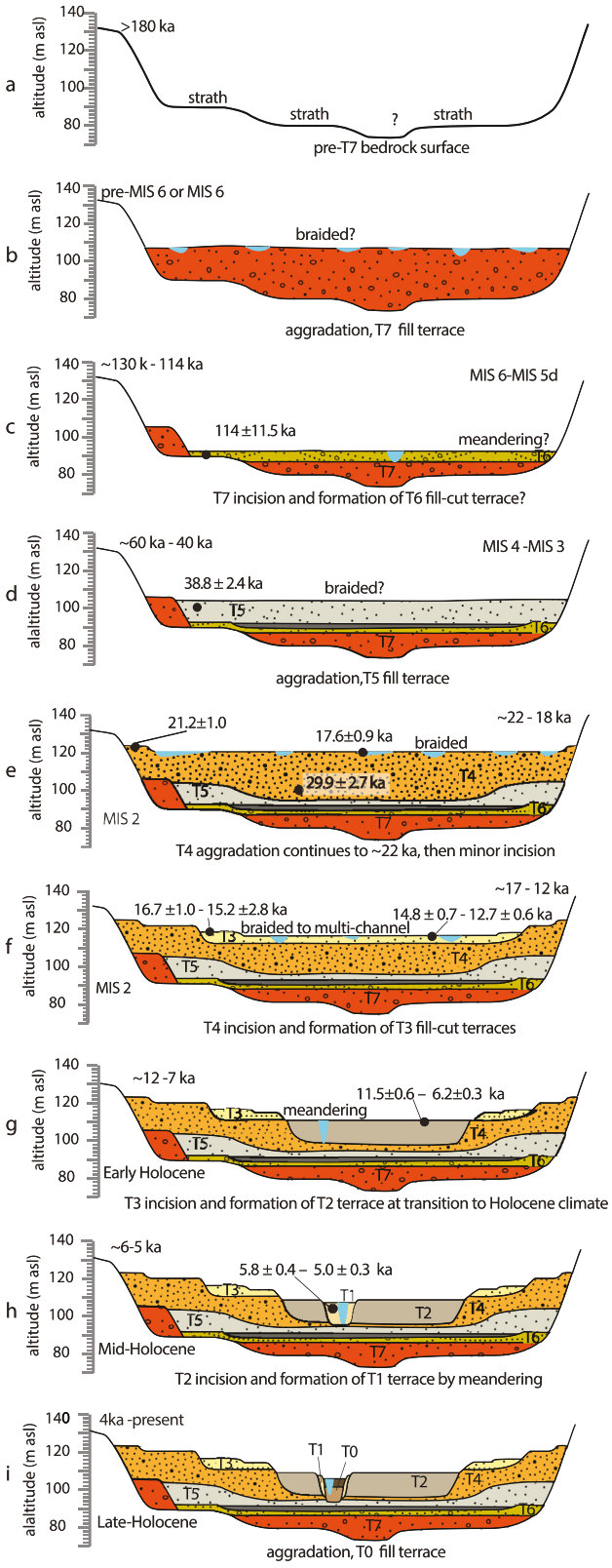

Fig. 13. Fluvial evolution of the Ohio River over the past ~160 ka. (a) Pre-T7 bedrock surface. (b) Aggradation, T7 fill terrace. (c) T7 incision and formation of T6 fill-cut terrace. (d) Aggradation, T5 fill terrace. (e) T4 aggradation continues to ~22 ka, then minor incision. (f) T4 incision and formation of T3 fill-cut terraces. (g) T3 incision and formation of T2 terrace at transition to Holocene climate. (h) T2 incision and formation of T1 terrace by meandering. (i) Aggradation, T0 fill terrace.

shifted from braided to meandering flow regimes at nearly the same time; after 11.3 ± 0.9 ka on the Mississippi River and by 11.5 ± 0.6 ka on the Ohio River (Fig. 12a).

Fluvial responses of the Ohio and Mississippi Rivers are expected to be largely synchronous because of similar climatic and glacial–hydrological forcing. Both rivers drain basins in the eastern United States that were covered by the Laurentide ice sheet. Additionally, the course of the modern Mississippi River, from Cairo, Illinois, to Memphis, Tennessee, was formerly occupied by the Ohio River until the Mississippi River was diverted through Thebes Gap ~12 ka (Rittenour et al., 2007) so some of the chronostratigraphies developed for the Mississippi valley are likely ages for lower Ohio River deposits.

6. Conclusions

The lower Ohio River valley is a terraced fluvial landscape that has been profoundly influenced by changes in hydrological flow regimes associated with late Pleistocene and Holocene climate changes. The application of OSL and radiocarbon dating combined with geologic mapping has allowed us to develop a detailed chronology of aggradation, terrace formation, and incision in the valley for the past ~110 ka that provides new insights into the evolution of the lower Ohio River valley.

Sediments from three major episodes of aggradation and incision are preserved in the valley. The basal T7 alluvium is typically severely weathered cobble gravel found in the deepest parts of the valley, and was deposited prior to or during the penultimate (MIS 6) glaciation. T6 sediments were deposited or reworked during the Last Interglacial (MIS 5e; Sangamon Interglacial) and are the oldest dated deposits in the valley. The presence of the Last Interglacial (Sangamon) paleosol on the valley margins (Figs. S13 and S14), ~18 m higher than the T6 alluvium, suggests that most if not all of the MIS 6 alluvium was scoured from the valley by the end of MIS 5e. There was no fluvial record identified in the main valley between MIS 5e and the middle of MIS 3. The stratigraphic positions and OSL ages (38.8 ± 2.4 ka and 38.4 ± 5.9 ka) for the T5 alluvium suggest that 10–14 m of aggradation occurred during MIS 3, or possibly during MIS 4 and was reworked during MIS 3. Whether the aggradation of T5 deposits began during MIS 4 and persisted through MIS 3, as was the case in the Mississippi valley, or if aggradation began during MIS 3 could not be conclusively resolved. Regardless of the precise timing, the aggradation of T5 alluvium is contemporaneous with aggradation in the Mississippi Valley and suggests there was active Laurentide ice in the Ohio River drainage basin sometime during the mid-Last Glacial (mid-Wisconsinan).

OSL ages of the highest fill terraces (T4) show that maximum aggradation occurred by 22.3 ± 4.7 ka, which is nearly synchronous with the maximum extent of the Laurentide Ice Sheet. The ages of T4 and T3 fill-cut terraces decrease as elevation decreases (Fig. 10a–b and Fig. S15 in supplementary data), indicating there was progressive incision as the Ohio River adjusted to fluxes in sediment load and discharge. The surface morphology of T4 and upper T3 terraces indicates the Ohio River had a braided channel pattern that changed to anastomosing by ~14.5 ka. There was 2–3 m of incision into the lower T3 terrace level from ~13.5 ± 0.8 ka to 12.7 ± 0.6 ka, and by 11.5 ± 0.6 ka the Ohio River began meandering and formed the T2 terrace level at the beginning of the Holocene. There was a relatively long period of stability and meandering from 11.5 ± 0.6 to 6.2 ± 0.3 ka, after which there was ~1 m of incision and the formation of the T1 terrace. The T1 terrace persisted until ~5.0 ± 0.3 ka, after which there was nearly 5 m of incision, likely in response to significant changes in the Holocene climate of North America. The Ohio River has aggraded at least 4 m since ~4 ka, averaging 1 m of aggradation per 1000 years.

Fluvial terraces and deeply buried alluvium are valuable archives for reconstructing paleoenvironmental changes, particularly in settings that link glaciated areas, where landforms and sediments from older glaciations are commonly eroded, to non-glaciated basins. The chronostratigraphic framework developed for Ohio River alluvium shows that the lower Ohio River has experienced multiple, large-amplitude cycles of aggradation and incision since MIS 6. Significant aggradation occurred during Last Glacial (Wisconsinan) glacial advances, and the OSL ages of late Pleistocene terraces appear to correspond to transitions from cooler intervals to warmer intervals (Fig. 10b). Similarly, the incision and formation of Holocene terraces appear to occur during changes in Holocene climate (Fig. 10a). This apparent synchronicity suggests that the Ohio River rapidly responded to glacial–interglacial transitions as well as changes in Holocene climate, and suggests the terrestrial fluvial record of the lower Ohio River valley is a viable proxy record of paleoenvironmental and climatic changes for the midcontinental United States.

Although a high degree of preservation along this relatively small reach of the Ohio River enabled us to construct a detailed terrace chronology, missing sediments from most of MIS 5 and all of MIS 4 make the record incomplete. Additional work in other areas, such as the abandoned Ohio River course through the Cache Valley in southern Illinois, downstream where the valley widens as it approaches the Mississippi Embayment, or the many tributary valleys may reveal additional insights to the late Pleistocene and Holocene history of the lower Ohio River.

Acknowledgments

This research was supported by multiple funding sources, including the U.S. Geological Survey's National Cooperative Geologic Mapping Program (STATEMAP and FEDMAP awards 03HQPA003, 04HQPA003, 05HQAG0007, 06HQAG0003, 07HQAG0062, 08HQPA0003, 09HQPA0003, and 11HQPA003), the U.S. Geological Survey's National Earthquakes Hazard Reduction Program (awards 06HQGR0192, 07HGGR0052, and G11AP20011), the Kentucky Geological Survey, and the University of Cincinnati. We thank Matt McCauley and Steve Neyhouse from the National Resource Conservation Service, Scott Waninger and Amy Bleithcroft from the Kentucky Geological Survey, and William Monaghan from the Indiana Geological Survey for help with coring and field mapping. We also thank Kristina Brady and Amy Myrbo from the Limnological Research Center, where some of the cores from this study were processed. We appreciate and acknowledge Kevin Kincare and an anonymous reviewer, whose comments and suggestions improved the quality of this manuscript. Any use of trade, product, or firm names is for descriptive purposes only and does not imply endorsement by the U.S. Government.

Appendix A. Supplementary data

Supplementary data related to this article can be found at http://dx.doi.org/10.1016/j.quascirev.2014.11.011.

References

Adamiec, G., Aitken, M., 1998. Dose rate conversion factors: update. Anc. TL 16, 37–49.
Aitken, M.J., 1998. An Introduction to Optical Dating: the Dating of Quaternary Sediments by the Use of Photon-stimulated Luminescence. Oxford University Press, Oxford, UK, p. 280.
Alexander, C.S., 1974. Some Observations on the Late Pleistocene and Holocene History of the Lower Ohio Valley, vol. 7. Occasional Publications of the University of Illinois Department of Geography.
Alexander, C.S., Prior, J.C., 1971. Holocene sedimentation rates in overbank deposits in the Black Bottom of the lower Ohio River, southern Illinois. Am. J. Sci. 270, 361–372.
Alexander, C.S., Nelson, R.N., 1972. Channel stability on the lower Ohio River. Ann. Assoc. Am. Geogr. 62, 411–417.
Bevington, P.R., Robinson, D.K., 2002. Data Reduction and Error Analysis for the Physical Sciences, third ed. McGraw-Hill Education, New York.
Blum, M.D., 2007. Large river systems and climate change. In: Gupta, A. (Ed.), Large Rivers: Geomorphology and Management. John Wiley & Sons, West Sussex, England, pp. 627–659.
Bodziak, R.M., 1999. High Resolution Seismic Reflection and Ground Penetrating Radar Studies across the Maunie Fault in the Wabash Valley Seismic Zone (unpublished MS thesis). Southern Illinois University, p. 175.
Booth, R.K., Jackson, S.T., Forman, S.L., Kutzbach, J.E., Bettis, E.A., Kreigs, J., Wright, D.K., 2005. A severe centennial-scale drought in midcontinental North America 4200 years ago and apparent global linkages. Holocene 15, 321–328.
Bronk Ramsey, C., 1995. Radiocarbon calibration and analysis of stratigraphy: the OxCal program. Radiocarbon 37, 425–430.
Bronk Ramsey, C., 2008. Deposition models for chronological records. Quat. Sci. Rev. 27, 42–60.
Bronk Ramsey, C., Dee, M., Lee, S., Nakagawa, T., Staff, R., 2010. Developments in the calibration and modeling of radiocarbon dates. Radiocarbon 52 (3), 953–961.
Bull, W.B., 1991. Geomorphic Responses to Climatic Change. Oxford University Press, New York, p. 326.
Clark, P.U., Clague, J.J., Curry, B.B., Dreimanis, A., Hicock, S.R., Miller, G.H., Berger, G.W., Eyles, N., Lamothe, M., Miller, B.B., Mott, R.J., Oldale, R.N., Stea, R.R., Szabo, J.P., Thorleifson, L.H., Vincent, J.S., 1993. Initiation and development of the Laurentide and Cordilleran ice sheets following the last interglaciation. Quat. Sci. Rev. 12, 79–114.
Counts, R.C., Martin, S.L., 2004a. Surficial Geology of the Henderson Quadrangle, Henderson County, Kentucky. In: Kentucky Geological Survey Draft Geologic Quadrangle, Map and Chart Series XII, 1:24,000 Scale.
Counts, Ronald C., Martin, Steven L., 2004b. Surficial Geology of the Wilson Quadrangle, Henderson County, Kentucky. In: Kentucky Geological Survey Draft Geologic Quadrangle, Map and Chart Series XII, 1:24,000 Scale.
Counts, R.C., 2006. Surficial Geology of the Smith Mills Quadrangle, Henderson County, Kentucky. In: Kentucky Geological Survey Draft Geologic Quadrangle, Map and Chart Series XII, 1:24,000 Scale.
Counts, R.C., 2007. Surficial Geology of the Uniontown Quadrangle, Union and Henderson Counties, Kentucky. In: Kentucky Geological Survey Draft Geologic Quadrangle, Map and Chart Series XII, 1:24,000 Scale.
Counts, R.C., 2008a. Surficial Geology of the Beech Grove Quadrangle, Webster, Hopkins, and Mclean Counties, Kentucky. In: Kentucky Geological Survey Draft Geologic Quadrangle, Map and Chart Series XII, 1:24,000 Scale.
Counts, R.C., 2008b. Surficial Geology of the Calhoun Quadrangle, Mclean and Hopkins Counties, Kentucky. In: Kentucky Geological Survey Draft Geologic Quadrangle, Map and Chart Series XII, 1:24,000 Scale.
Counts, R.C., Wang, H., Grimley, D., Mahan, S., 2008. Luminescence and radiocarbon chronology of loess-paleosol sequences in the lower Ohio River valley. Geol. Soc. Am. Abstr. Progr. 40 (5), 3.
Counts, R.C., Monaghan, G.W., 2014. Quaternary geology and geoarchaeology of the lower Ohio River valley, southwestern Indiana. In: Guidebook for the 56th Midwest Friends of the Pleistocene Field Conference, p. 86.
Crittenden, M.D., Hose, R.K., 1965. Geology of the Rome Quadrangle in Kentucky. In: U.S. Geological Survey Geologic Quadrangle 362, Scale 1:24,000.
De Rego, Kathryn, 2012. Holocene Landscape Evolution of the Ohio River Valley from Knob Creek to Rosewood Bottom (unpublished M.S. thesis). Indiana State University, p. 193.
Dean, W.E., Ahlbrandt, T.S., Anderson, R.Y., Bradbury, J.P., 1996. Regional aridity in North America during the middle Holocene. Holocene 6, 145–155.
Dorale, J.A., Edwards, R.L., Ito, E., González, L.A., 1998. Climate and vegetation history of the midcontinent from 75 to 25 ka: a speleothem record from Crevice Cave, Missouri, USA. Science 282 (5395), 1871–1874.
Driese, S.G., Li, Z.-H., Horn, S.P., 2005. Late Pleistocene and Holocene climate and geomorphic histories as interpreted from a 23,000 14C yr B.P. paleosol and floodplain soils, southeastern West Virginia, USA. Quat. Res. 63, 136–149.
Driese, S.G., Li, Z.-H., McKay, L.D., 2008. Evidence for multiple, episodic, mid-Holocene Hypsithermal recorded in two soil profiles along an alluvial floodplain catena, southeastern Tennessee, USA. Quat. Res. 69, 276–291.
Duller, G.A.T., 1996. Recent developments in luminescence dating of Quaternary sediments. Prog. Phys. Geogr. 20, 127–145.
Duller, G.A.T., 2008. Luminescence Dating: Guidelines on Using Luminescence Dating in Archaeology. English Heritage, Swindon, p. 45.
Eggert, D.L., Woodfield, M.C., 1996. Geological Terrain Map of the Indiana Portion of the Newburgh Quadrangle, Indiana-Kentucky. Indiana Geological Survey Open-File Study 96–09, 3 plates.
Fenneman, N.M., 1928. Physiographic divisions of the United States. Ann. Assoc. Am. Geogr. 18, 261–353.
Forman, S.L., Oglesby, R., Webb, R.S., 2001. Temporal and spatial patterns of Holocene dune activity on the Great Plains of North America: megadroughts and climate links. Glob. Planet. Change 29, 1–29.
Forman, S.L., Pierson, J., 2002. Late Pleistocene luminescence chronology of loess deposition in the Missouri and Mississippi River valleys, United States. Palaeogeogr. Palaeoclimatol. Palaeoecol. 186, 25–46.
Foster, D.R., Oswald, W.W., Faison, E.K., Doughty, E.D., Hansen, B.C.S., 2006. A climatic driver for abrupt mid-Holocene vegetation dynamics and the Hemlock decline in New England. Ecology 87, 2959–2966.
Fowke, G., 1925. The genesis of the Ohio River. Proc. Indiana Acad. Sci. 34, 81–102.

Fraser, G.S., 1986. Origin of Mid-channel Islands in the Ohio River Near Evansville, Indiana. In: Indiana Geological Survey Special Report, 38, 15 p.
Fraser, G.S., 1994. Sequences and sequence boundaries in glacial sluiceways beyond glacial margins. In: Dalrymple, Robert W., Boyd, R., Zaitlin Brian, A. (Eds.), Incised-valley Systems; Origin and Sedimentary Sequences, SEPM Special Publication 51, pp. 337–351.
Fraser, G.S., Fishbaugh, D.A., 1986. Alluviation of the Ohio River Valley Near Evansville, Indiana and its Effect on the Distribution of Sand and Gravel in the Area. In: Indiana Geological Survey Special Report 36, 26 p.
Frye, J.C., Leonard, A., Willman, H., Glass, H., 1972. Geology and paleontology of Late Pleistocene Lake Saline, Southeastern Illinois. Ill. State Geol. Surv. Circ. 471, 44.
Fuller, M.L., Ashley, G.H., 1902. Ditney Folio, Indiana. In: U.S. Geological Survey Geologic Atlas of the United States, Folio 84.
Fuller, M.L., Clapp, F.G., 1904. Patoka Folio, Indiana-Illinois. In: U.S. Geological Survey Geologic Atlas of the United States, Folio 105.
Gibbons, A.B., 1972. Geologic Map of Parts of the Burlington and Addyston Quadrangles, Boone County, Kentucky. In: U.S. Geological Survey Geologic Quadrangle 1025, Scale 1:24,000.
Granger, D.E., Fabel, D., Palmer, A.N., 2001. Pliocene-Pleistocene incision of the Green River, Kentucky, determined from radioactive decay of cosmogenic ^{26}Al and ^{10}Be in Mammoth Cave sediments. Geol. Soc. Am. Bull. 113 (7), 825–836.
Grover, N.C., Mansfield, G.R., 1938. Floods of Ohio and Mississippi Rivers, January–February 1937. In: U.S. Geological Survey Water Supply Paper 838, p. 746.
Grün, R., 2009. The "AGE" program for the calculation of luminescence age estimates. Anc. TL 27, 45–46.
Hayward, R.K., Lowell, T.V., 1993. Variations in loess accumulation rates in the midcontinent, United States, as reflected by magnetic susceptibility. Geology 21 (9), 821–824.
Jackson, S.T., Overpeck, J.T., Webb- Iii, T., Keattch, S.E., Anderson, K.H., 1997. Mapped plant-macrofossil and pollen records of late Quaternary vegetation change in eastern North America. Quat. Sci. Rev. 16 (1), 1–70.
Jackson, S.T., Webb, R.S., Anderson, K.H., Overpeck, J.T., Webb III, T., Williams, J.W., Hansen, B.C.S., 2000. Vegetation and environment in eastern North America during the Last Glacial Maximum. Quat. Sci. Rev. 19 (6), 489–508.
Jain, M., Singhvi, A.K., 2001. Limits to depletion of blue-green light stimulated luminescence in feldspars: implications for quartz dating. Radiat. Meas. 33 (6), 883–892.
Johnson, G.H., 1965. The Stratigraphy, Paleontology, and Paleoecology of the Peoria Loess (Upper Pleistocene) of Southwestern Indiana (unpublished Doctoral thesis). Indiana University, Bloomington, IN, p. 400.
Johnson Jr., W.D., 1972. Geologic Map of the Newburgh and Yankeetown Quadrangles, Henderson and Daviess Counties, Kentucky. In: U.S. Geological Survey Geologic Quadrangle Map 1045, Scale 1:24,000.
Johnson Jr., W.D., 1973a. Geologic Map of Part of the Wilson Quadrangle, Henderson County, Kentucky. In: U.S. Geological Survey Geologic Quadrangle Map 1136, Scale 1:24,000.
Johnson Jr., W.D., 1973b. Geologic Map of Part of the Henderson Quadrangle, Henderson County, Kentucky. In: U.S. Geological Survey Geologic Quadrangle Map 1074, Scale 1:24,000.
Johnson Jr., W.D., Norris, R.L., 1974. Geologic Map of the Smith Mills Quadrangle, Henderson and Union Counties, Kentucky. In: U.S. Geological Survey Geologic Quadrangle Map 1215, Scale 1:24,000.
Johnson, W.D. Jr., 1974. Geologic map of the West Franklin, Caborn, and Mount Vernon Quadrangles, Henderson and Union Counties, Kentucky, U.S. Geological Survey Geologic Quadrangle Map 1152, Scale 1:24:000.
Johnson Jr., W.D., Schwalb, H., 2010. Geology and structure of the Rough Creek area, western Kentucky. Ky. Geol. Surv. Bull. 1, 139.
Kepferle, R.C., 1974. Geologic Map of Parts of the Louisville West and Lanesville Quadrangles, Jefferson County, Kentucky. In: U.S. Geological Survey Geologic Quadrangle Map 1202, Scale 1:24,000.
Kottek, M., Grieser, J., Beck, C., Rudolf, B., Rubel, F., 2006. World map of the Koppen-Geiger climate classification updated. Meteorol. Z. 15 (3), 259–263.
Kvale, E., Archer, A., 2007. Paleovalley fills: trunk vs. tributary. AAPG Bull. 91 (6), 809–821.
Leidy, J., 1856. Notice of some fossil bones discovered by Mr. Francis A. Lincke, in the banks of the Ohio River, Indiana. In: Proceedings of the Academy of Natural Sciences of Philadelphia, Filadélfia 7, pp. 199–201.
Leigh, D.S., Knox, J.C., 1992. AMS radiocarbon age of the Upper Mississippi Valley Roxana Silt. Quat. Res. 39, 282–289.
Leopold, L.B., Wolman, M.G., Miller, J.P., 1964. Fluvial Processes in Geomorphology. W.H. Freeman and Company, San Francisco and London, 535 p.
Leverett, F., 1902. Glacial Formations and Drainage Features of the Erie and Ohio Basins. In: U.S. Geological Survey Monograph 41, 802 p.
Liseicki, L.E., Raymo, M.E., 2005. A Pliocene-Pleistocene stack of 57 globally distributed benthic δ18O records. Palaeogeogr. Palaeoclimatol. Palaeoecol 20, PA1003.
Lowell, T.V., Savage, K.M., Brockman, C.S., Stuckenrath, R., 1990. Radiocarbon analyses from Cincinnati, Ohio, and their implications for glacial stratigraphic interpretations. Quat. Res. 34 (1), 1–11.
Luft, S.J., 1971. Geologic Map of Part of the Covington Quadrangle, Northern Kentucky. In: U.S. Geological Survey Geologic Quadrangle Map 955, Scale 1:24,000.
Maddy, D., Bridgland, D., Westaway, R., 2001. Uplift-driven valley incision and climate-controlled river terrace development in the Thames Valley, UK. Quat. Int. 79 (1), 23–36.
Maddy, D., Bridgland, D.R., Green, C.P., 2000. Crustal uplift in southern England: evidence from the river terrace records. Geomorphology 33, 167–181.
Markewich, H.W., Wysocki, D.A., Pavich, M.J., Rutledge, E.M., Millard, H.T., Rich, F.J., Maat, P.B., Rubin, M., McGeehin, J.P., 1998. Paleopedology plus TL, ^{10}Be, and ^{14}C dating as tools in stratigraphic and paleoclimatic investigations, Mississippi River valley, U.S.A. Quat. Int. 51–52, 143–167.
Mayewski, P.A., Rohling, E.E., Curt Stager, J., Karlén, W., Maasch, K.A., David Meeker, L., Meyerson, E.A., Gasse, F., van Kreveld, S., Holmgren, K., Lee-Thorp, J., Rosqvist, G., Rack, F., Staubwasser, M., Schneider, R.R., Steig, E.J., 2004. Holocene climate variability. Quat. Res. 62, 243–255.
McDowell, R.C., 1986. The Geology of Kentucky—a Text to Accompany the Geologic Map of Kentucky. U.S. Geological Survey Professional Paper 1151-H, p. 76.
Meade, R.H., Yuzyk, T.R., Day, T.J., 1990. Movement and storage of sediment in rivers of the United States and Canada in Surface Water Hydrology. Geological Society of America, Boulder, Colorado, pp. 255–280.
Melhorn, W.N., Kempton, J.P., 1991. The Teays system; a summary. In: Melhorn, W.N., Kempton, J.P. (Eds.), Geology and Hydrogeology of the Teays-Mahomet Bedrock Valley Systems, Geological Society of America Special Paper 258, pp. 125–128.
Miao, X., Mason, J.A., Johnson, W.C., Wang, H., 2007. High-resolution proxy record of Holocene climate from a loess section in southwestern Nebraska, USA. Palaeogeogr. Palaeoclimatol. Palaeoecol. 245, 368–381.
Moore, D.W., Newell, W.L., Counts, R.C., Fraser, G.S., Fishbaugh, D.A., Brandt, T.R., 2007. Surficial Geologic Map of the West Franklin Quadrangle, Vanderburgh and Posey Counties, Indiana, and Henderson County, Kentucky. In: U.S. Geological Survey Scientific Investigations Map 2967, Scale 1:24,000.
Moore, D.W., Lundstrom, S.C., Counts, R.C., Martin, S.L., Andrews Jr., W.M., Newell, W.L., Murphy, M.L., Thompson, M.F., Taylor, E.M., Kvale, E.P., Brandt, T.R., 2009. Surficial Geologic Map of the Evansville, Indiana, and Henderson, Kentucky Area. In: U.S. Geological Survey Scientific Investigations Map 3069, Scale 1:50,000.
Murray, A.S., Wintle, A.G., 2000. Luminescence dating of quartz using an improved single-aliquot regenerative-dose protocol. Radiat. Meas. 32, 57–73.
NOAA-NCDC, 2014. 1981–2010 Climate Normals. National Climatic Data Center, National Oceanic and Atmospheric Administration. Available online at: http://www.ncdc.noaa.gov/data-access/land-based-station-data/land-based-datasets/climate-normals/1981-2010-normals-data.
Nelson, J.W., 1991. Structural Styles of the Illinois Basin. In: Leighton, M.W., Kolata, D.R., Oltz, D.F., Eidel, J.J. (Eds.), Interior Cratonic Basins, American Association of Petroleum Geologists Memoir 51, pp. 209–243.
Nuttli, O.W., 1979. Seismicity of the central United States. Eng. Geol. 4, 67–94.
Obermeier, S.F., Bleuer, N.R., Munson, C.A., Munson, P.J., Martin, W.S., McWilliams, K.M., Tabaczynski, D.A., Odum, J.K., Rubin, M., Eggert, D.L., 1991. Evidence of strong earthquake shaking in the Lower Wabash Valley from prehistoric liquefaction features. Science 251 (4997), 1061–1063.
Owen, D.D., 1861. Fourth Report of the Geological Survey in Kentucky, Made during the Years 1858 and 1859. Yeoman Office, Frankfort, KY, p. 617.
Owen, D.D., 1859. Report of a Geological Reconnaissance of the State of Indiana, Made in the Year 1837 [-1838], in Conformity to an Order of the Legislature. Indianapolis, IN, p. 71.
Porat, N., 2006. Use of magnetic separation for purifying quartz for luminescence dating. Anc. TL 24, 33–36.
Prescott, J.R., Hutton, J.T., 1994. Cosmic ray contributions to dose rates for luminescence and ESR dating: large depths and long-term time variations. Radiat. Meas. 23, 497–500.
Ray, L.L., 1957. Two significant new exposures of Pleistocene deposits along the Ohio River valley in Kentucky. J. Geol. 65, 542–545.
Ray, L.L., 1960. Significance of Loess Deposits along the Ohio River Valley. U.S. Geological Survey Professional Paper 400-B, p. 211.
Ray, L.L., 1963. Quaternary Events along the Unglaciated Lower Ohio River Valley. U.S. Geological Survey Professional Paper 475, pp. B125–B128.
Ray, L.L., 1965. Geomorphology and Quaternary Geology of the Owensboro Quadrangle, Indiana and Kentucky. U.S. Geological Survey Professional Paper 488, 72 p.
Ray, L.L., 1974. Geomorphology and Quaternary Geology of the Glaciated Ohio River Valley; a Reconnaissance Study. U.S. Geological Survey Professional Paper 876, 77 p.
Reimer, P.J., Baillie, M.G.L., Bard, E., Bayliss, A., Beck, J.W., Blackwell, P.G., Bronk Ramsey, C., Buck, C.E., Burr, G.S., Edwards, R.L., Friedrich, M., Grootes, P.M., Guilderson, T.P., Hajdas, I., Heaton, T.J., Hogg, A.G., Hughen, K.A., Kaiser, K.F., Kromer, B., McCormac, F.G., Manning, S.W., Reimer, R.W., Richards, D.A., Southon, J.R., Talamo, S., Turney, C.S.M., van der Plicht, J., Weyhenmeyer, C.E., 2009. IntCal09 and Marine09 radiocarbon age calibration curves, 0–50,000 years cal BP. Radiocarbon 51 (4), 1111–1150.
Rice, C.L., Sable, Edward G., Dever Jr., Garland R., Kehn, Thomas M., 1979. The Mississippian and Pennsylvanian (Carboniferous) Systems in the United States—Kentucky. U.S. Geological Survey Professional Paper 1110-F, 32 p.
Rittenour, T.M., Goble, R.J., Blum, M.D., 2003. An optical age chronology of Late Pleistocene fluvial deposits in the northern lower Mississippi valley. Quat. Sci. Rev. 22, 1105–1110.
Rittenour, T.M., Goble, R.J., Blum, M.D., 2005. An 85,000 yr OSL chronology for late Pleistocene channel belts in the lower Mississippi valley. Quat. Sci. Rev. 24, 2539–2554.
Rittenour, T.M., Blum, M.D., Goble, R.J., 2007. Fluvial evolution of the lower Mississippi River valley during the last 100-kyr glacial cycle: response to glaciation and sealevel change. Geol. Soc. Am. Bull. 119, 586–608.

Rodbell, D.T., Forman, S.L., Pierson, J., Lynn, W.C., 1997. Stratigraphy and chronology of Mississippi Valley loess in western Tennessee. Geol. Soc. Am. Bull. 109, 1134–1148.
Rodnight, H., 2008. How many equivalent dose values are needed to obtain a reproducible distribution? Anc. TL 26, 3–9.
Ruhe, R.V., Hall, R.D., Canepa, A.P., 1974. Sangamon paleosols of southwestern Indiana, U.S.A. Geoderma 12, 191–200.
Ruhe, R.V., Olson, C.G., 1980. Clay-mineral indicators of glacial and nonglacial sources of Wisconsinan loesses in southern Indiana, U.S.A. Geoderma 24, 283–297.
Ruhe, R.V., Olson, C.G., 1978. Loess stratigraphy and paleosols in southwest Indiana. In: Guidebook of the Midwestern Friends the Pleistocene 25th Field Conference, Indiana University Water Resources Research Center and Dept. of Geology, p. 72.
Rutledge, F.A., 2004. High Resolution Geophysical Investigation of Late Quaternary Deformation in the Lower Wabash Valley Fault System (unpublished M.S. thesis). University of Kentucky, 147 p.
Sambrook Smith, G.H., Ashworth, P.J., Best, J.L., Woodward, J., Simpson, C.J., 2006. The sedimentology and alluvial architecture of the sandy braided South Saskatchewan River, Canada. Sedimentology 53, 413–434.
Saucier, R.T., 1994. Geomorphology and Quaternary Geologic History of the Lower Mississippi Valley, vol. 1. U.S. Army Corps of Engineers Waterways Experiment Station, Vicksburg, MS, p. 364.
Schumm, S., Mosley, M., Weaver, W., 1987. Experimental Fluvial Geomorphology. Wiley, New York, p. 413.
Schumm, S.A., 1977. The Fluvial System. Wiley, New York, p. 338.
Shaw, E., 1911. Preliminary statement concerning a new system of Quaternary lakes in the Mississippi Basin. J. Geol. 19, 481–491.
Shaw, E.W., 1915. On the origin of loess in southwestern Indiana. Science 41 (1046), 104–108.
Shen, Z., Törnqvist, T., Autin, W.J., Zenon, R.P.M., Straub, K.M., Mauz, B., 2012. Rapid and widespread response of the Lower Mississippi River to eustatic forcing during the last glacial–interglacial cycle. GSA Bull. 124, 690–704.
Smith, D.G., 1976. Effect of vegetation on lateral migration of anastomosed channels of a glacier meltwater river. Geol. Soc. America Bull. 87, 857–860.
Smith III, M., 2007. A Geological and Geophysical Study of the Maunie Fault (unpublished MS thesis). Southern Illinois University at Carbondale, 158 p.
Snyder, S.L., Duval, J.S., 2003. Design and Construction of a Gamma-ray Spectrometer System for Determining Natural Radioelement Concentrations in Geological Samples at the U.S. Geological Survey in Reston, Virginia. U.S. Geological Survey Open File Report 03–029.
Steig, E.J., 1999. Mid-Holocene climate change. Science 286 (5444), 1485–1487.
Stokes, S., 1999. Luminescence dating applications in geomorphological research. Geomorphology 29, 153–171.
Straw, W.T., 1968. The upper alluvial terrace along the Ohio River valley in south-central Indiana. Proc. Indiana Acad. Sci. 77, 231–235.
Stuiver, M., Braziunas, T.F., Grootes, P.M., Zielinski, G.A., 1997. Is there evidence for solar forcing of climate in the GISP2 oxygen isotope record? Quat. Res. 48, 259–266.
Stuiver, M., Reimer, P.J., Bard, E., Beck, J.W., Burr, C., Hughen, K.A., Kromer, B., McCormac, G., Plicht, J., Spurk, M., 1998. INTCAL98 radiocarbon age calibration, 24,000-0 cal BP. Radiocarbon 40, 1041–1084.
Swadley, W.C., 1969. Geologic Map of Parts of the Patriot and Florence Quadrangles, North-central Kentucky. In: U.S. Geological Survey Geologic Quadrangle Map 873, Scale 1:24,000.
Swadley, W.C., 1976. Geologic Map of Part of the Carrollton Quadrangle, Carroll and Trimble Counties, Kentucky. In: U.S. Geological Survey Geologic Quadrangle Map 1281, Scale 1:24,000.
Szabo, J.P., Angle, M.P., Eddy, A.M., 2011. Pleistocene glaciation of Ohio, USA. In: Jürgen Ehlers, P.L.G., Philip, D.H. (Eds.), Quaternary Glaciations—extent and Chronology: a Closer Look, Developments in Quaternary Science 15. Elsevier, Amsterdam, pp. 513–520.
Theis, C.V., 1922. Geology of Henderson County, Kentucky (unpublished Doctoral thesis). University of Cincinnati, p. 215.
Tight, W.G., 1903. Drainage Modifications in Southeastern Ohio and Adjacent Parts of West Virginia and Kentucky. U.S. Geological Survey Professional Paper 13, 111 p.
Ver Steeg, K., 1946. The Teays River. Ohio Jour. Sci. 46, 297–307.
Walker, E.H., 1957. The Deep Channel and Alluvial Deposits of the Ohio Valley in Kentucky. U.S. Geological Survey Water-Supply Paper 1411, 25 p.
Wallinga, J., 2002. Optically stimulated luminescence dating of fluvial deposits: a review. Boreas 31, 303–322.
Wang, H., Hughes, R.E., Steele, J.D., Lepley, S.W., Tian, J., 2003. Correlation of climate cycles in middle Mississippi Valley loess and Greenland ice. Geology 31, 179–182.
Wang, H., Lundstrom, C.C., Zhang, Z., Grimley, D.A., Balsam, W.L., 2009. A mid-late Quaternary loess-paleosol record in Simmons Farm in southern Illinois, USA. Quat. Sci. Rev. 28, 93–106.
Wanner, H., Beer, J., Bütikofer, J., Crowley, T.J., Cubasch, U., Flückiger, J., Goosse, H., Grosjean, M., Joos, F., Kaplan, J.O., Küttel, M., Müller, S.A., Prentice, I.C., Solomina, O., Stocker, T.F., Tarasov, P., Wagner, M., Widmann, M., 2008. Mid- to late Holocene climate change: an overview. Quat. Sci. Rev. 27, 1791–1828.
Wayne, W., 1952. Pleistocene evolution of the Ohio and Wabash Valleys. J. Geology 60, 575–585.
Wilkins, G.R., Delcourt, P.A., Delcourt, H.R., Harrison, F.W., Turner, M.R., 1991. Paleoecology of central Kentucky since the last glacial maximum. Quat. Res. 36, 224–239.
Williams, J.W., 2003. Variations in tree cover in North America since the last glacial maximum. Glob. Planet. Change 35, 1–23.
Wintle, A.G., 2008. Luminescence dating: where it has been and where it is going. Boreas 37, 471–482.
Wintle, A.G., Murray, A.S., 2006. A review of quartz optically stimulated luminescence characteristics and their relevance in single-aliquot regeneration dating protocols. Radiat. Meas. 41, 369–391.
Wood, J.R., Forman, S.L., Everton, D., Pierson, J., Gomez, J., 2010. Lacustrine sediments in Porter Cave, central Indiana, USA and possible relation to Laurentide ice sheet marginal positions in the middle and late Wisconsinan. Palaeogeogr. Palaeoclimatol. Palaeoecol. 298, 421–431.
Woodfield, M.C., 1998. Wabash and Ohio River Megasequences: Little Pigeon Creek Basin, Evansville (unpublished M.S. thesis). Indiana University, Bloomington, IN, p. 73.
Woods, A.J., Omernik, J.M., Brockman, C.S., Gerber, T.D., Hosteter, W.D., Azevedo, S.H., 1998. Ecoregions of Indiana and Ohio (Map) and Supplementary Text.
Woolery, E.W., 2005. Geophysical and geological evidence of neotectonic deformation along the Hovey Lake fault, lower Wabash Valley Fault System, Central United States. Bull. Seismol. Soc. Am. 95, 1193–1201.

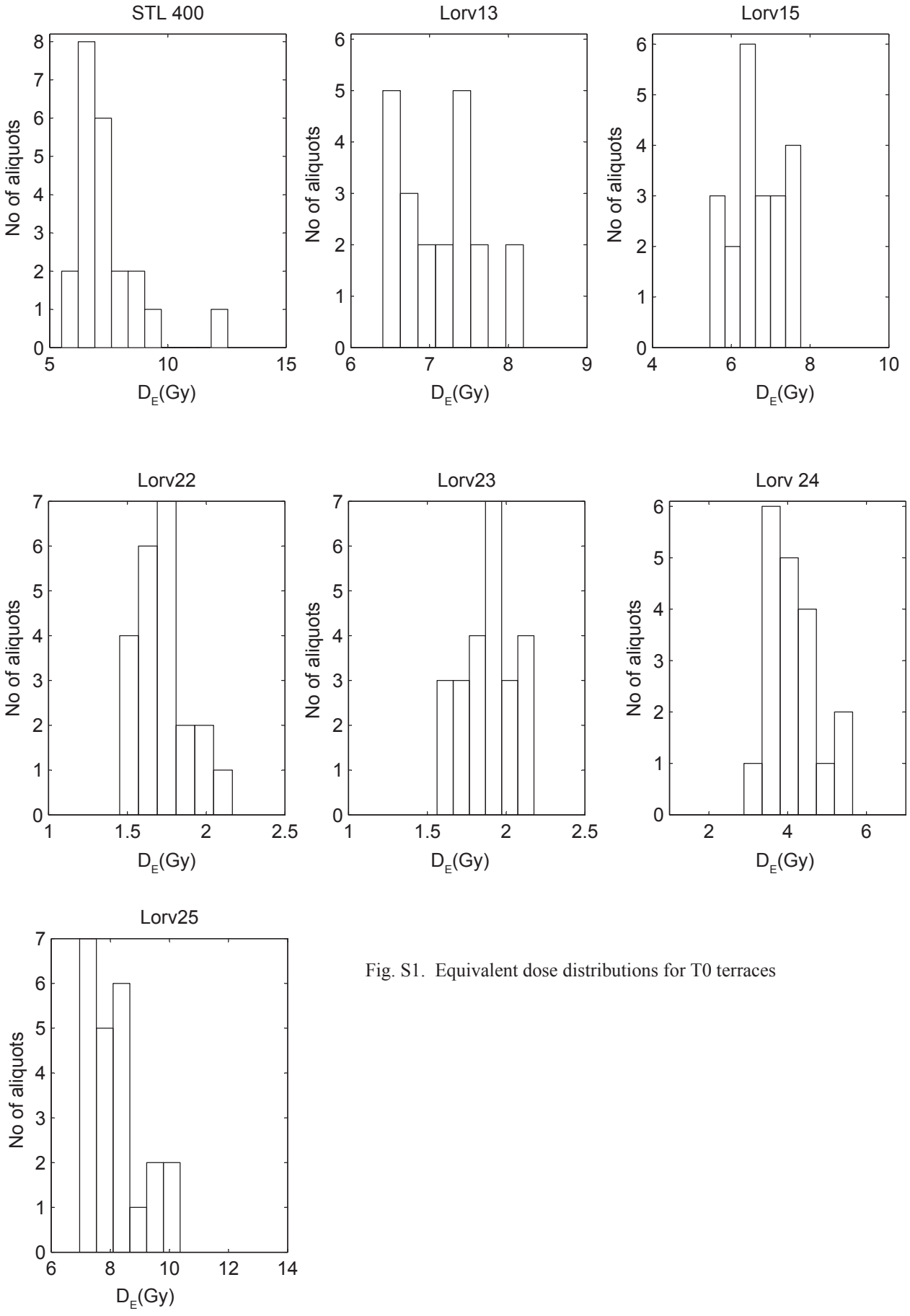

Fig. S1. Equivalent dose distributions for T0 terraces

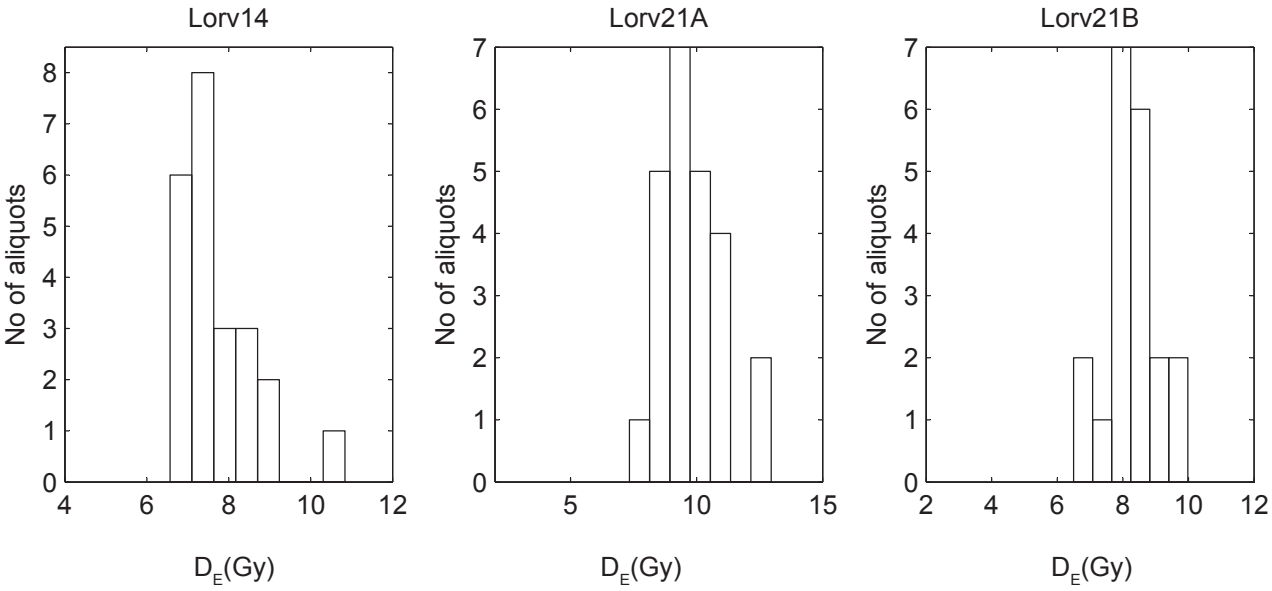

Fig. S2. Equivalent dose distributions for T1 terraces.

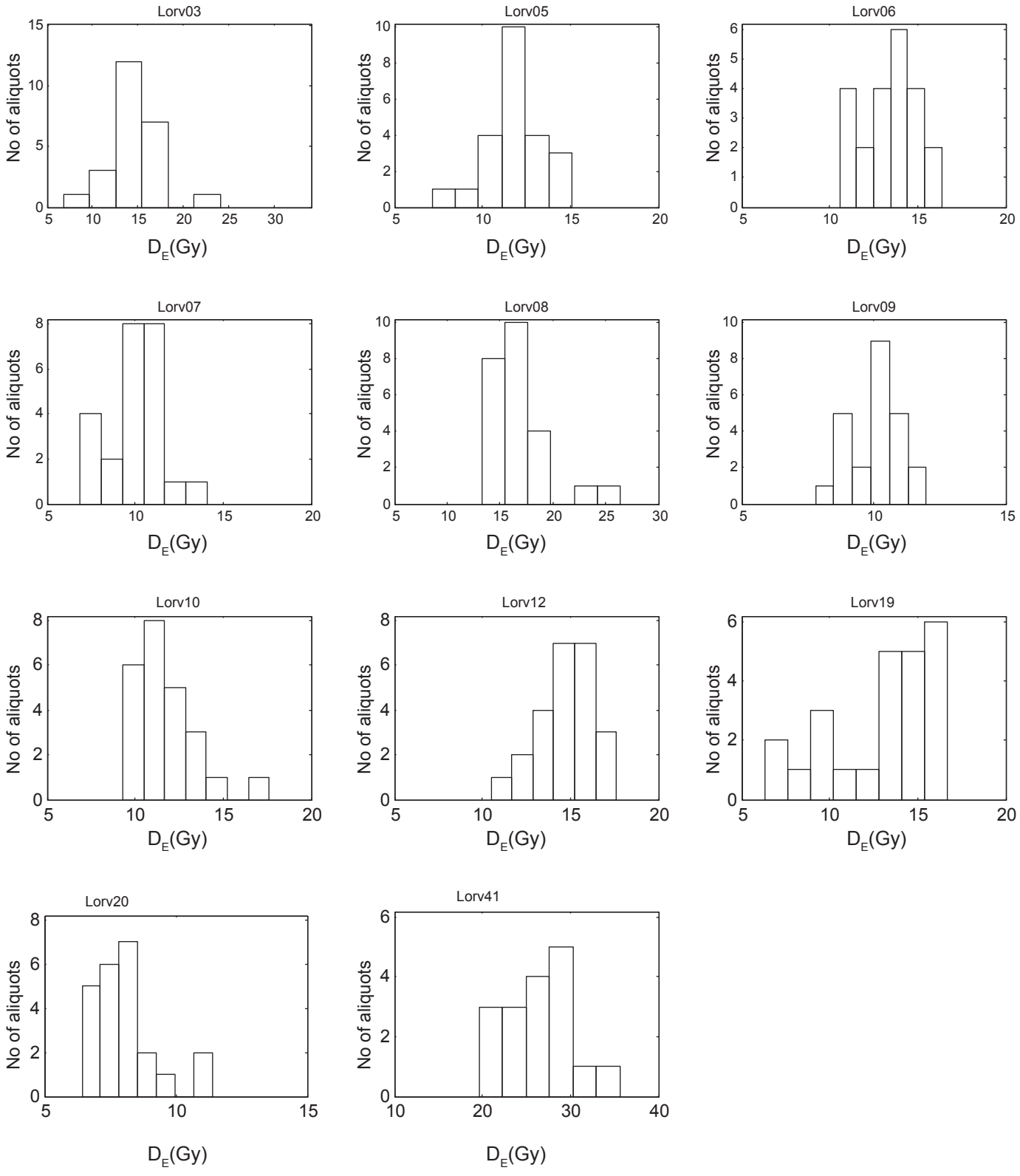

Fig. S3. Equivalent dose distributions for T2 terraces.

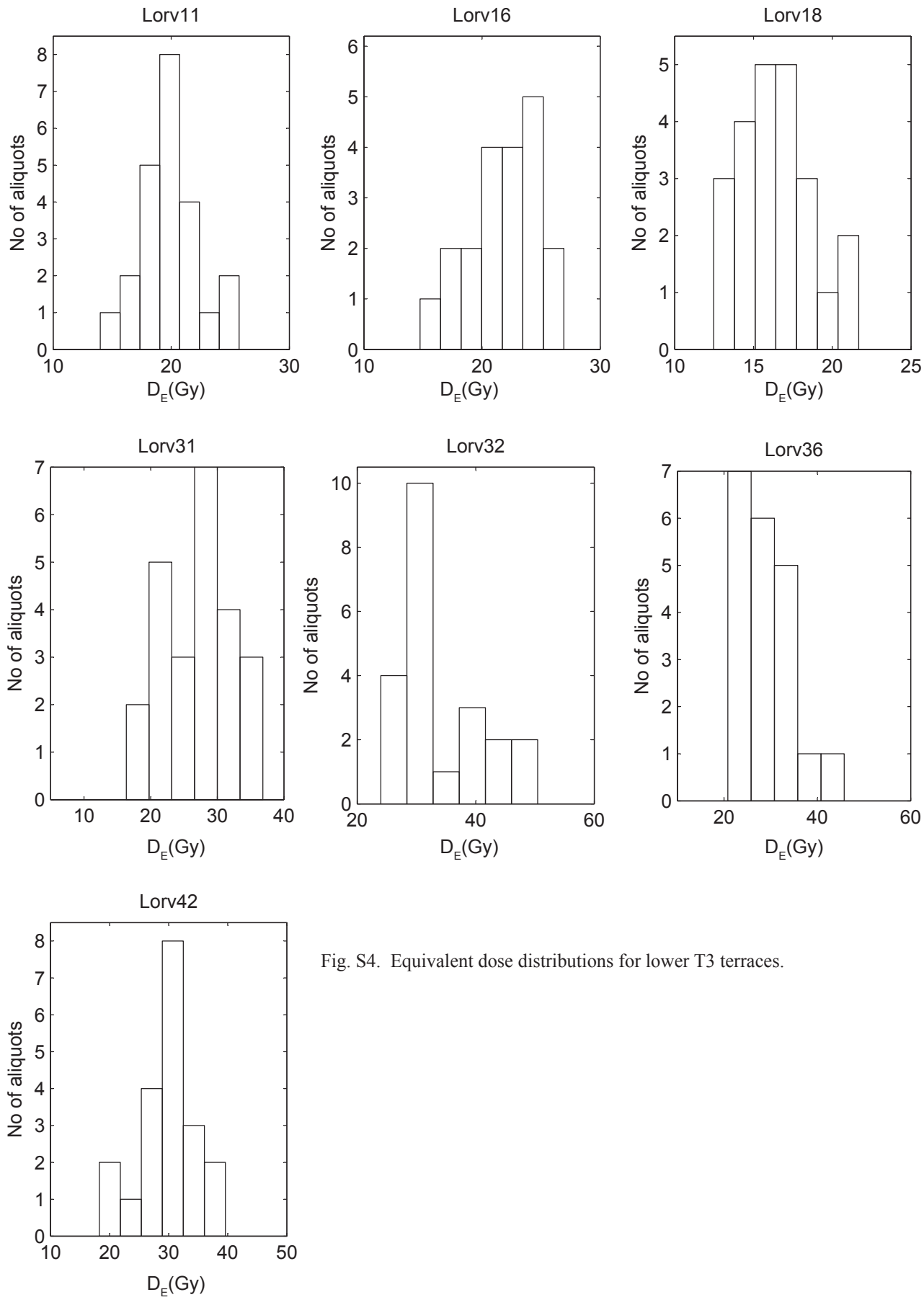

Fig. S4. Equivalent dose distributions for lower T3 terraces.

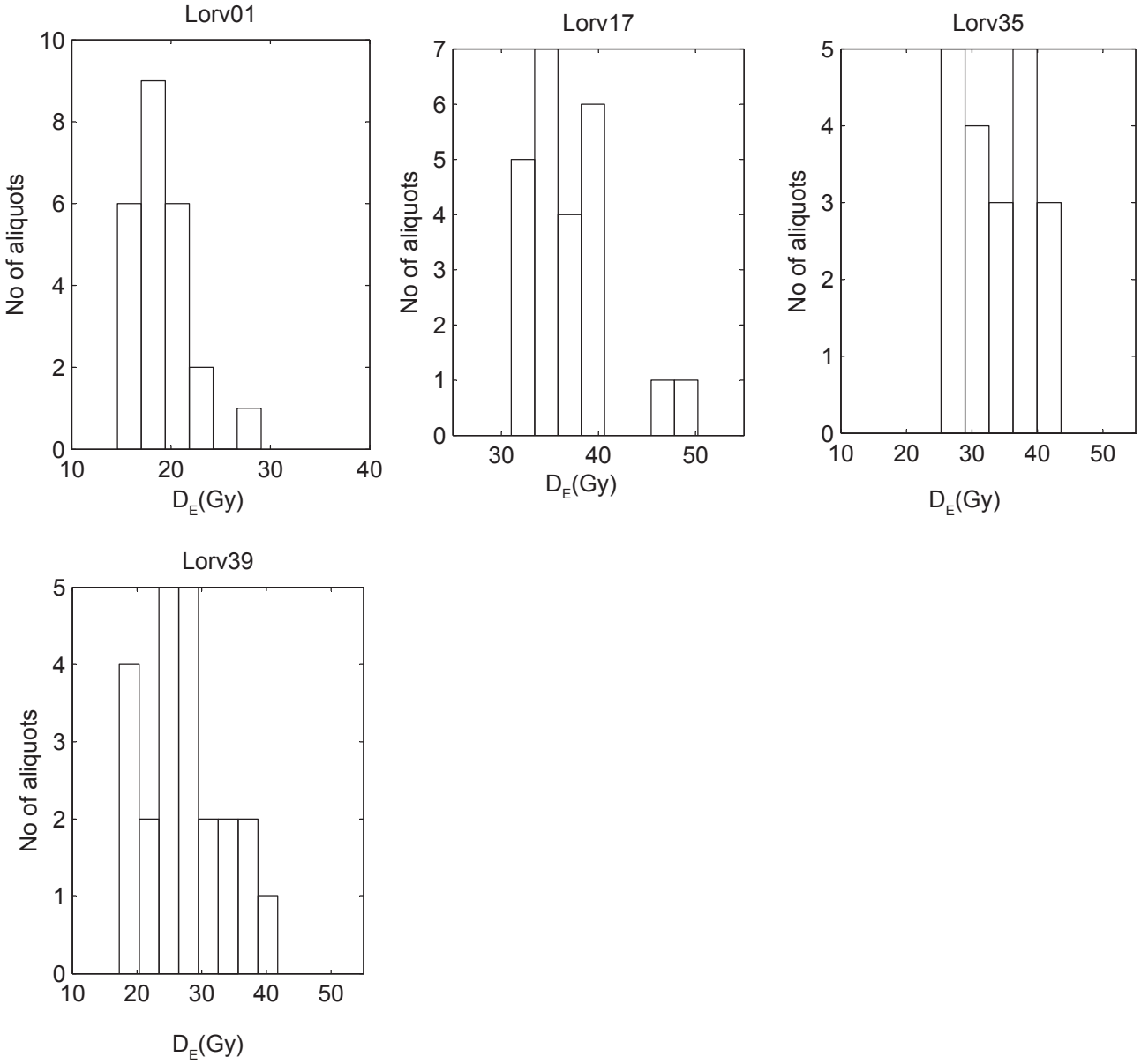

Fig. S5. Equivalent dose distributions for upper T3 terraces.

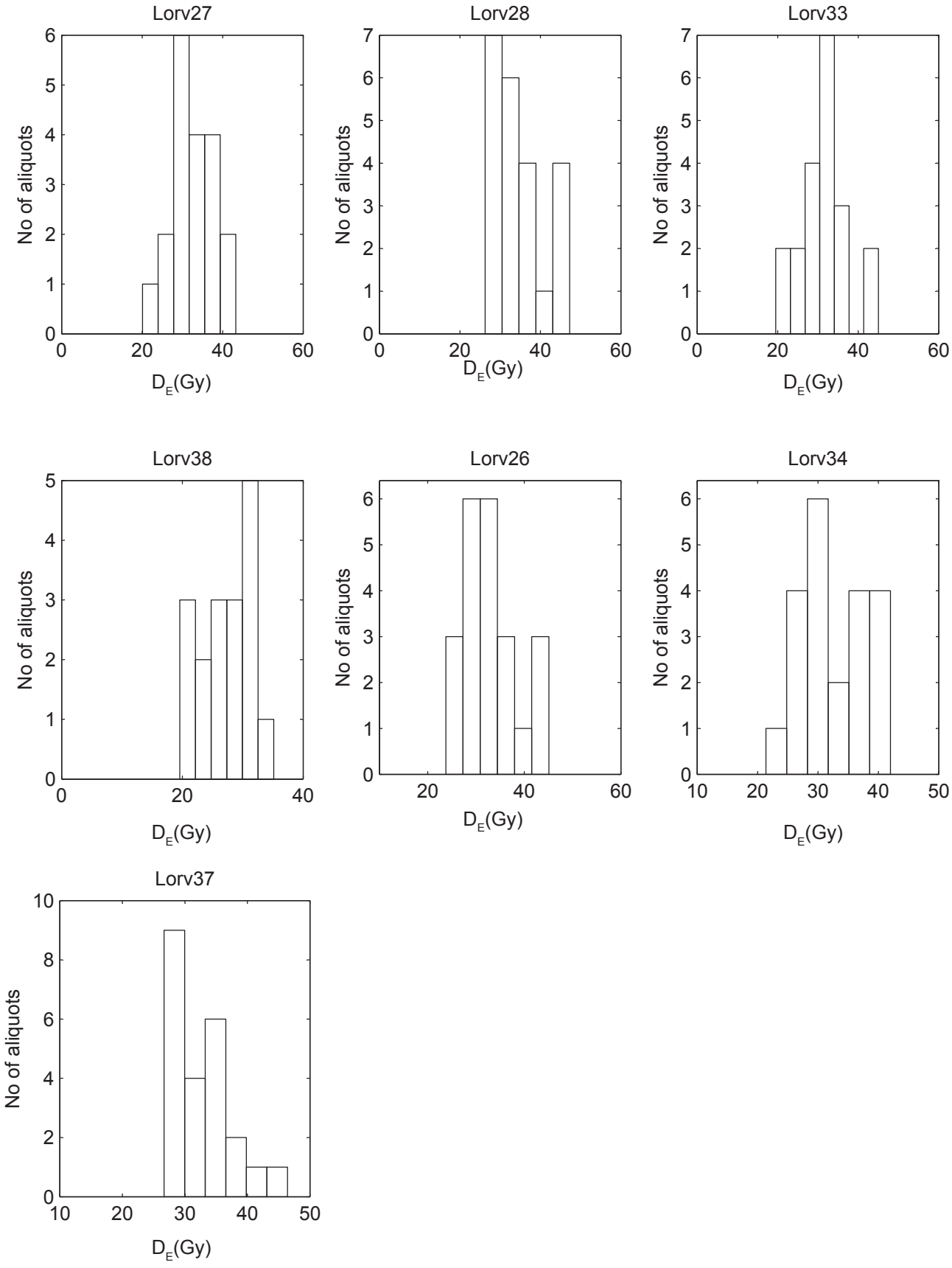

Fig. S6. Equivalent dose distributions for T4 terraces.

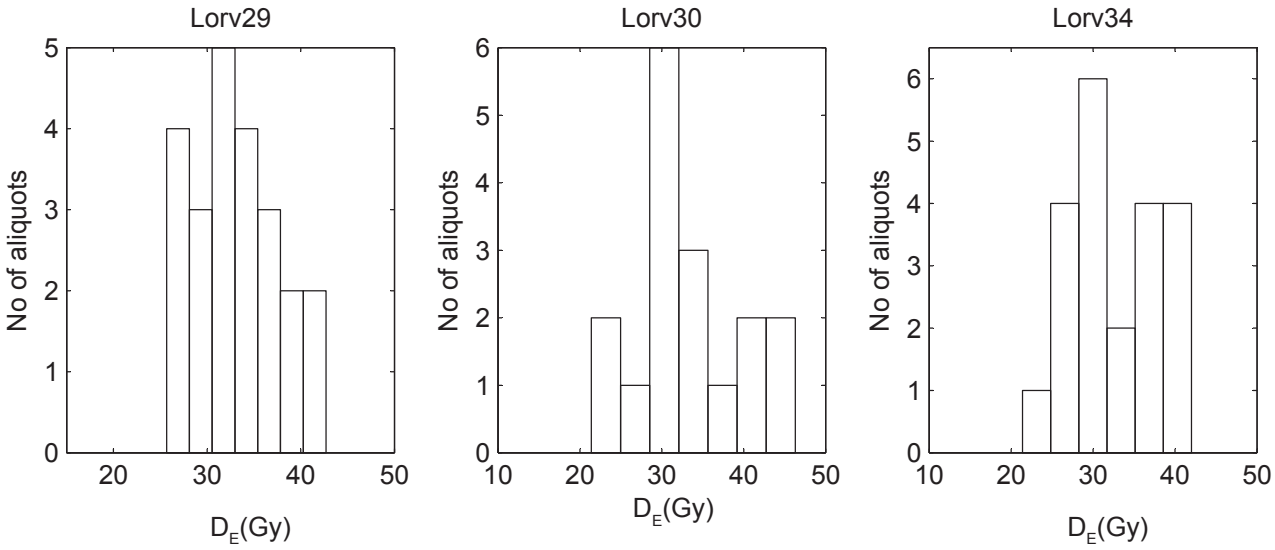

Fig. S7. Equivalent dose distributions for dunes on T4 terraces.

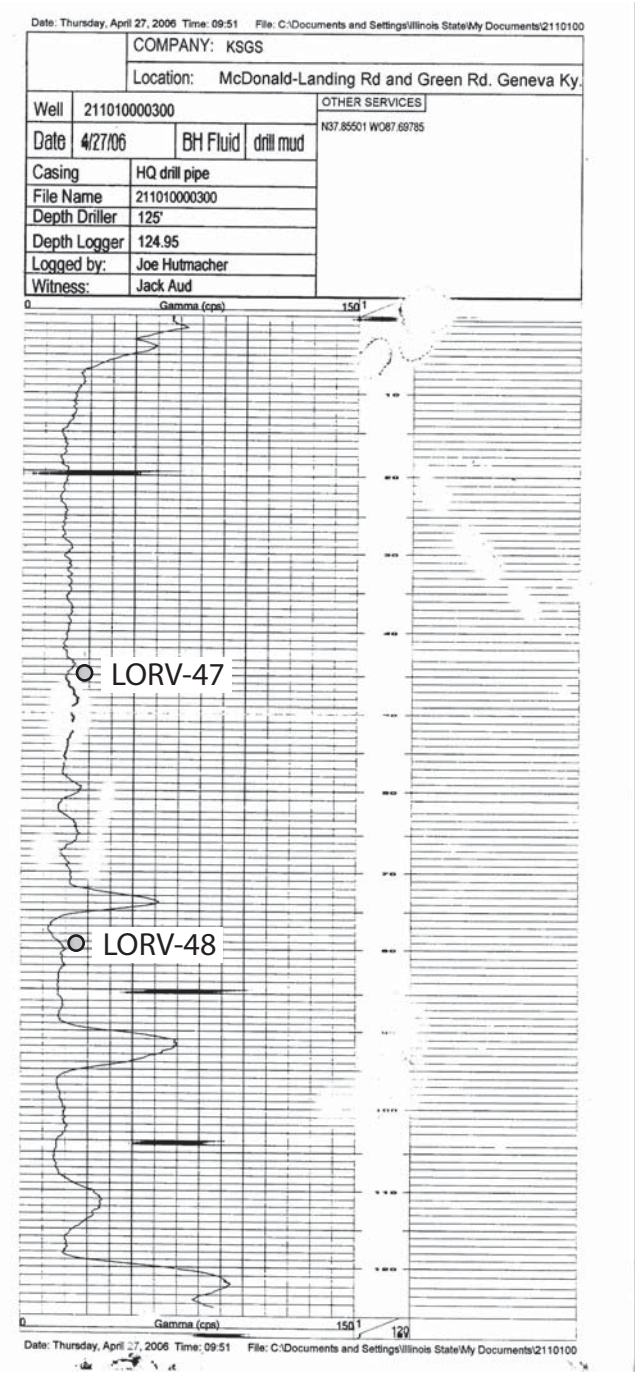

Fig S8a. Gamma log for deep borehole containing samples LORV-47 and LORV-48.

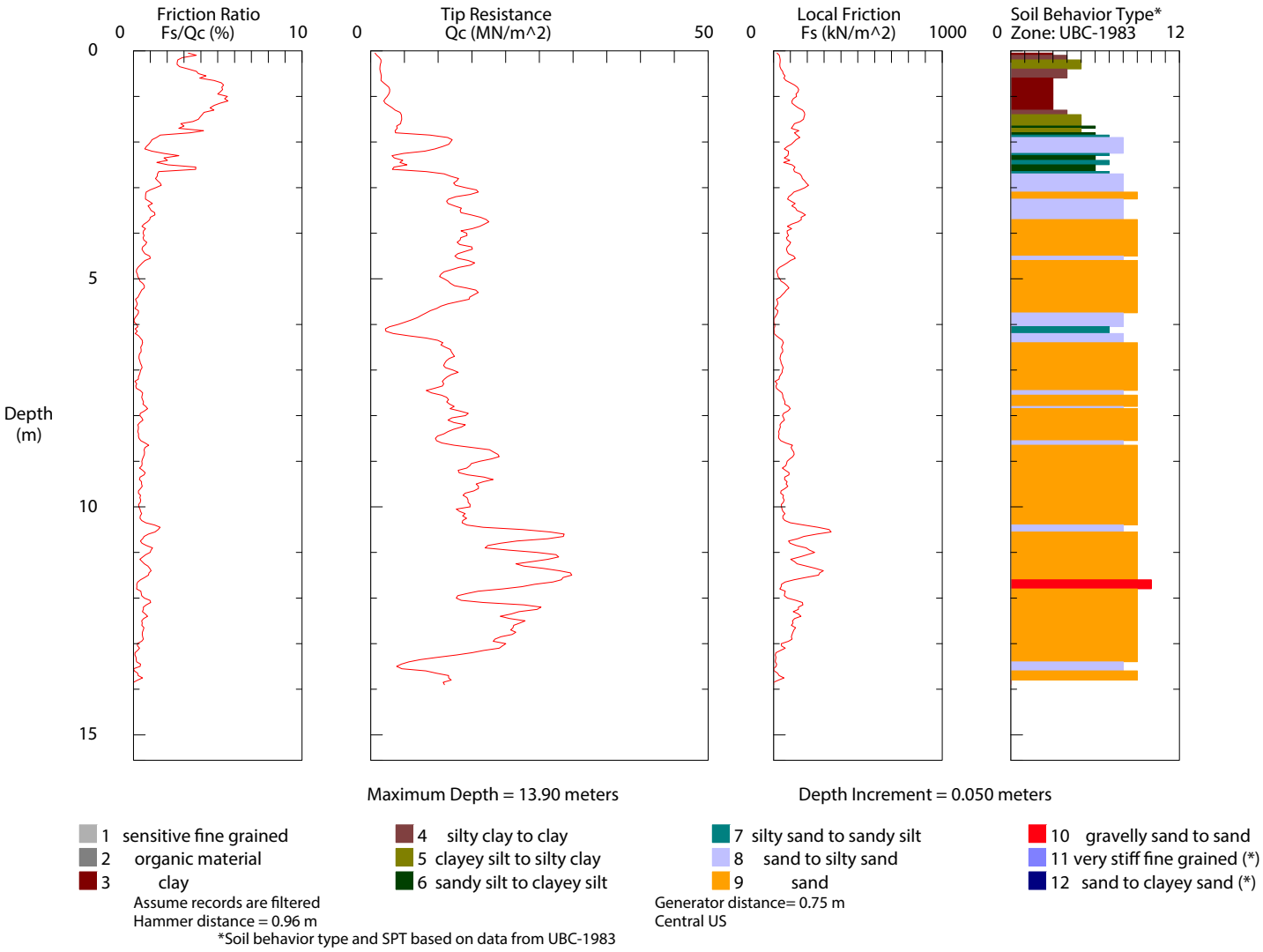

Fig. S8b. Cone penetrometer sounding, to depth of 20 meters, at the site containing samples LORV-47 and LORV-48.

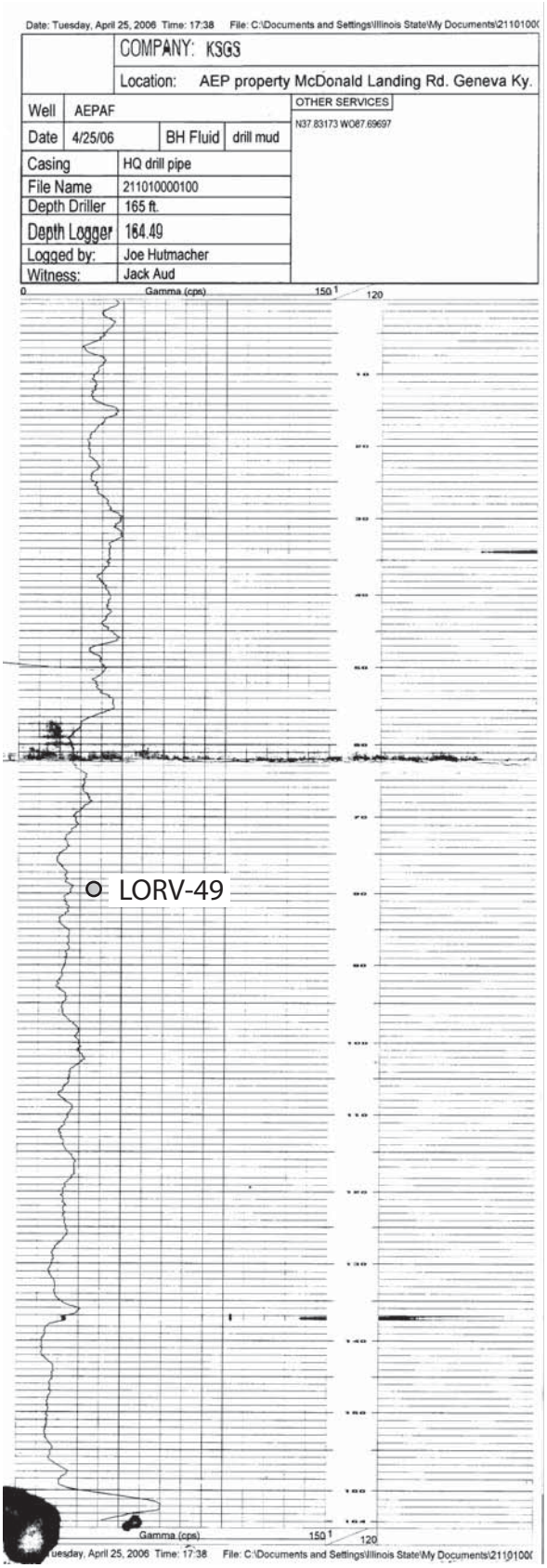

Fig. S9. Gamma log for deep borehole containing samples LORV-49.

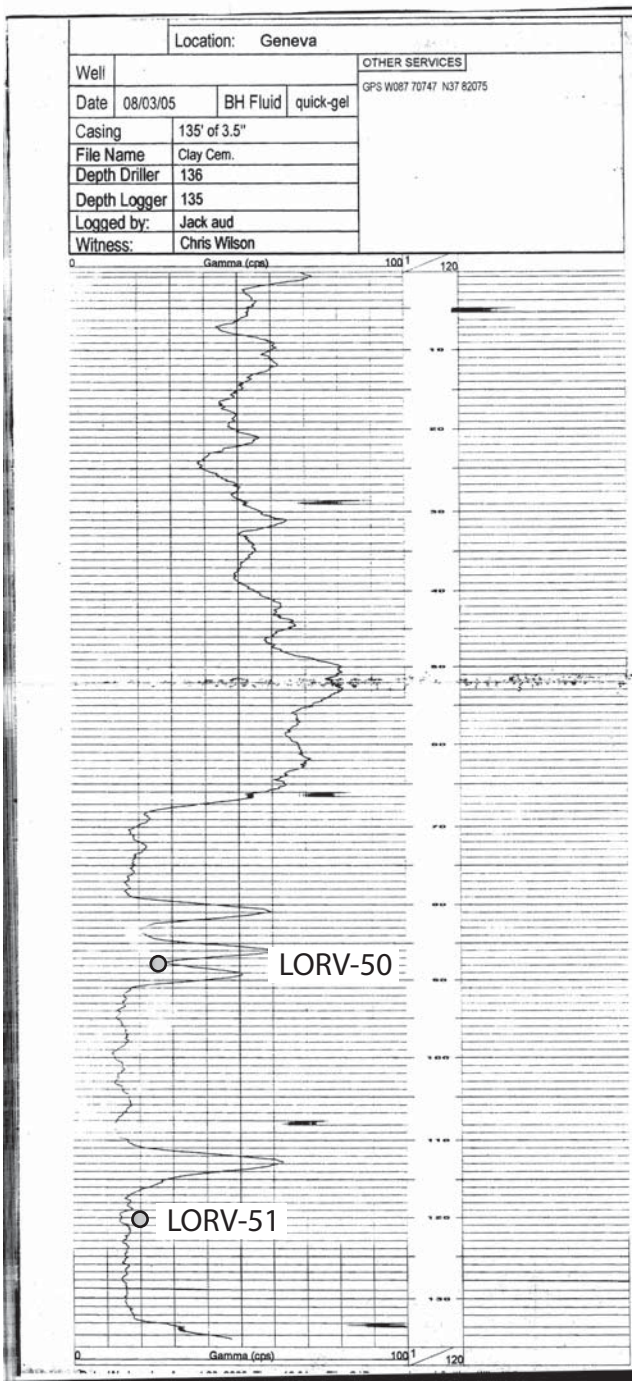

Fig. S10a. Gamma log for deep borehole containing samples LORV-50 and LORV-51.

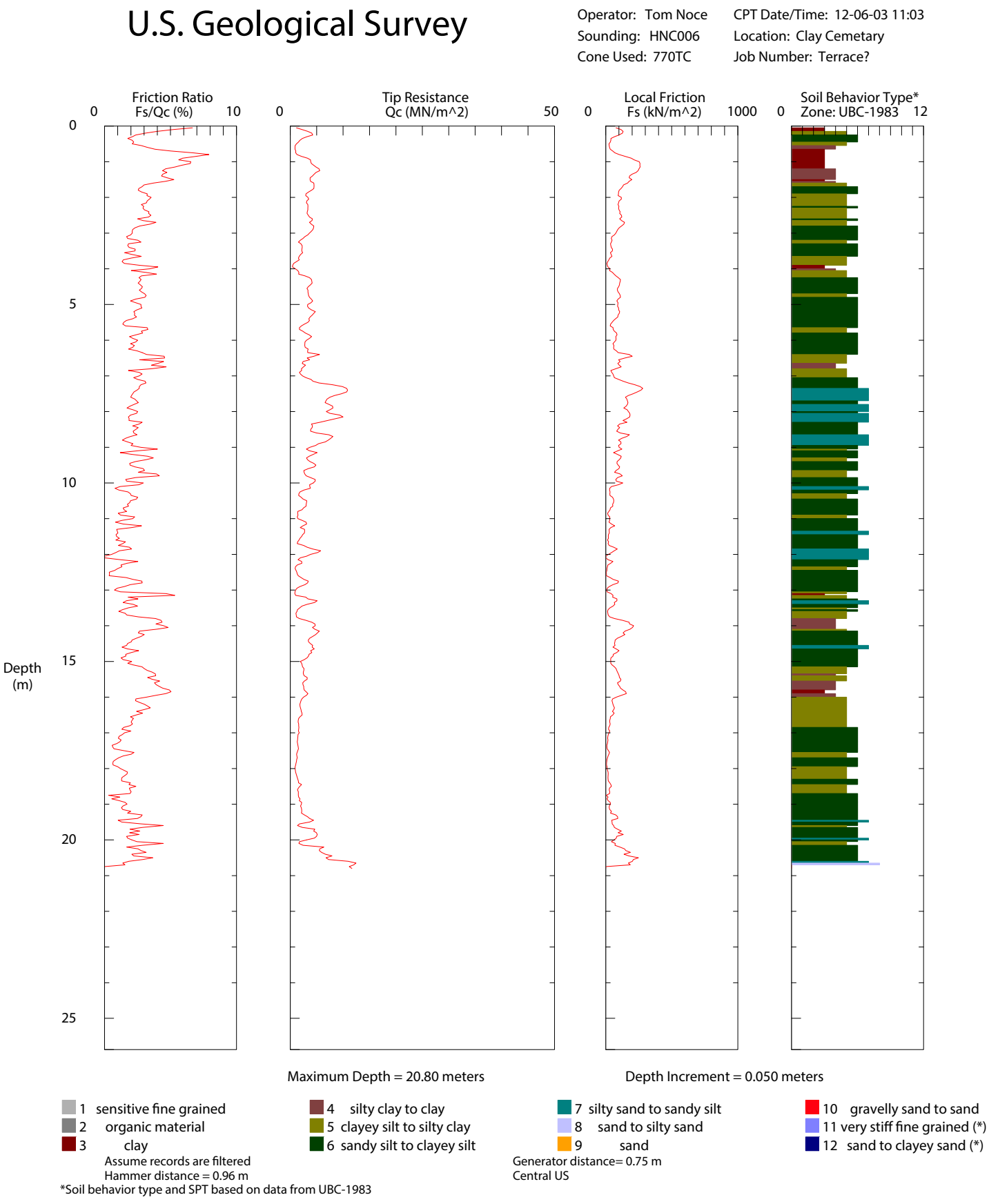

Fig. S10b. Cone penetrometer sounding, to depth of 21 meters, at the site containing samples LORV-50 and LORV-51.

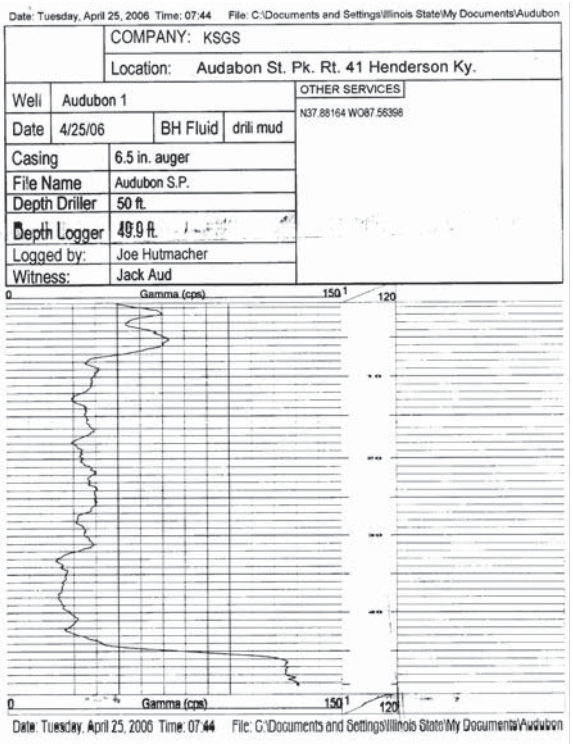

Fig. S11. Gamma log for deep borehole on S4 terrace.

Figure S12. Digital line scan of a 7.72 cm (3 inch) diameter core drilled on T4 terrace just west of Owensboro, KY (location shown on Figure 2). This is not a continuous core; the core is incomplete because recovery was very poor in the saturated sandy alluvium, so many intervals are missing.

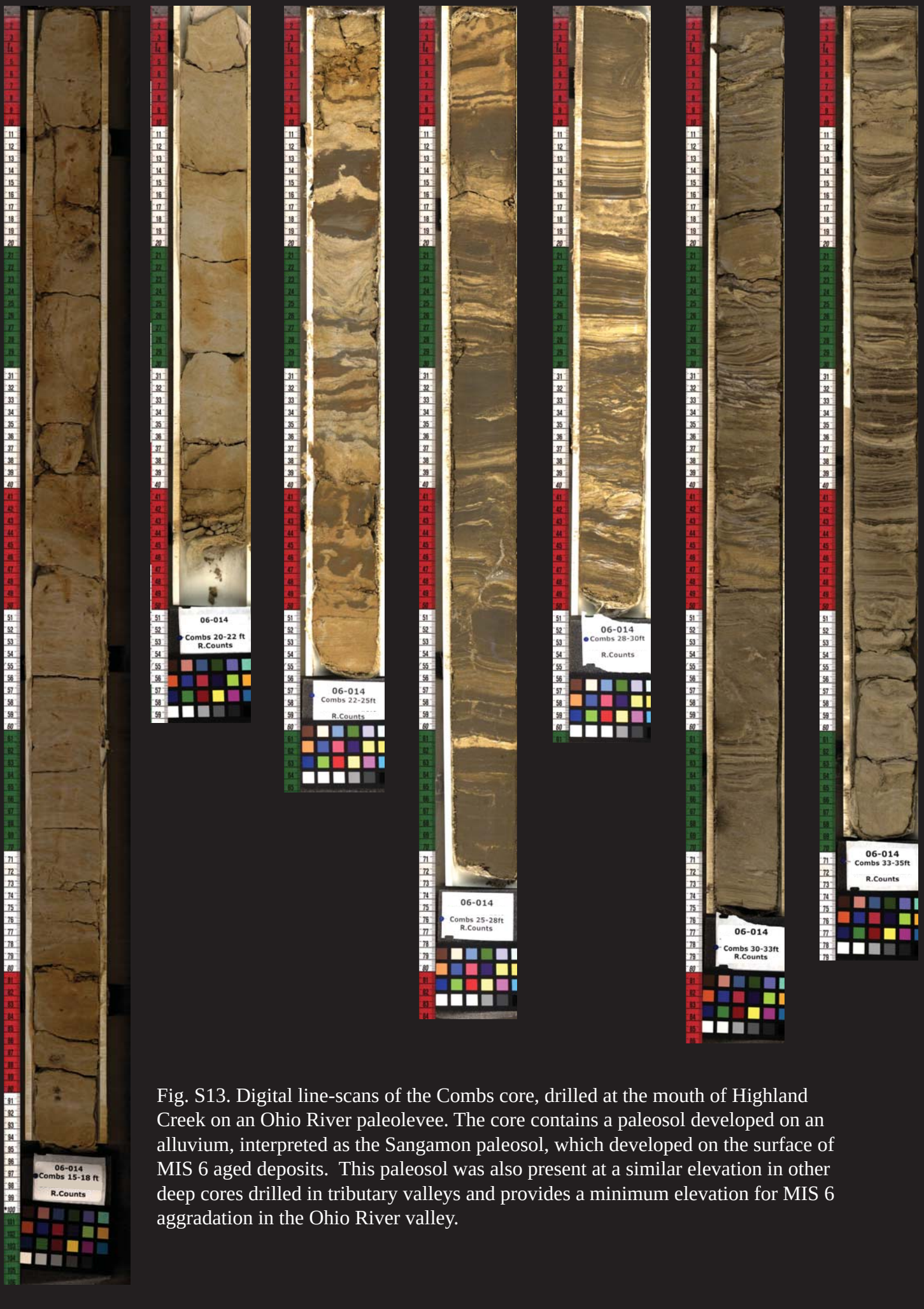

Fig. S13. Digital line-scans of the Combs core, drilled at the mouth of Highland Creek on an Ohio River paleolevee. The core contains a paleosol developed on an alluvium, interpreted as the Sangamon paleosol, which developed on the surface of MIS 6 aged deposits. This paleosol was also present at a similar elevation in other deep cores drilled in tributary valleys and provides a minimum elevation for MIS 6 aggradation in the Ohio River valley.

Fig. S13 (cont). Digital line-scans of the Combs core, drilled at the mouth of Highland Creek on an Ohio River paleolevee. The core contains a paleosol developed on an alluvium, interpreted as the Sangamon paleosol, which developed on the surface of MIS 6 aged deposits. This paleosol was also present at a similar elevation in other deep cores drilled in tributary valleys and provides a minimum elevation for MIS 6 aggradation in the Ohio River valley.

Fig. S13 (cont). Digital line-scans of the Combs core, drilled at the mouth of Highland Creek on an Ohio River paleolevee. The core contains a paleosol developed on an alluvium, interpreted as the Sangamon paleosol, which developed on the surface of MIS 6 aged deposits. This paleosol was also present at a similar elevation in other deep cores drilled in tributary valleys and provides a minimum elevation for MIS 6 aggradation in the Ohio River valley.

Fig. S13 (cont). Digital line-scans of the Combs core, drilled at the mouth of Highland Creek on an Ohio River paleolevee. The core contains a paleosol developed on an alluvium, interpreted as the Sangamon paleosol, which developed on the surface of MIS 6 aged deposits. This paleosol was also present at a similar elevation in other deep cores drilled in tributary valleys and provides a minimum elevation for MIS 6 aggradation in the Ohio River valley.

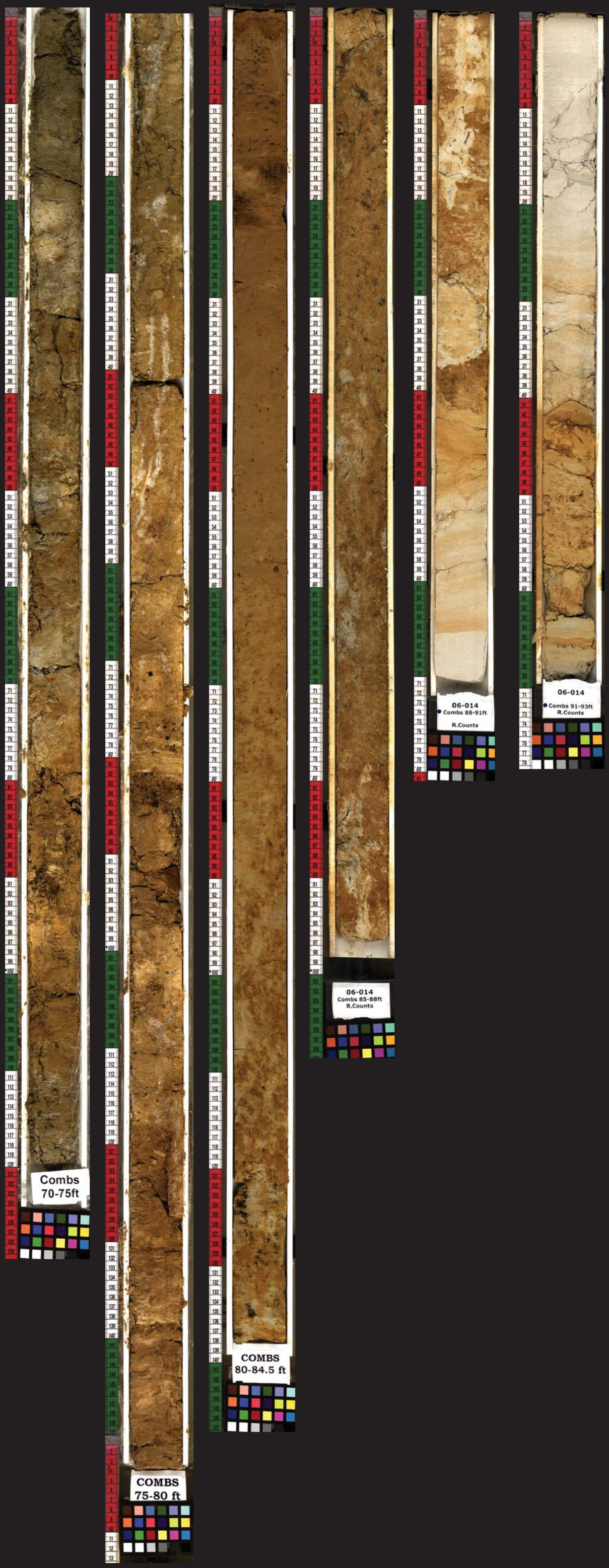

INITIAL CORE DESCRIPTION

LAKE Combs | SECTION LENGTH (cm) 91.4 | mblf top 4.57 | Describer Ron Counts

CORE ID 15-18 ft | SED. LENGTH (cm) 94 | mblf bot 5.48 | Date 01.26.09

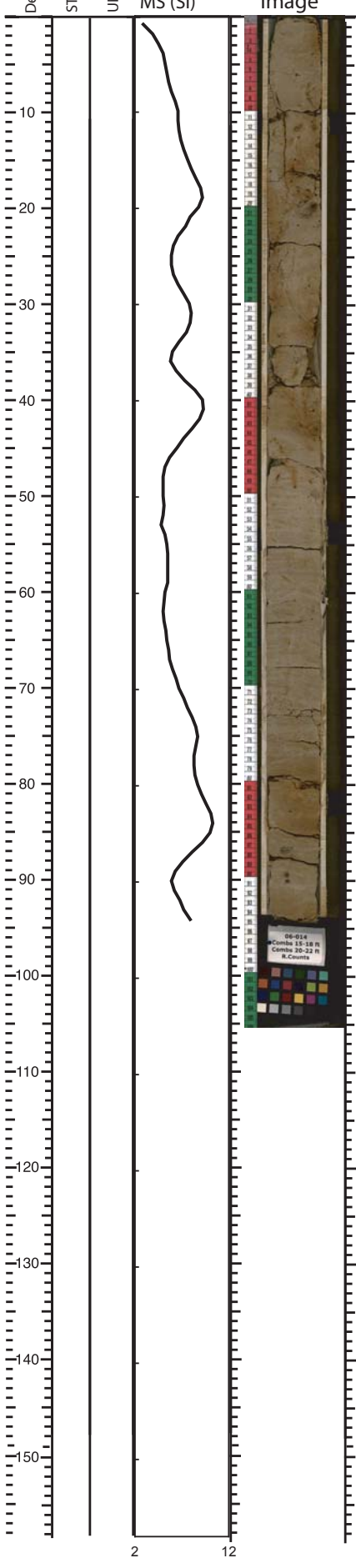

LITHOLOGIC DESCRIPTION

0-6 cm: massive silt, 2.5 Y6/3 (dry), faint oxidized or redoximorphic areas that are 10YR 6/8; very slight rxn with 10% HCl (looks like an individual grain reacts)

6- 50 cm: massive coarse silt with paleosol development; matrix is 2.5Y 6/3 (dry) and oxidized areas are 10YR 5/6 (dry); most of this interval reacts strongly with 10% HCl; Mn concretions, Mn nodules (up to 5 mm in diameter), and areas of Mn accumulation are common; 1.5 mm wide, Mn coated root trace from 8 to 19 cm and from 24 to 28 cm; faint evidence of burrowing from 8-12 cm, 12 -15 cm, 21-30 cm, and 47-50 cm; white flecks that appear to be gastropod shell fragments at 20.5, 24.5, 25, and 27 cm

50-70 cm: massive coarse silt with weak paleosol development; matrix is 2.5Y 6/3 (dry) and oxidized areas are 10YR 5/6 and 10 YR 6/8 (dry); 50-66 cm does not react with10% HCl, 66-70 very weak reaction that gets stronger with depth; few fine linear features (small burrows?) that have faint Mn accumulations or coatings, Mn nodules or concretions absent

70-78 cm:massive coarse silt with weak paleosol development; matrix is 2.5Y 6/3 (dry) and oxidized areas are 10YR 5/6 and 10 YR 6/8 (dry); slight rxn with 10% HCl; Mn coated, linear root or burrow traces pervasive

78-86 cm: massive silt (finer than previous intervals), entire interval is oxidized 2.5 Y 6/8 (dry); small zones of Mn accumulation at 82 and 83 cm; moderate rxn with 10% HCL

86-92 cm: massive coarse silt, partially oxidized, matrix is 2.5 Y 6/3, oxidized areas are 2.5Y 6/8, interval has black accumulations (Mn?)

92-94 cm: massive silt (finer than previous intervals), entire interval is oxidized 2.5 Y 6/8 (dry); small zones of Mn accumulation at 82 and 83 cm; moderate rxn with 10% HCL

Fig. S14. Detailed core description of the Combs core shown in Figure S13.

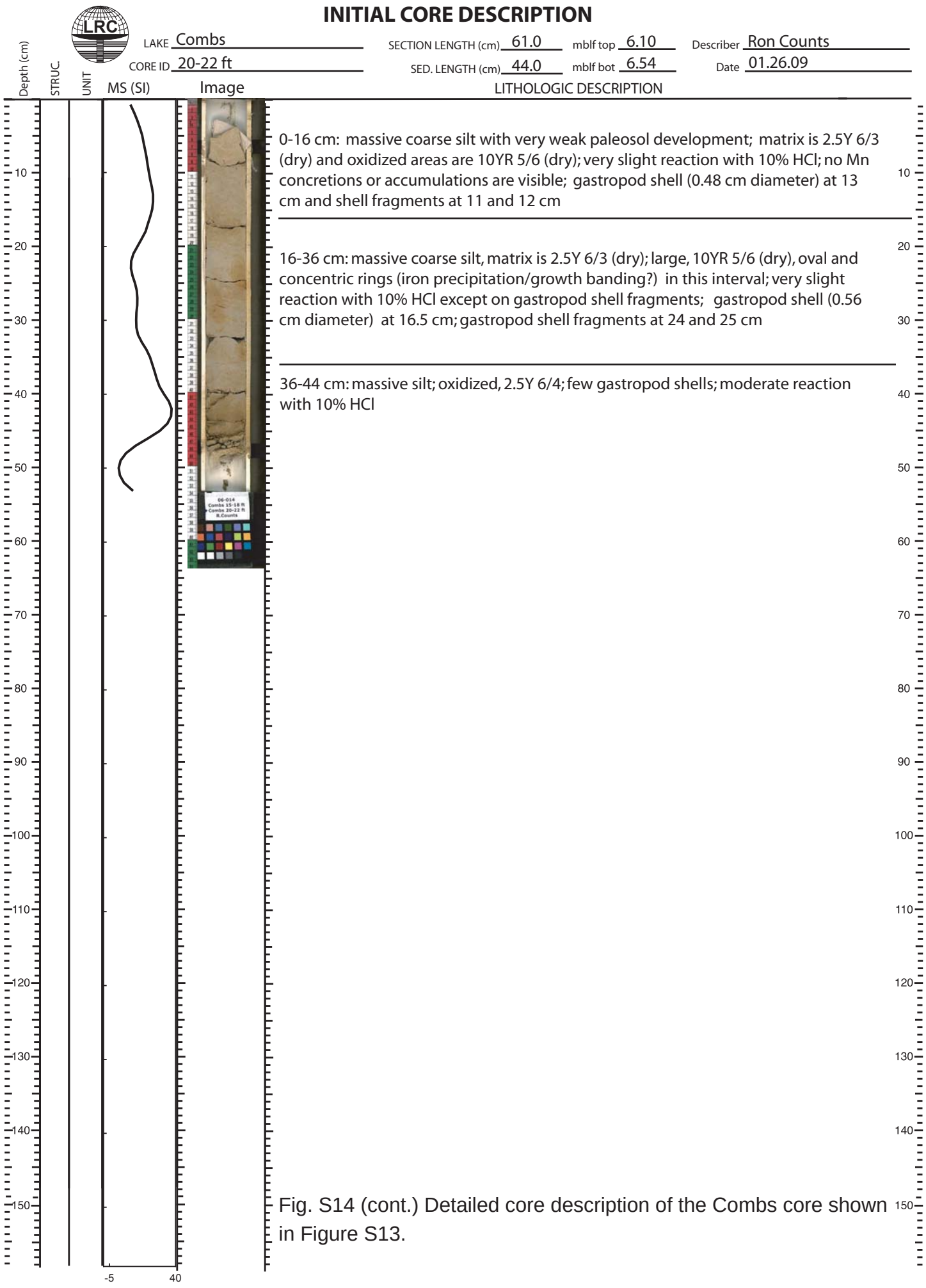

Fig. S14 (cont.) Detailed core description of the Combs core shown in Figure S13.

INITIAL CORE DESCRIPTION

LAKE 06-014 Combs Farm
CORE ID 22-25 ft
SECTION LENGTH (cm) 91.4 mblf top 6.71 Describer Ron Counts
SED. LENGTH (cm) 55.5 mblf bot 7.26 Date 01.26.09

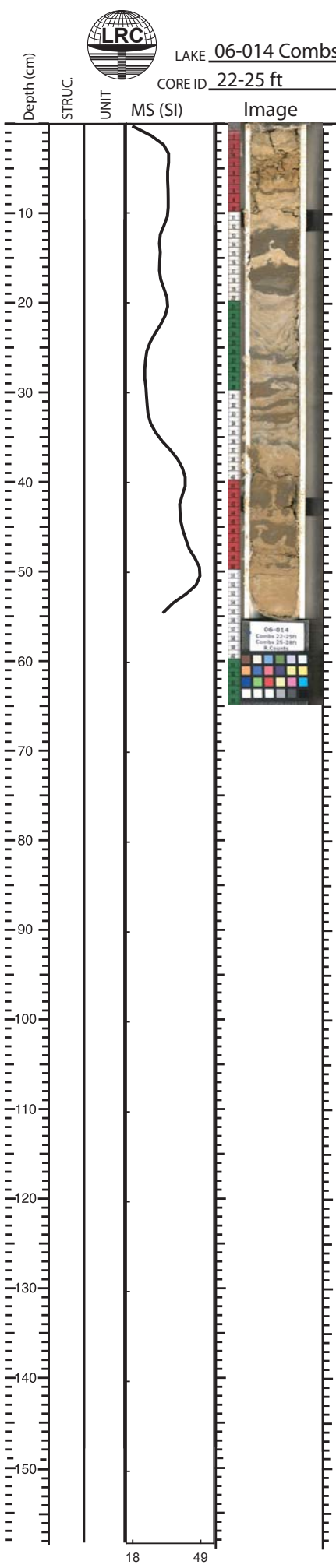

LITHOLOGIC DESCRIPTION

0-3 cm: coarse silt with minor, very fine sand; 2.5Y 6/3 (dry); has warped, 2mm thick bands of clay that are 2.5Y 4/2 (deformed during drilling); gastropod shell fragment at 1cm; weak, delayed reaction with 10% HCl

3-8 cm: silt; oxidized; 10YR 5/6 (dry), strong reaction with 10% HCl; 2.5Y 4/3 clay bands at 6 cm (0.6 cm thick) and at 7.5 cm (0.7 cm thick)

8-12 cm: coarse silt with some very fine sand; 2.5Y 6/3 (dry); has faint mottled or redoximorphic areas that are 10YR 5/6; very strong reaction with 10% HCl

12-15.45cm: clay; 2.5Y 4/2, moderate reaction with 10% HCl

15.45-16.13 cm: silt; 2.5Y 6/3 (dry); approximately 0.7 cm thick originally but has been deformed, looks like a minor liquefaction feature, moderate to strong reaction with 10% HCl

16.13-19.5 cm: clay; 2.5Y 4/2, moderate reaction with 10% HCl

19.5-26 cm: coarse silt; 2.5Y 6/2.5 (dry); has few faint mottled or redox areas that are 10YR 5/6, that could also be oxidation but there is no oxidation halo at core edges; no rxn with 10% HCl, clay from lower interval disturbed upward

26-27 cm: clay; 2.5Y 4/2, no reaction with 10% HCl; silt from lower interval is injected up into the clay

27-28.5 cm: coarse silt with fine sand; 2.5Y 6/2.5 (dry); silt is injected upward into overlying clay bed forming mushroom structure, no rxn with 10% HCl

28.5-31 cm: clay; 2.5Y 4/2, no reaction with 10% HCl; silt from lower interval is injected up into the clay

31-32 cm: silt; 2.5Y 5/3; very slight rxn with acid, slightly warped bed

32-32.5 cm: clay; 2.5Y 4/2, slight reaction with 10% HCl; silt from lower interval is injected up into the clay

32.5-33 cm: silt; 2.5Y 5/3; slight to moderate rxn with acid, deformed and injected upward into overlying clay

33-33.5cm: clay, 2.5Y 4/2; very slight to moderate rxn with acid, has very thin silt bed that is deformed and injected upward

33.5-35.5 cm: silt, 2.5Y 5/3; slight rxn with acid, has very thin disrupted clay bed

35.5-36.5 cm: clay, 2.5Y 4/2; very slight rxn with acid, silt from lower interval is injected up into the clay

36.5-39.5 cm: silt, 2.5Y 5/4; very slight rxn with acid, has very thin disrupted clay

39.5-43 cm: clay, 2.5Y 4/2; very slight rxn with acid, silt from lower interval is injected up into the clay

43-45 cm: silt, 2.5Y 5/4; very slight rxn with acid, silt is injected upward into overlying clay bed

45-47.5 cm: clay, 2.5Y 4/2; very slight rxn with acid, silt from lower interval is injected up into the clay forming mushroom structure

47.5-49 cm: silt, 2.5Y 5/4; slight rxn with acid, silt is injected upward into overlying clay bed forming mushroom structure in the clay

49-50 cm: disrupted, broken clay laminae, 2.5Y 4/2; very slight rxn with acid, could be part of overylying clay bed (45-47.5 cm)that has been seperated by injected silt from below

50-55.5 cm: silt, 2.5Y 5/4; slight rxn with acid, silt may be source of silt in 47.5-49 interval,

Fig. S14 (cont.) Detailed core description of the Combs core shown in Figure S13.

INITIAL CORE DESCRIPTION

LAKE 06-014 Combs Farm
CORE ID 25-28 ft
SECTION LENGTH (cm) 91.4 mblf top 7.62
SED. LENGTH (cm) 72.5 mblf bot 8.35
Describer Ron Counts
Date 01.26.09

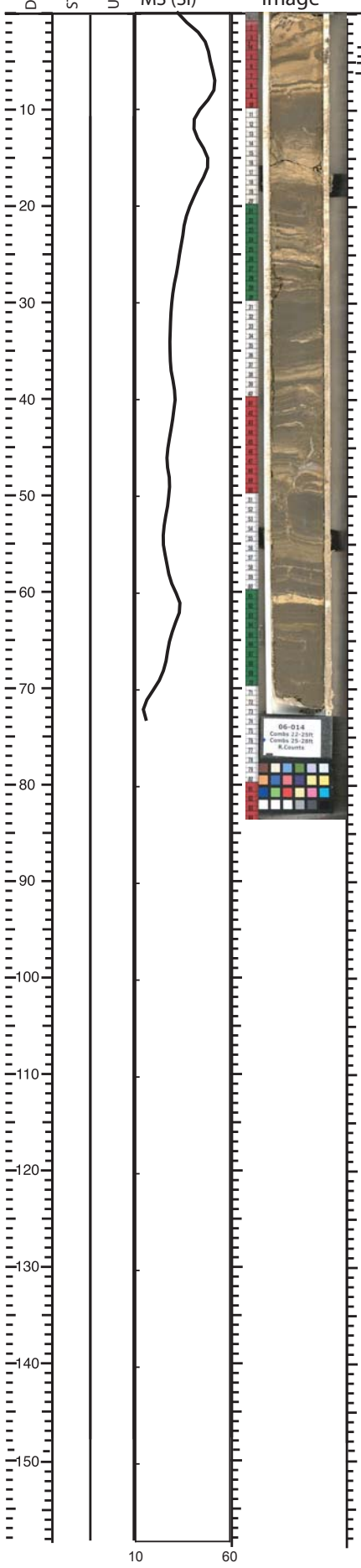

LITHOLOGIC DESCRIPTION

0-3.5 cm: silt, 2.5Y 5/4; slight rxn with acid, contains clay clasts form interval below and appears to be disrupted and possibly injected upward into overlying interval

3.5-4.0 cm: clay, 2.5Y 4/3; very slight rxn with acid, silt from lower interval is injected up into the clay

4.0-5.0 cm: silt, 2.5Y 5/4; slight rxn with acid, injected upward into overlying clay laminae

5.0-6.0 cm: clay, 2.5Y 4/3; slight rxn with acid, silt from lower interval is injected up into the clay

6.0-7.5 cm: silt, 2.5Y 5/4; slight rxn with acid, silt is disrupted and injected upward into overlying clay laminae

7.5-7.9 cm: clay, 2.5Y 4/3; very slight rxn with acid,

7.9-8.5 cm: silt, 2.5Y 5/4; slight to moderate rxn with acid, silt is disrupted and penetrates downward into underlying clay laminae laminae (from 8.3-8.5 cm)

8.5-13.5 cm: clay, 5Y 3/2; slight rxn with acid

13.5-18 cm: silt, 2.5Y 5/4; slight to moderate rxn with acid, has very thin clay stringers > 1 mm thick (approx 5 total)

18-22.5 cm: clay, 5Y 3/2; slight to moderate rxn with acid, has silt stringers > 1 mm thick through interval (approx 7 total)

22.5-26 cm: silt, 2.5Y 5/4; slight to moderate rxn with acid, has thin clay stringers 2-3 mm thick (approx 6 total) that are slightly disturbed

26-30 cm: clay, 5Y 3/2; moderate rxn with acid, has silt stringers has approximately 4 that are > 1 mm thick and three that are 1.5-3 mm thick

30-36.5 cm: clay, 5Y 3/2; moderate rxn with acid, has one deformed, 3 mm thick silt bed at 34.5 cm

36.5-38.5 cm: silt, 2.5Y 5/4; moderate rxn with acid, has a few thin clay stringers 2-3 mm thick and several > 1 mm thick, all clay stringers are slightly disturbed

38.5-39 cm: clay, 5Y 3/2; slight rxn with acid, silt from lower interval is injected up into the clay

39-40 cm: deformed silt, 2.5Y 5/4; slight rxn with acid; silt is injected upward into overlying clay laminae

40-50 cm: clay, 5Y 3/2, slight rxn with acid, interbedded with mm scale silt, many interbeds from 46-50, interval is bioturbated, especially around a burrow that runs from 43-50 cmburrow

50-54 cm: clay, 5Y 3/2, slight rxn with acid, few interbeds of silt (2.5Y 5/4) from 53-54 cm, interval is bioturbated around a burrow that runs from 50-54 and continues into overlying unit cmburrow

54-55.5 cm: silt, 2.5Y 5/4; slight rxn with acid, has thin clay stringers > 1 mm thick that are disrupted by a burrow

55.5-57 cm: silt, 2.5Y 5/4; slight rxn with acid

57-60.5 cm: clay, 5Y 3/2; slight rxn with acid, has several beds of silt that look like sills from underlying silt that was injected up into the clay

60.5-61.5 cm: very coarse silt and very fine sand, 2.5Y 6/3, slight rxn with acid, source bed for features in overlying interval

60.5-72.5 cm: clay, 5Y 3/2; slight rxn with acid, has silt bed from 63.5-64 cm and mm thick silt beds at 65 and 69.5 cm, faint traces of thin, vertical silt zones that may be from an underlying silt bed but they are too faint and discontinuous to be certain

Fig. S14 (cont.) Detailed core description of the Combs core shown in Figure S13.

INITIAL CORE DESCRIPTION

LAKE 06-014 Combs Farm
CORE ID 28-30 ft
SECTION LENGTH (cm) 61 mblf top 8.53 Describer Ron Counts
SED. LENGTH (cm) 49.5 mblf bot 9.03 Date 01.27.09

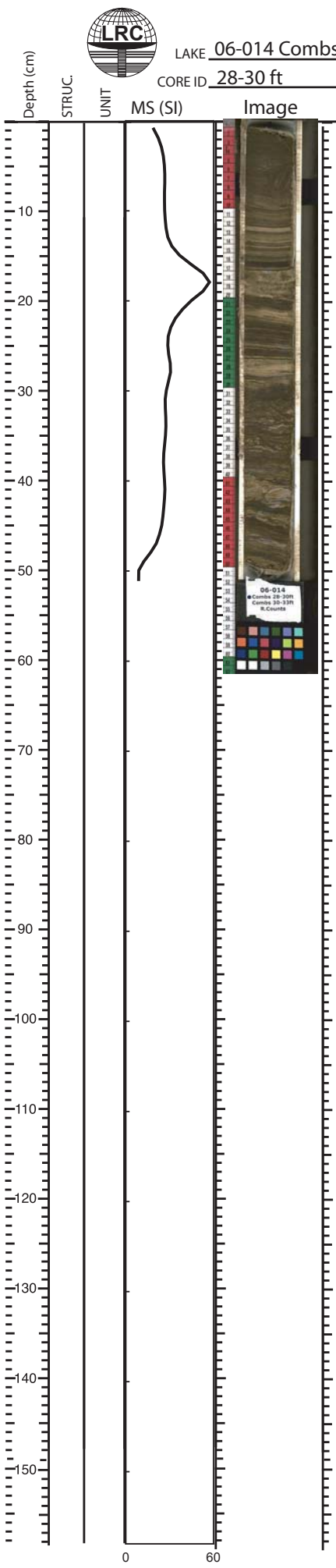

LITHOLOGIC DESCRIPTION

0-8 cm: clay, 5Y 3/2; slight to moderate rxn with acid, disturbed from 3-7 cm by bioturbation or SSD

8-11 cm: interbeded silt and clay, silt is 2.5Y 5/4; clay is 2.5Y 3/2; both have slight rxn with acid; load structure at the bottom of interval
11-11.5 cm: very coarse silt and vf sand; 2.5Y 6/3, slight rxn with acid

11.5-16 cm: interbeded silt and clay, silt is 2.5Y 5/4; clay is 2.5Y 3/2; both have slight rxn with acid; beds are < 1 mm except a 7 mm clay bed from 15.0-15.7 cm

16-19 cm: very coarse silt and vf sand; 2.5Y 6/3, moderate rxn with acid

19-28 cm: interbeded silt and clay, silt is 2.5Y 5/4; clay is 2.5Y 3/2; both have moderte rxn with acid; beds are ~ 1 mm thick except silt from 20.5-21cm and 26-28 cm and clay from 21.5-22.5, 24.5-25.5 cm

28-40 cm: dominately clay with interbeded silt; clay is 2.5Y 3/2; silt interbeds are disrupted by SSD; both have moderate rxn with acid

40-42.5 cm: silt with interbedded clay, silt is 2.5Y 5/4; clay is 2.5Y 3/2; both have moderte rxn with acid; beds are disrupted

42.5-49.5 cm: interbedded silt and clay; clay is 2.5Y 3/2; silt is 2.5Y 6/2 and 2.5Y 5/4; both have moderte rxn with acid; beds are slightly disrupted

Fig. S14 (cont.) Detailed core description of the Combs core shown in Figure S13.

INITIAL CORE DESCRIPTION

LAKE 06-014 Combs Farm
CORE ID 30-33 ft
SECTION LENGTH (cm) 91.4 mblf top 9.14
SED. LENGTH (cm) 75.0 mblf bot 9.89
Describer Ron Counts
Date 01.27.09

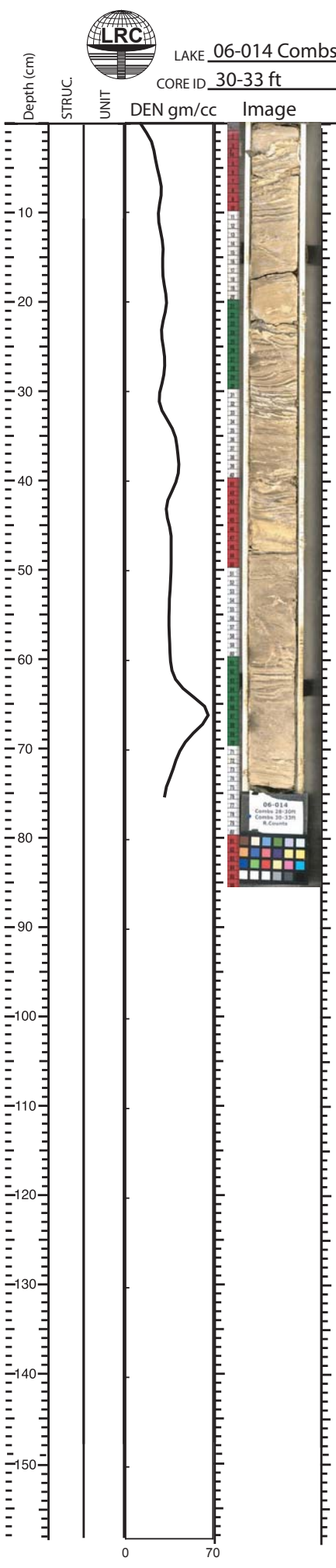

LITHOLOGIC DESCRIPTION

MUNSELL COLORS ARE FOR DRY SEDIMENT UNLESS NOTED OTHERWISE

0-11.5 cm: dominantly silt with mm scale laminae of clay; silt is 2.5 Y 6/2; clay is 2.5Y 5/1; 3/2; moderate to stong rxn with acid, sediments are disturbed and folded (SSD)isturbed from 3-7 cm by bioturbation or SSD

12-21.5 cm: silt; 2.5Y 6/3, has zones that are 2.5Y 6/1, hard to tell if the browner zone is discolored from drying and oxidation or if the 2.5Y 6/1 color is original color; moderate to stong rxn with acid; contains dark zones that may be Mn accumulations; has a few mm scale clay laminae at 17 cm that are deformed and a deformed v coarse silt with vf sand lens at 21 cm

21.5-34 cm: interbeded silt and clay laminae, silt is 2.5Y 5/4 and 2.5Y 7/2; clay is 2.5Y 3/2; interval has moderte rxn with acid; laminae are deformed, folded, and have burrows

34-39 cm: silt; 2.5Y 6/3, has laminae of coarser silt or vf sand, slight rxn with acid;

39-42 cm: disturbed coarse silt and/or vf sand bed with disturbed clay laminae, silt is 2.5Y 6/4, clay is 2.5Y 3/2; strong rxn with acid;

42-45.5 cm: silt with interbeded clay laminae, silt is 2.5Y 5/4 and 2.5Y 7/2; clay is 2.5Y 3/2; interval has moderate rxn with acid; laminae are deformed

45.5-47 cm: silt; 2.5Y 6/4; moderate moderate rxn with acid; 46-46 has vf black sand that look like truncated climbing ripples

47-48.5 cm: interval has 7 silt-clay couplets; silt is 2.5Y 6/4 and is 1 mm thick; clay is 2.5Y 3/2 and is 0.1 mm thick; strong to very strong rxn with acid;

48.5-48.8 cm: clay laminae; 2.5Y 3/2; relatively undisturbed and horizontal;

45.8-60.5 cm: silt; 2.5Y 6/3; has a few clay laminae; interval is burrowed and appears to be homoginized; strong rxn with acid;

60.5-65 cm: interbeded silt and clay laminae, silt is 2.5Y 6/3; clay is 2.5Y 3/2; beds are relatively horizontal with one slightly folded bed at 64 cm; moderate rxn with acid

65-72.5 cm: silt; 2.5Y 6/3; has broken remnants of clay laminae but interval appears to be homoginized; strong rxn with acid;

72.5-75 cm: interbeded silt laminae, silt is 2.5Y 7/2 and 2.5Y 6/3; beds are relatively horizontal; moderate rxn with acid

Fig. S14 (cont.) Detailed core description of the Combs core shown in Figure S13.

INITIAL CORE DESCRIPTION

LAKE 06-014 Combs Farm
CORE ID 33-35 ft
SECTION LENGTH (cm) 61.0 mblf top 10.06
SED. LENGTH (cm) 68.5 mblf bot 10.74
Describer Ron Counts
Date 01.27.09

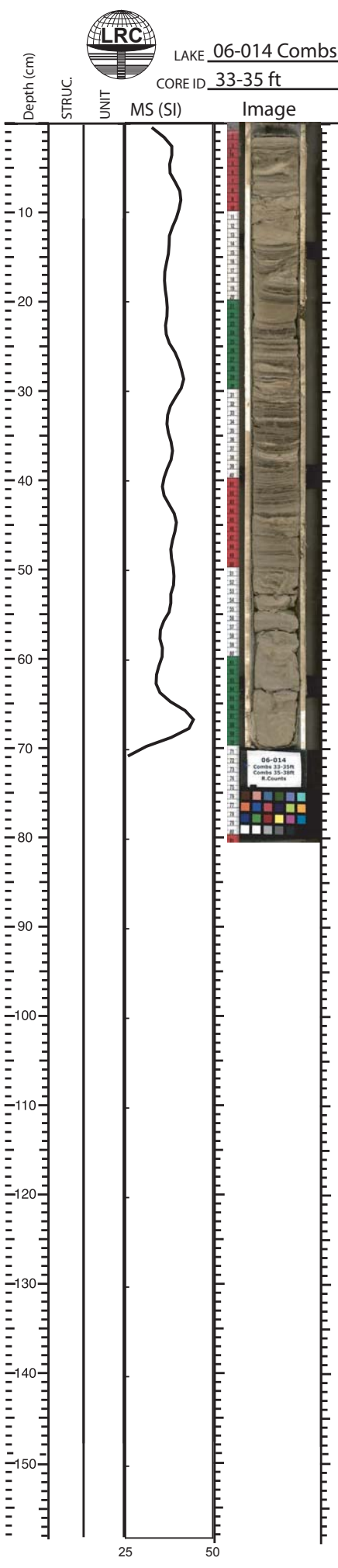

LITHOLOGIC DESCRIPTION

0-2 cm: interbeded silt and clay laminae, silt is 2.5Y 6/3; clay is 2.5Y 4/2; beds are relatively horizontal and undisturbed; moderate rxn with acid

2- 4.5 cm: silt; 2.5Y 5/3 and 2.5Y 6/3; has a few remnant clay laminae; appears to be homoginized by bioturbation; strong rxn with acid;

4.5-7 cm: silt with interbedded clay laminae, silt is 2.5Y 6/3; clay is 2.5Y 4/2; beds are relatively horizontal, clay laminae are slightly broken (minor burrowing?); moderate rxn with acid

7-12 cm: v coarse silt; 2.5Y 5/3 at least one remnant clay laminae; appears to be homoginized by bioturbation; very strong rxn to acid

12-19 cm: interbeded silt and clay laminae, silt is 2.5Y 7/3; clay is 2.5Y 4/2; beds from 12-17 are pushed upward by a large horizontal burrow 5 cm in diameter; beds from 17-19 are horizontal and undisturbed are relatively horizontal and undisturbed; strong rxn to acid

19-21 cm: v coarse silt; 2.5Y 6/3; very strong rxn to acid

21-42 cm: interbeded silt and clay laminae, silt is 2.5Y 6/3; clay is 2.5Y 4/2; beds are relatively horizontal but some are wavy (SSD?), vertical burrow from 26-29 cm; interval has numerous small burrows >1 cm; very strong rxn to acid

42-48.5 cm: silt with interbedded clay laminae, silt is 2.5Y 5/3; clay is 2.5Y 4/2; clay laminae are wavy but relatively horizontal, some clay laminae are broken or discontinuous (minor burrowing?); slight to moderate rxn with acid

48.5-51 cm: silt with interbedded clay laminae, silt is 2.5Y 5/3; clay is 2.5Y 4/2; clay laminae are deformed upward by liquefaction or de-gassing of underlying unit; slight to moderate rxn with acid

51-53 cm: vc silt and vf sand; 2.5Y 6/3; slight to moderate rxn with acid

53-63.5: silt; with interbedded clay laminae, silt is 2.5Y 6/3; clay is 2.5Y 4/2; clay laminae at 57 cm has load structure; slight rxn with acid

63.5-65: vf sand; 2.5y 5/3; very slight rxn with acid

65-68.5 cm: vc silt and vf sand; 2.5Y 6/3; slight to moderate rxn with acid; bioturbated

Fig. S14 (cont.) Detailed core description of the Combs core shown in Figure S13.

INITIAL CORE DESCRIPTION

LAKE 06-014 Combs Farm
CORE ID 35-38 ft
SECTION LENGTH (cm) 91.4 mblf top 10.7
SED. LENGTH (cm) 67.5 mblf bot 11.3
Describer Ron Counts
Date 01.27.09

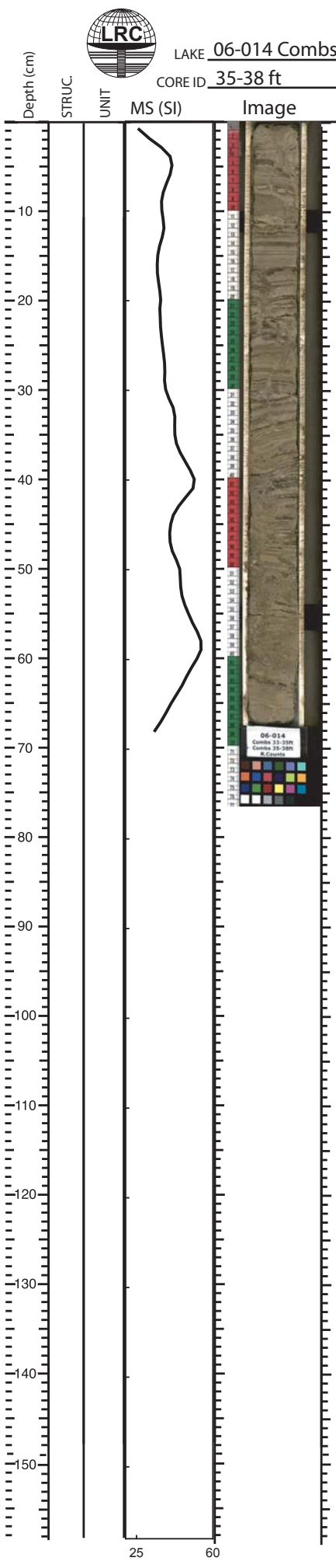

LITHOLOGIC DESCRIPTION

0-8 cm: interbeded silt and clay laminae, silt is 2.5Y 5/3; clay is 2.5Y 4/1; interval has vertical burrows or root casts filled with vf sand from overlying interval, moderate rxn to acid

8-10.5 cm: silt; 2.5Y 5/3; vertical burrow or root at core edge filled with vf sand from overlying interval, moderate rxn to acid

10.5-13 cm: interbeded silt and clay laminae, silt is 2.5Y 7/3; clay is 2.5Y 4/1; interval has vertical burrows or root casts filled with vf sand from overlying interval, moderate rxn to acid

13-16.5 cm: silt with interbedded clay laminae, silt is 2.5Y 5/3; clay is 2.5Y 4/1; laminae are horizontal and undisturbed; moderate rxn to acid

16.5-65.5 cm: interbeded silt and clay laminae, silt is 2.5Y 5/3 and 2.5Y 6/1; clay laminae are 2.5Y 4/1; interval has many vertical burrows and bioturbated zones; vf sand from 30-31 cm; interval has slight to moderate rxn to acid

65.5-67.5 cm: silt; 2.5Y 5/3; remnant clasts of clay laminae still visible; zone has been homoginized by bioturbation; slight rxn to acid

Fig. S14 (cont.) Detailed core description of the Combs core shown in Figure S13.

INITIAL CORE DESCRIPTION

LAKE 06-014 Combs Farm
CORE ID 38-40 ft
SECTION LENGTH (cm) 61.0 mblf top 11.6
SED. LENGTH (cm) 68.0 mblf bot 12.3
Describer Ron Counts
Date 01.27.09

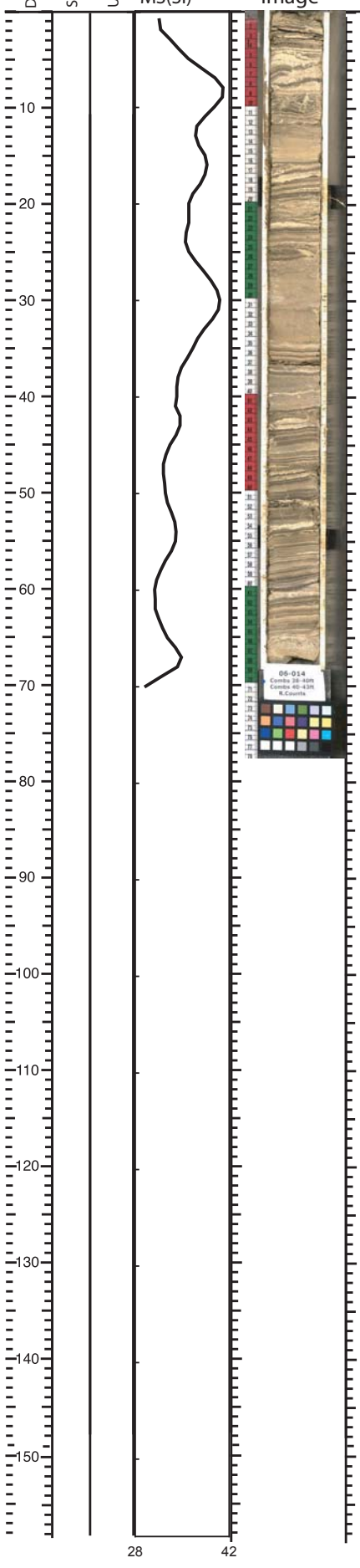

LITHOLOGIC DESCRIPTION

0-4 cm: interbeded silt and clay laminae, silt is 2.5Y 5/3; clay laminae are 2.5Y 4/2; interval from 0-3 cm is bioturbated, interval from 3-4 cm is undisturbed; moderate rxn to acid

4-9 cm: silt with clay laminae, silt is 2.5Y 6/3; clay laminae are 2.5Y 4/2; clay laminae are disturbed from bioturbation; moderate rxn to acid

6-7 cm: interbeded silt and clay laminae, silt is 2.5Y 5/3; clay laminae are 2.5Y 4/2; right half of interval had been destroyed by horizontal burrowfrom 3-4 cm is undisturbed; moderate rxn to acid

9-11 cm: interbeded silt and clay laminae, silt is 2.5Y 5/3; clay laminae are 2.5Y 4/2; interval disrupted by vertical burrows; slight rxn to acid

11-13 cm: silt with clay laminae, silt is 2.5Y 6/3; clay laminae are 2.5Y 4/2; clay laminae are disturbed from small vertical burrows; moderate rxn to acid

13-16 cm: silt; 2.5Y 5/3, slight rxn to acid

16-18 cm: silt with clay laminae, silt is 2.5Y 6/3; clay laminae are 2.5Y 4/1; clay laminae are disturbed from bioturbation; slight rxn to acid

22.5-24 cm: interbeded silt and clay laminae, silt is 2.5Y 6/3; clay laminae are 2.5Y 4/1; interval undisturbed; slight rxn to acid

20-22.5 cm: silt with clay laminae, silt is 2.5Y 6/3; clay laminae are 2.5Y 4/1; clay laminae are slightly disrupted (bioturbation or dessication?); interval from 22-22.5 is vc silt; slight to moderate rxn to acid

22.5-24 cm: interbeded silt and clay laminae, silt is 2.5Y 6/3; clay laminae are 2.5Y 4/1; interval undisturbed; slight rxn to acid

24-26.5 cm: interbeded silt and clay laminae, silt is 2.5Y 6/3; clay laminae are 2.5Y 4/1; interval disrupted by horizontal burrow and bioturbation, slight rxn to acid

26.5-35 cm: coarse silt from 26.5-31.0 cm; 2.5Y 5/3; moderate rxn to acid; finer silt from 31.2-35 cm; 2.5Y 6/3; slight to moderate rxn to acid; silts are seprerated by several horizontal clay laminae that are microns thick,

35-38 cm: interbeded silt and clay laminae, silt is 2.5Y 6/3; clay laminae are 2.5Y 4/1; laminae are horizontal and undisturbed except for disrupted laminae from 37-37.5; slight rxn to acid

38-41.5 cm: silt from 38-40 cm; 2.5Y 5/3; slight to moderate rxn to acid; coarser silt from 40-41.5 cm; 2.5Y 5/3; moderate rxn to acid; silts are seprerated by several slightly disrupted clay laminae

41.5-54 cm: interbedded silt and clay laminae, silts are 2.5Y 5/3 and 2.5Y 6/3; clay laminae are 2.5Y 4/1 and 2.5Y 4/2; slight to moderate rxn to acid throughout interval; interval contains wide, vertical burrows and very narrow vertical burrows or root casts

54-65 cm: interbedded silt and clay laminae, silts are 2.5Y 5/3 and 2.5Y 7/2, and from 59.5-60 cm silt is 2.5Y 6/1; beds are horizontal and undisturbed except for a few, very narrow vertical root casts; moderate rxn to acid

65-66 cm: interbedded silt and clay laminae, silt is 2.5Y 6/3; clay is 2.5Y 4/1; clay laminae are disrupted; beds are horizontal and undisturbed except for a few, very narrow vertical root casts; slight to moderate rxn to acid

66-68 cm: vc silt and/or vf sand; 2.5Y 5/3; moderate rxn to acid

Fig. S14 (cont.) Detailed core description of the Combs core shown in Figure S13.

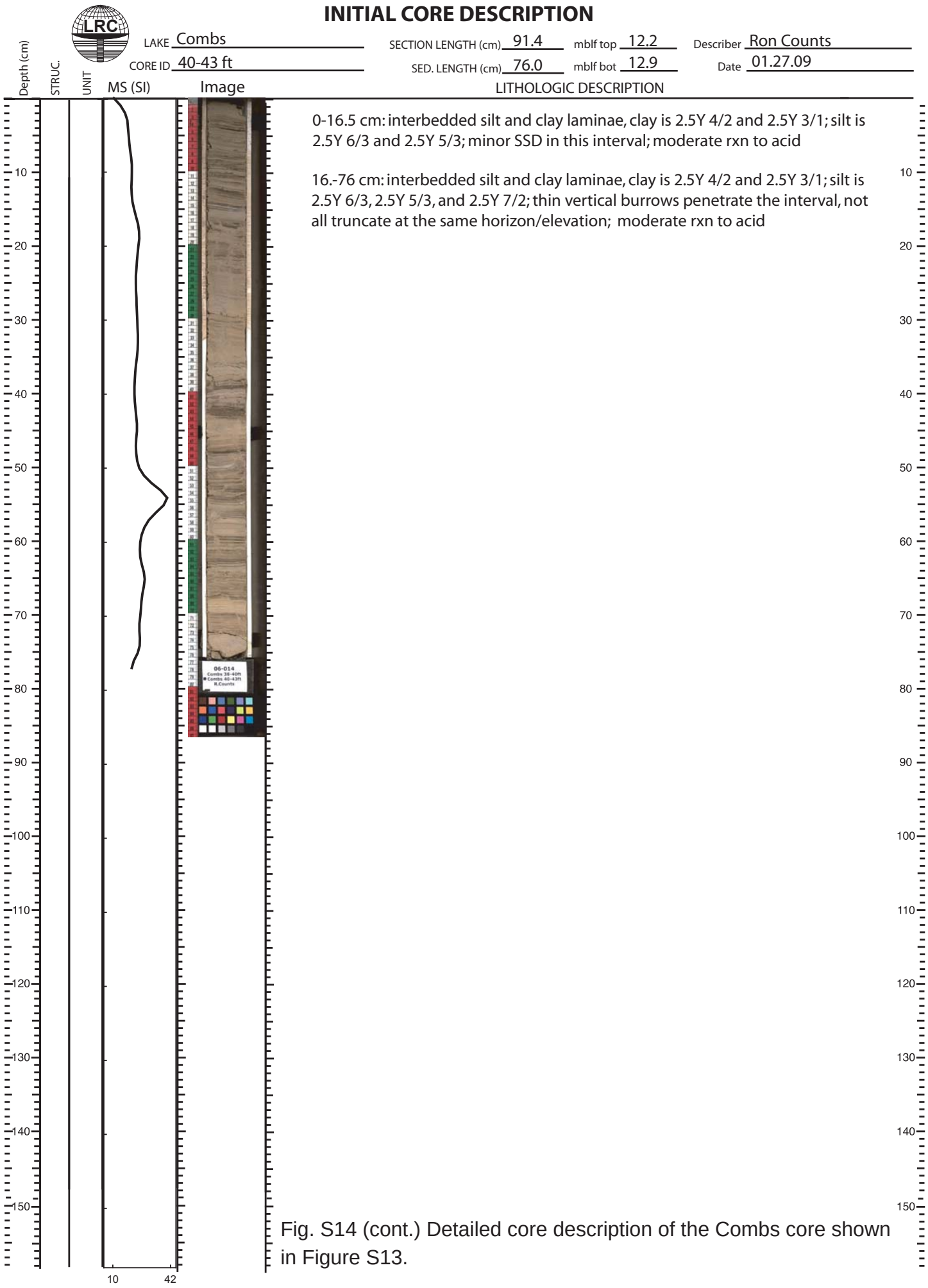

Fig. S14 (cont.) Detailed core description of the Combs core shown in Figure S13.

INITIAL CORE DESCRIPTION

LAKE 06-014 Combs Farm | SECTION LENGTH (cm) 61 | mblf top 13.1 | Describer Ron Counts

CORE ID 43-45 ft | SED. LENGTH (cm) 61 | mblf bot 13.7 | Date 01.27.09

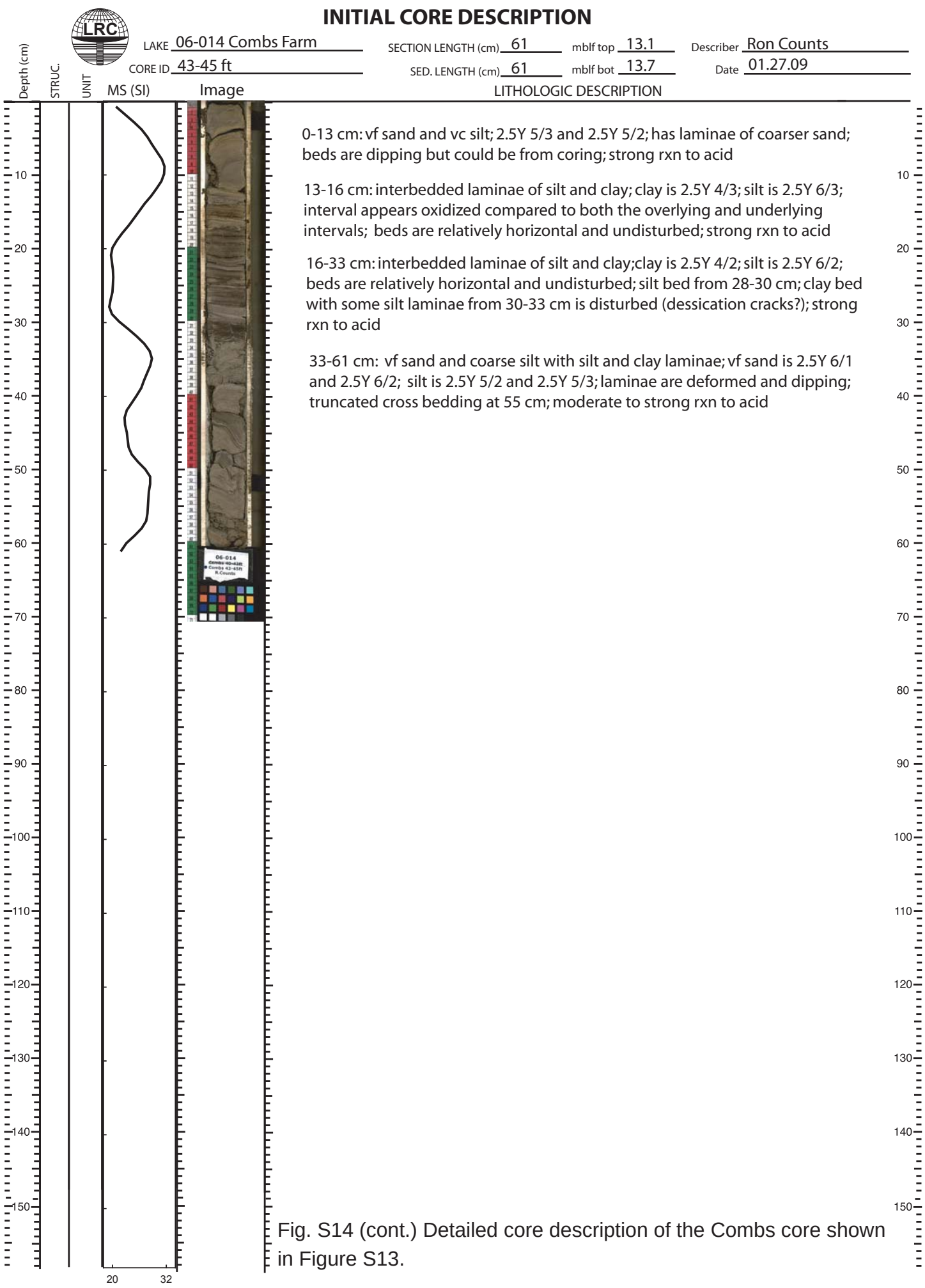

Fig. S14 (cont.) Detailed core description of the Combs core shown in Figure S13.

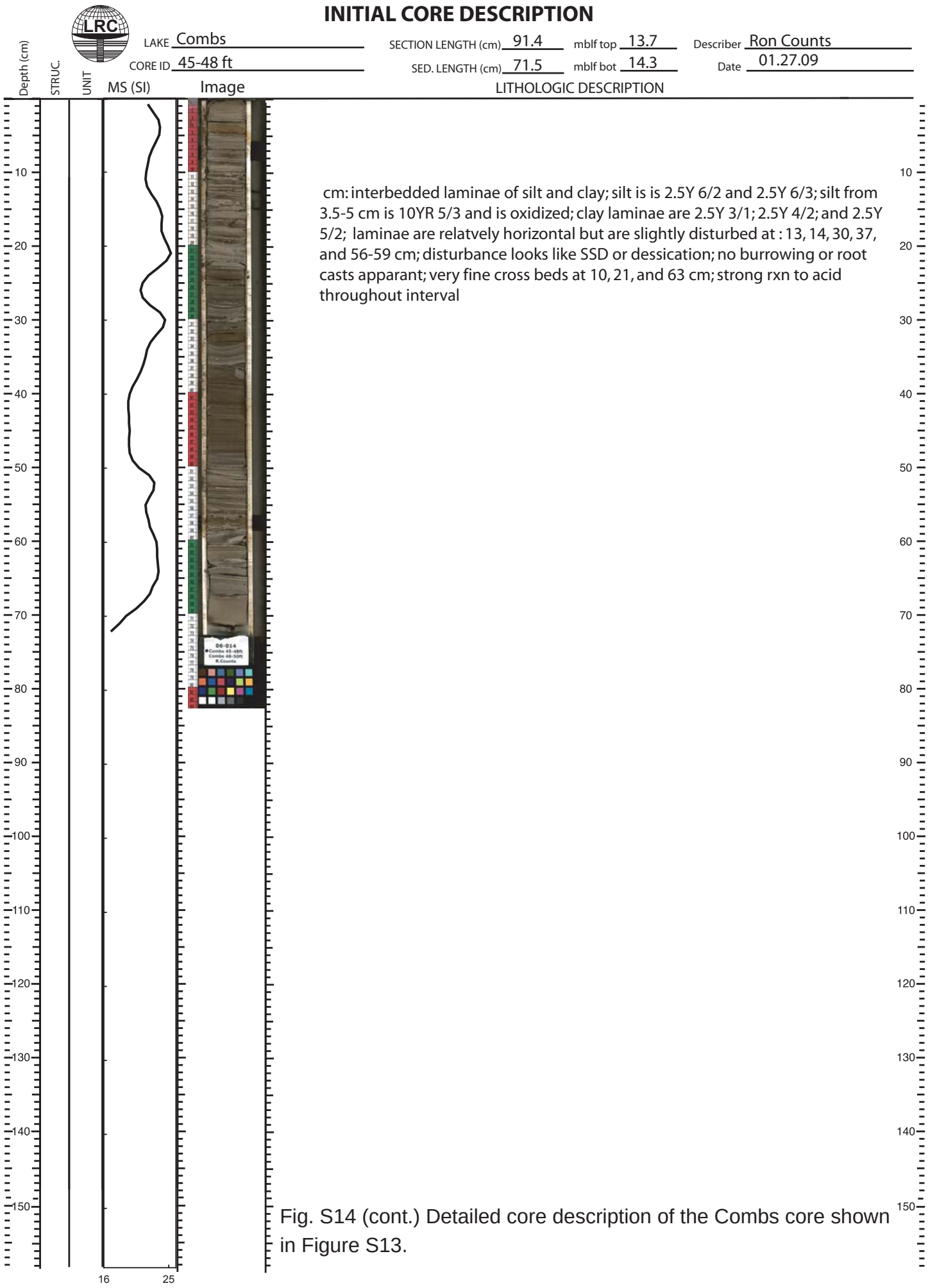

Fig. S14 (cont.) Detailed core description of the Combs core shown in Figure S13.

INITIAL CORE DESCRIPTION

LAKE Combs
CORE ID 48-50 ft
SECTION LENGTH (cm) 61.0 mblf top 14.6
SED. LENGTH (cm) 58.5 mblf bot 15.2
Describer Ron Counts
Date 01.27.09

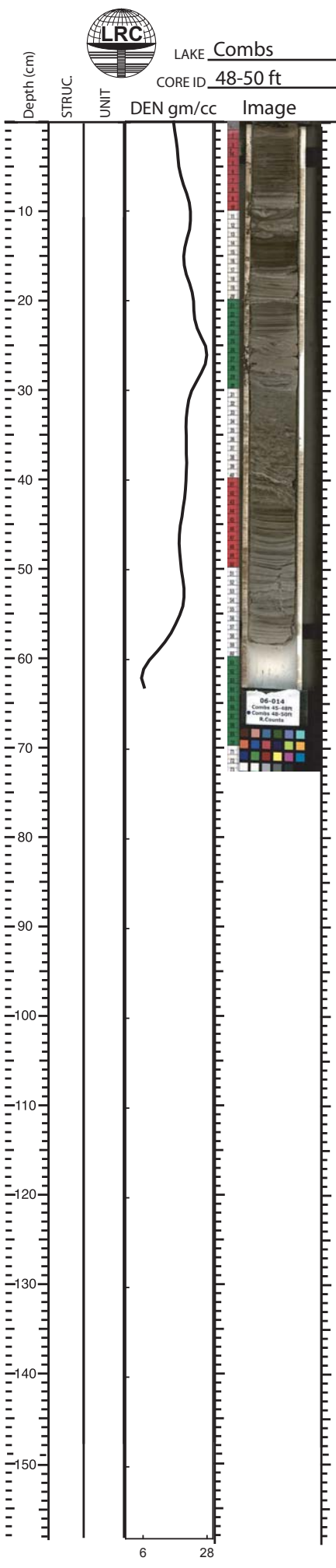

LITHOLOGIC DESCRIPTION

0-17 cm: clay beds with thin silt laminae; silt laminae are 2.5Y 6/2; clay is 2.5Y 3/1; interval is very slightly disturbed; silt bed with clay laminae from 8.5-10 cm; zone from 10-13 is folded and has augen structures; moderate to strong rxn to acid

17-24 cm: laminations of silt and clay; silt laminae are 2.5Y 6/2; clay laminae are 2.5Y 3/1; laminae are horizontal and undisturbed; moderate to strong rxn to acid

24-26 cm: vf sand with silt and clay laminae; sand is 2.5Y 6/2; slight to moderate rxn to acid

26-28 cm: vc silt, 2.5Y 5/2; moderate rxn to acid

28-30 cm: laminations of silt and clay; silt laminae are 2.5Y 6/2; clay laminae are 2.5Y 3/1; laminae are disturbed (dessication?); moderate rxn to acid

30-34 cm: silt and clay, heavily bioturbated, dominate color is 2.5Y 5/2; moderate rxn to acid

34-43 cm: laminations of silt and clay; silt laminae are 2.5Y 6/2 and one is 2.5Y 7/2; clay laminae are 2.5Y 3/1; laminae are broken and rotated (rip-up clasts or possibly dessication; moderate to strong rxn to acid

43-48.5 cm: laminations of silt and clay; silt laminae are 2.5Y 6/2; clay laminae are 2.5Y 3/1; laminae are horizontal and undisturbed; moderate rxn to acid

48.5-58.5 cm: laminations of silt and clay; silt laminae are 2.5Y 6/2; clay laminae are 2.5Y 3/1; laminae are slightly disrupted and interval from 51-55 cm is penetrated by 2 vertical burrows; moderate to strong rxn to acid

Fig. S14 (cont.) Detailed core description of the Combs core shown in Figure S13.

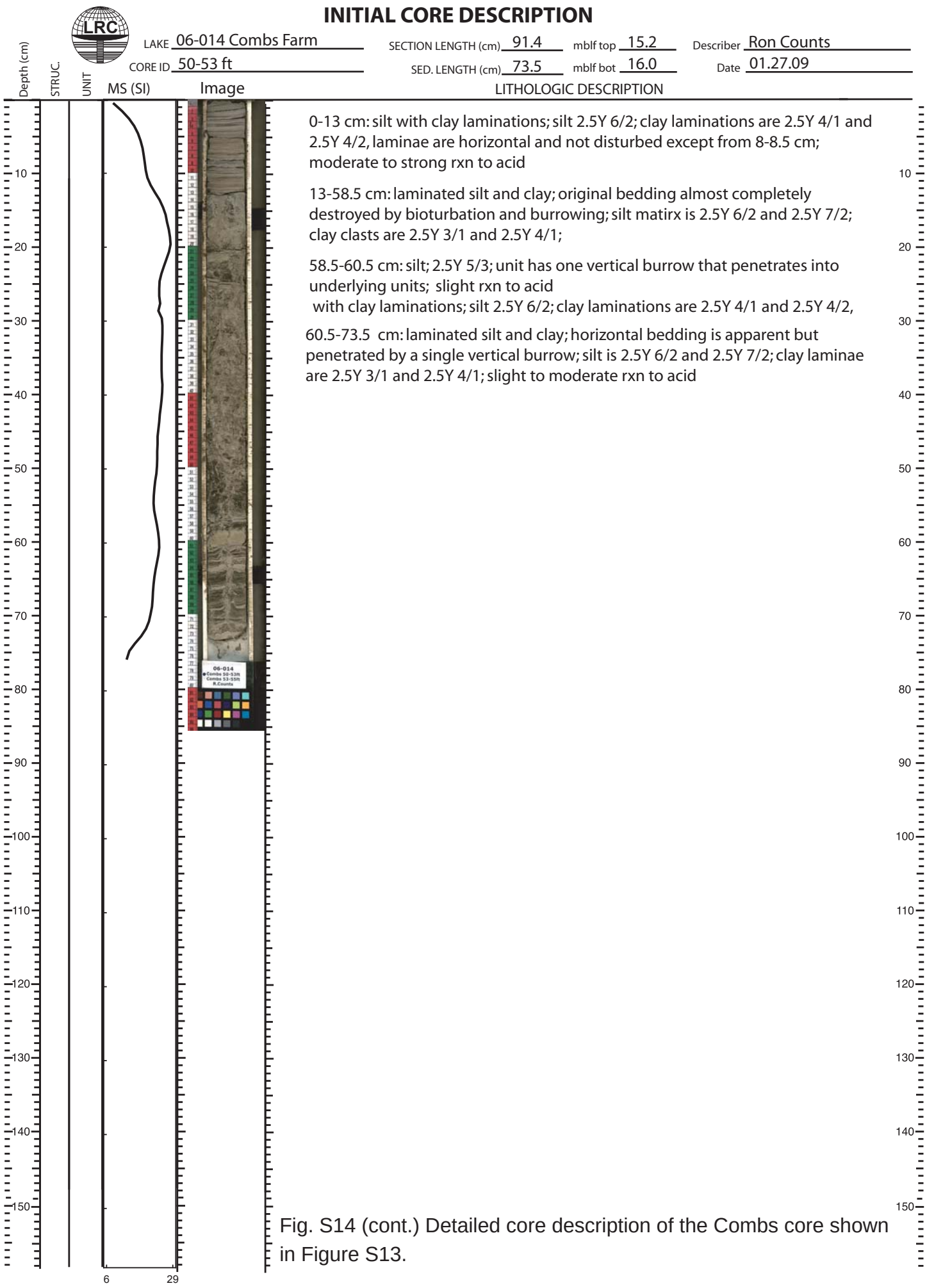

Fig. S14 (cont.) Detailed core description of the Combs core shown in Figure S13.

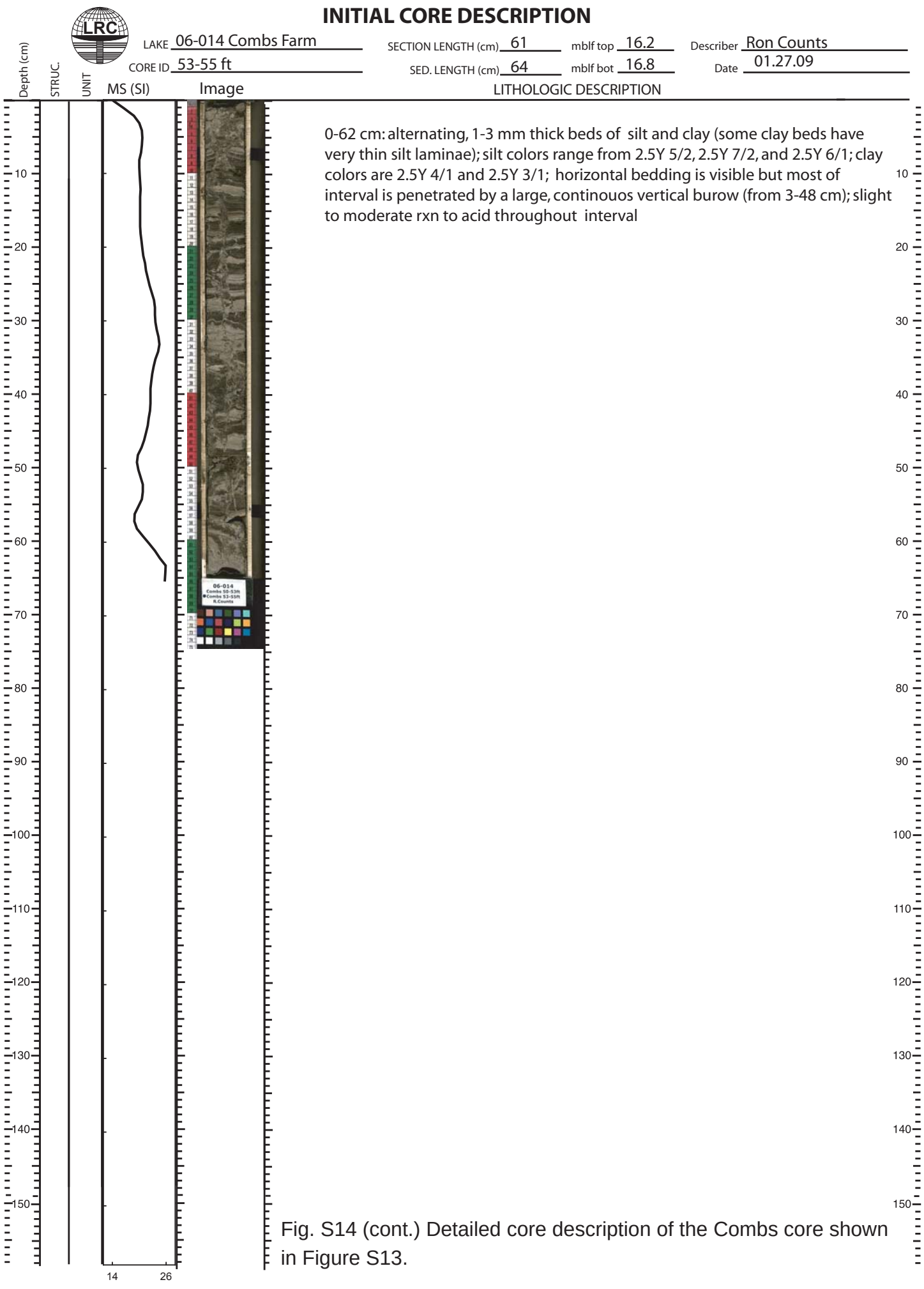

Fig. S14 (cont.) Detailed core description of the Combs core shown in Figure S13.

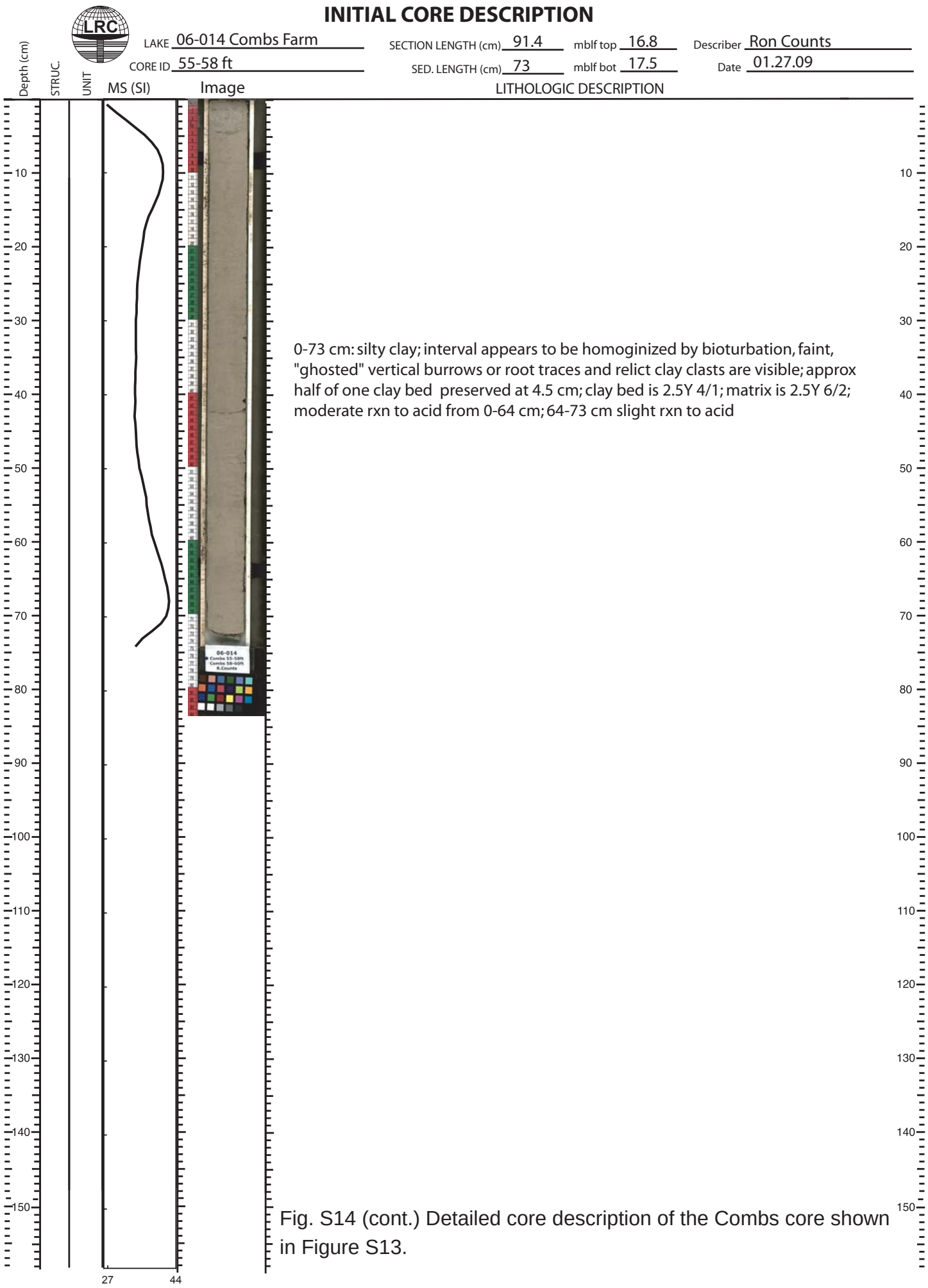

Fig. S14 (cont.) Detailed core description of the Combs core shown in Figure S13.

INITIAL CORE DESCRIPTION

LAKE 06-014 Combs Farm
CORE ID 58-60 ft
SECTION LENGTH (cm) 61 mblf top 17.7 Describer Ron Counts
SED. LENGTH (cm) 64 mblf bot 18.3 Date 01.27.09

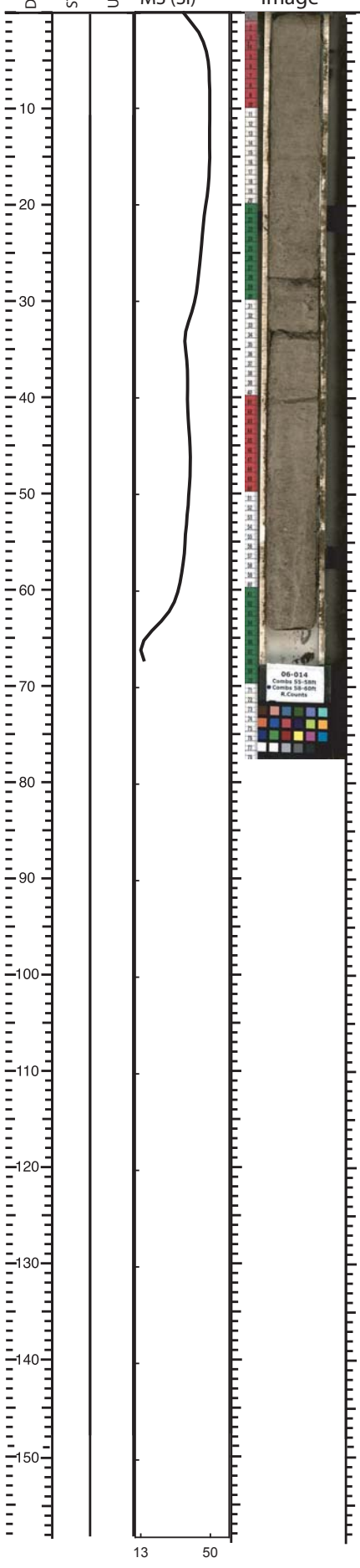

LITHOLOGIC DESCRIPTION

0-4 cm: clayey silt; 2.5Y 6/2; interval appears to be homoginized by bioturbation, faint, "ghosted" vertical burrows or root traces and relict clay clasts are visible; slight rxn to acid

4-64 cm: silty clay; 2.5Y 6/2; interval appears to be homoginized by bioturbation, faint, "ghosted" vertical burrows or root traces and relict clay clasts are visible throughout core, (though fewer clay clast relicts are visibe from 4-17cm);silt beds less than 1 cm thick lie at 28; 33.5, and 41.5 cm; moderate rxn to acid;

Fig. S14 (cont.) Detailed core description of the Combs core shown in Figure S13.

INITIAL CORE DESCRIPTION

LAKE 06-014 Combs Farm
CORE ID 60-63 ft
SECTION LENGTH (cm) 91.4 mblf top 18.3
SED. LENGTH (cm) 72.5 mblf bot 19.0
Describer Ron Counts
Date 01.27.09

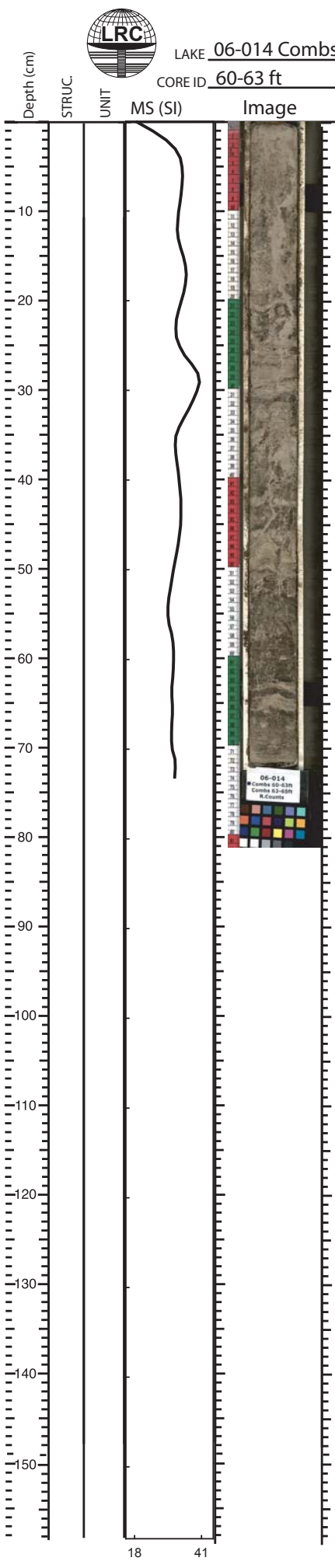

LITHOLOGIC DESCRIPTION

0-5 cm: clayey silt; 2.5Y 6/2; interval appears homoginized by bioturbation, faint, "ghosted" vertical burrows or root traces and relict clay clasts are visible ; slight to moderate rxn to acid

5-18.5 cm; clayey silt; interval is heavily bioturbated and original bedding is mostly destroyed but appears to have been laminated silt and clay; clay zones are 2.5Y 3/1; matrix is 2.5Y 6/2; slight to moderate rxn to acid
vertical disturbance that gets narrow with depth (root trace) extends from 7-66 cm;

18.5-35cm: laminated clay and silt beds, silt is 2.5Y 6/2 and clay is 2.5Y 4/1; interval disturbed by bioturbation and root trace but original bedding is not completely destroyed and discernable; silt bed from 27-29 cm; moderate rxn to acid

35-51 cm: laminated clay and silt beds, silt is 2.5Y 6/2 and clay is 2.5Y 4/1; interval disturbed by bioturbation and root trace but original bedding primarily destroyed and not readily visible except fropm 43-46 cm; moderate rxn to acid

51-72-5 cm: primarily clay with silt laminae; clay is 2.5Y 4/1; silt laminae are 2.5Y 6/2; interval disturbed by bioturbation and root trace but original bedding is not completely destroyed and discernable; silt beds (not laminae from 63.5-64 cm and 65-66.5 cm; moderate to strong rxn to acid

Fig. S14 (cont.) Detailed core description of the Combs core shown in Figure S13.

INITIAL CORE DESCRIPTION

LAKE Combs | SECTION LENGTH (cm) 61 | mblf top 19.2 | Describer Ron Counts

CORE ID 63-65 ft | SED. LENGTH (cm) 52 | mblf bot 19.7 | Date 01.27.09

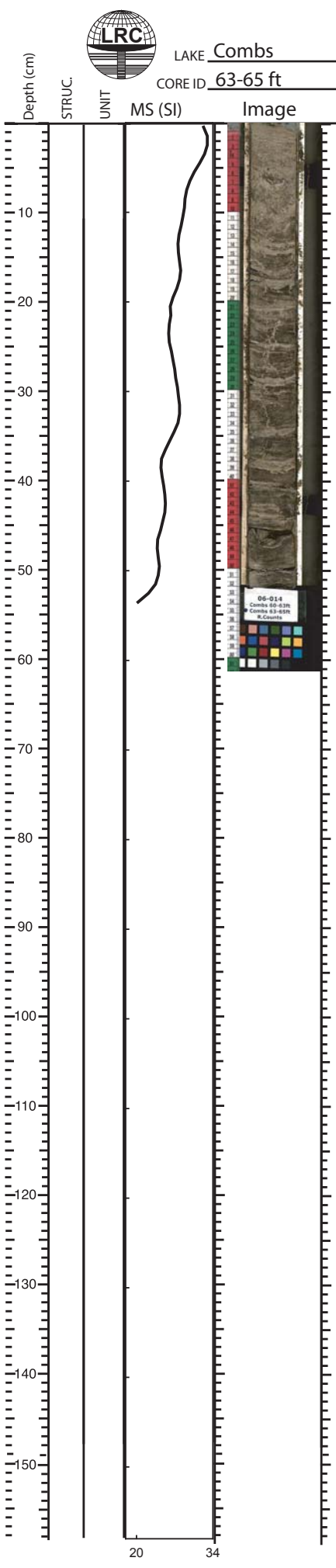

LITHOLOGIC DESCRIPTION

0-13 cm: clayey silt to silty clay; interval is heavily bioturbated and original bedding is destroyed except for a few laminae from 1-2 cm; matrix is 2.56Y 6/2; clay clasts are 2.5Y 4/1; very strong rxn to acid

13-38 cm; primarily clay beds (with very fine laminae of silt) with laminae of silt; silt is 2.5 Y 6/2; clay is 2.5Y 4/2; original bedding is not completely destroyed and discernable but is mildly bioturbatedand contains multiple, thin,vertical root traces or burrows; very strong rxn to acid

38-39 cm: silty zone with clay clasts and Fe concretions; silt is 2.5 Y 6/2; clay is 2.5Y 4/2; very strong rxn to acid

39-52 cm: laminated clay and silt beds, silt is 2.5Y 6/2 and clay is 2.5Y 4/1; SSD features (load structures and folded sediment) in this interval but lacks bioturbation seen in overlying interval; strong rxn to acid

Fig. S14 (cont.) Detailed core description of the Combs core shown in Figure S13.

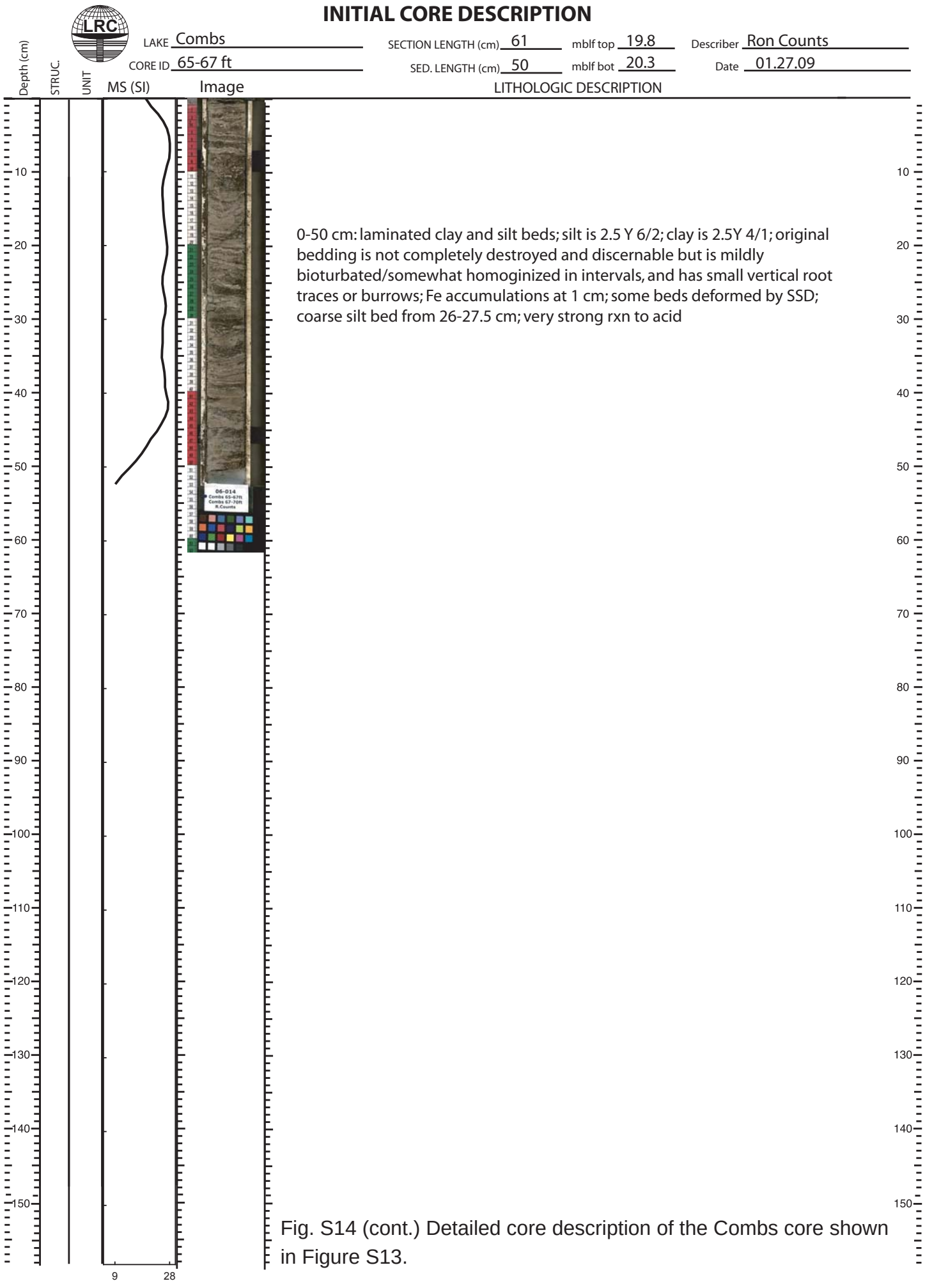

Fig. S14 (cont.) Detailed core description of the Combs core shown in Figure S13.

INITIAL CORE DESCRIPTION

LAKE Combs | SECTION LENGTH (cm) 91.4 | mblf top 20.4 | Describer Ron Counts

CORE ID 67-70 ft | SED. LENGTH (cm) 73.5 | mblf bot 21.2 | Date 01.27.09

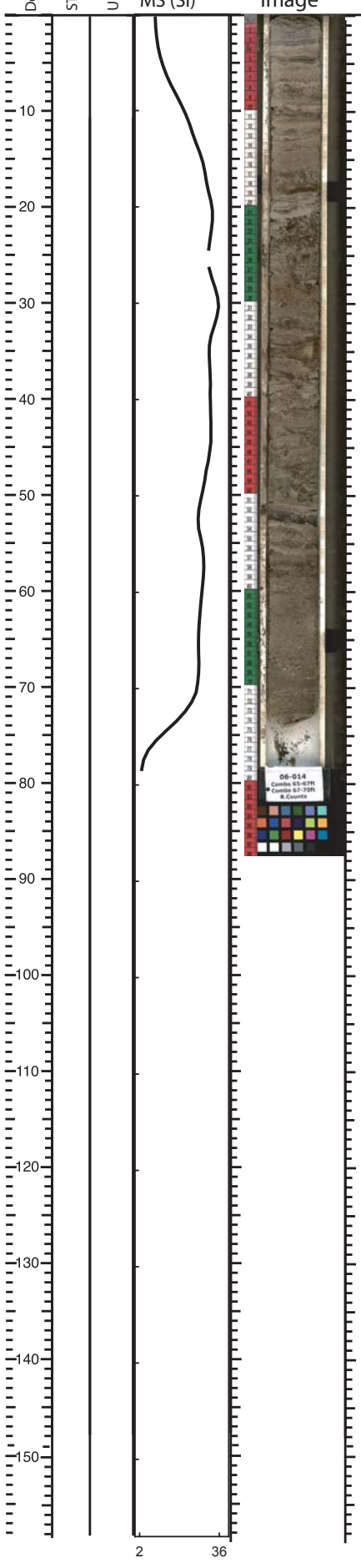

LITHOLOGIC DESCRIPTION

0-2 cm: fine silt; 2.5Y 6/1; very strong rxn with acid

2-5 cm: laminated clay and silt beds; silt is 10YR 5/210YR 6/3; clay is 10YR 4/1; beds are horizontal and undisturbed; strong rxn to acid

5-59 cm: interval is heavily bioturbated and original bedding is mostly destroyed but appears to have been laminated silt and clay; clay clasts are 10YR 4/2 and 10YR 4/1; silt is 10YR 6/2 and 2.5Y 6/2; oxidized zones are at 18, 29, and 35 cm; gastropod shell at 45.5 cm; weathered green lithic clast 1.3 x 3.8 mm at 58 cm; silt has strong rxn to acid, clay clasts have moderate rxn to acid; interval from 50.5-52 is undisturbed

59-73.5 cm: silt; interval is extremely bioturbated and original bedding is totally destroyed; matrix is 2.5Y 5/2 and 2.5Y 6/2; clay clasts are 2.5Y 4/1; gastropod shell at 68.5 cm; rounded, green, weathered lithic clast measuring 3.8 x 3.1 mm at 69 cm; strong rxn to acid

Fig. S14 (cont.) Detailed core description of the Combs core shown in Figure S13.

INITIAL CORE DESCRIPTION

LAKE Combs | SECTION LENGTH (cm) | mblf top 21.3 | Describer Ron Counts

CORE ID 70-75 ft | SED. LENGTH (cm) 120 | mblf bot 22.5 | Date 01.27.09

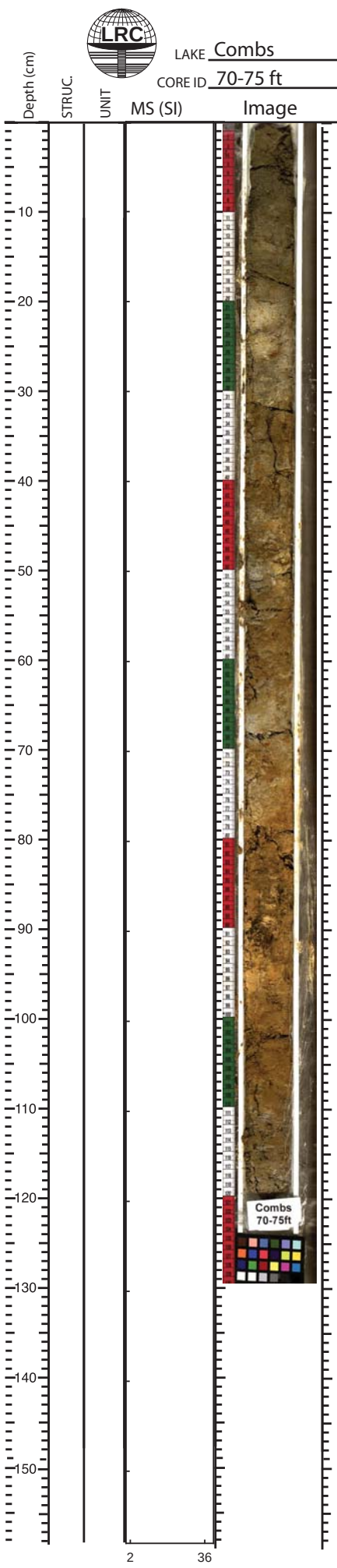

0-16 cm: silt to silt loam; 2.5Y 6/2; bioturbated but some originan bedding is visible; moderate rxn with acid

16-31 cm: silt to silty clay; 5Y 7/1; no rxn to acid; appears to be top of a paleosol

31-120 cm: interval is heavily bioturbated and mottled, original bedding is mostly destroyed; but appears to have been laminated silt and clay; matrix is 10YR 5/8; with 5Y 7/1 mottles

Fig. S14 (cont.) Detailed core description of the Combs core shown in Figure S13.

INITIAL CORE DESCRIPTION

LAKE Combs | SECTION LENGTH (cm) | mblf top 22.9 | Describer Ron Counts

CORE ID 75-80 ft | SED. LENGTH (cm) 153 | mblf bot | Date 01.27.09

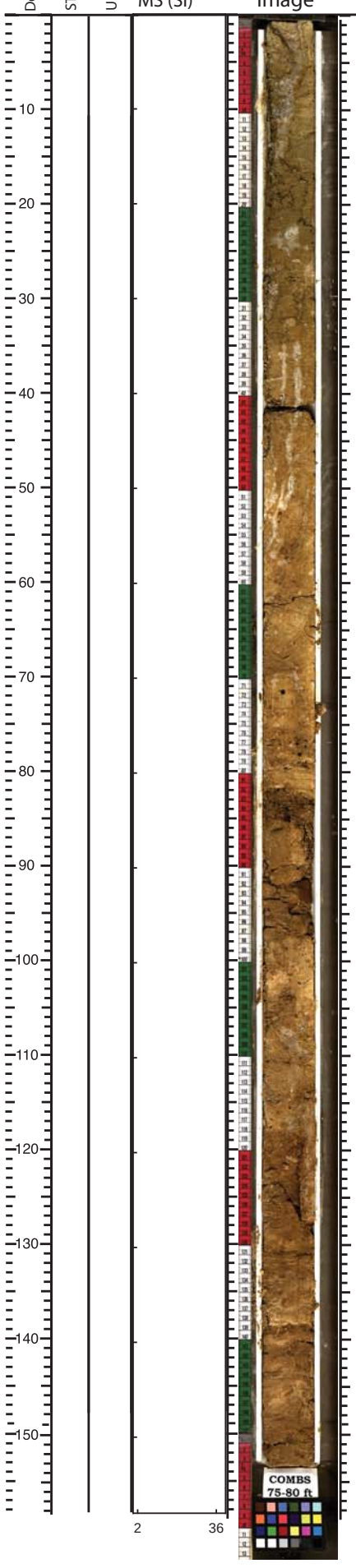

Fig. S14 (cont.) Detailed core description of the Combs core shown in Figure S13.

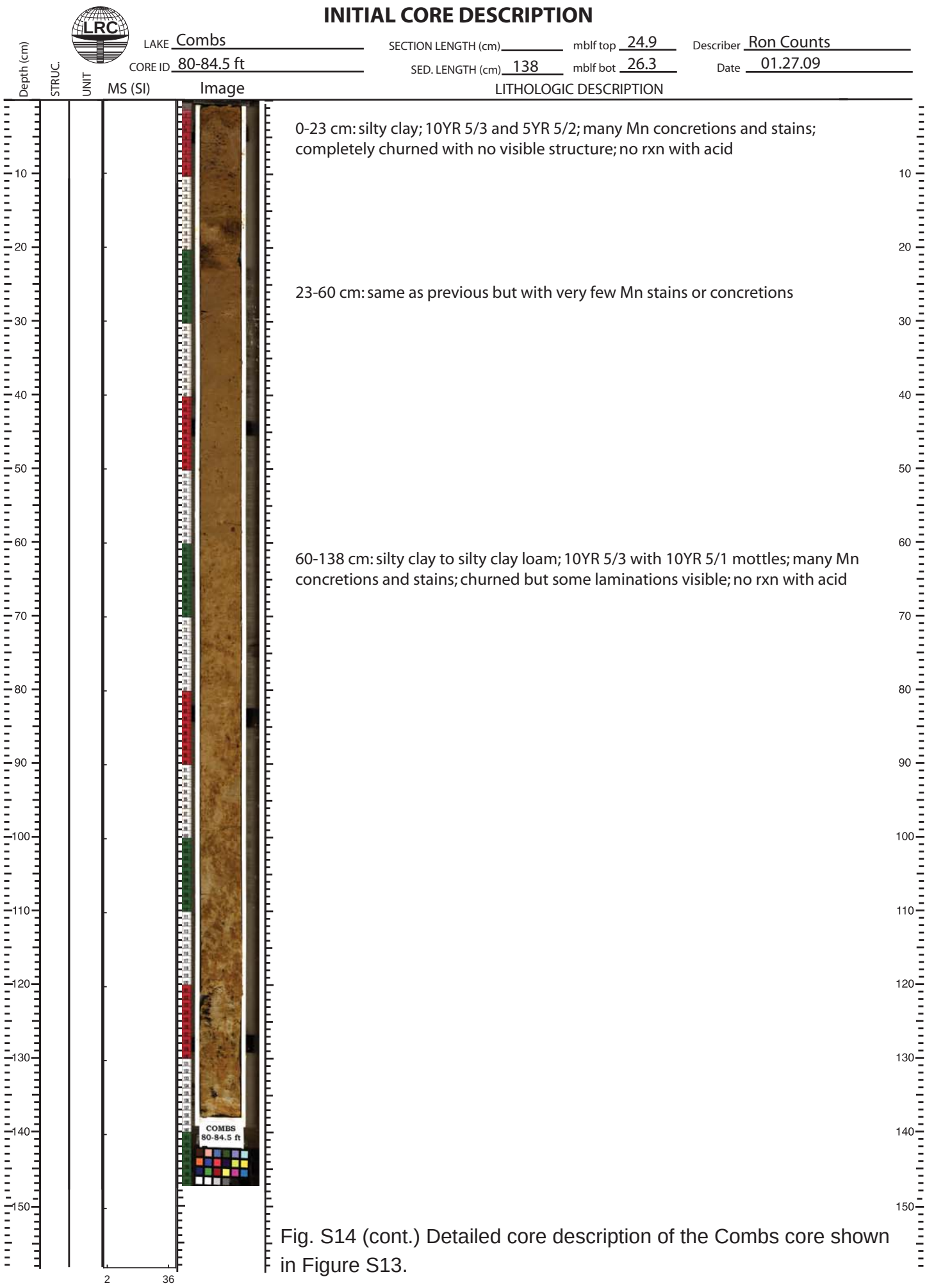

Fig. S14 (cont.) Detailed core description of the Combs core shown in Figure S13.

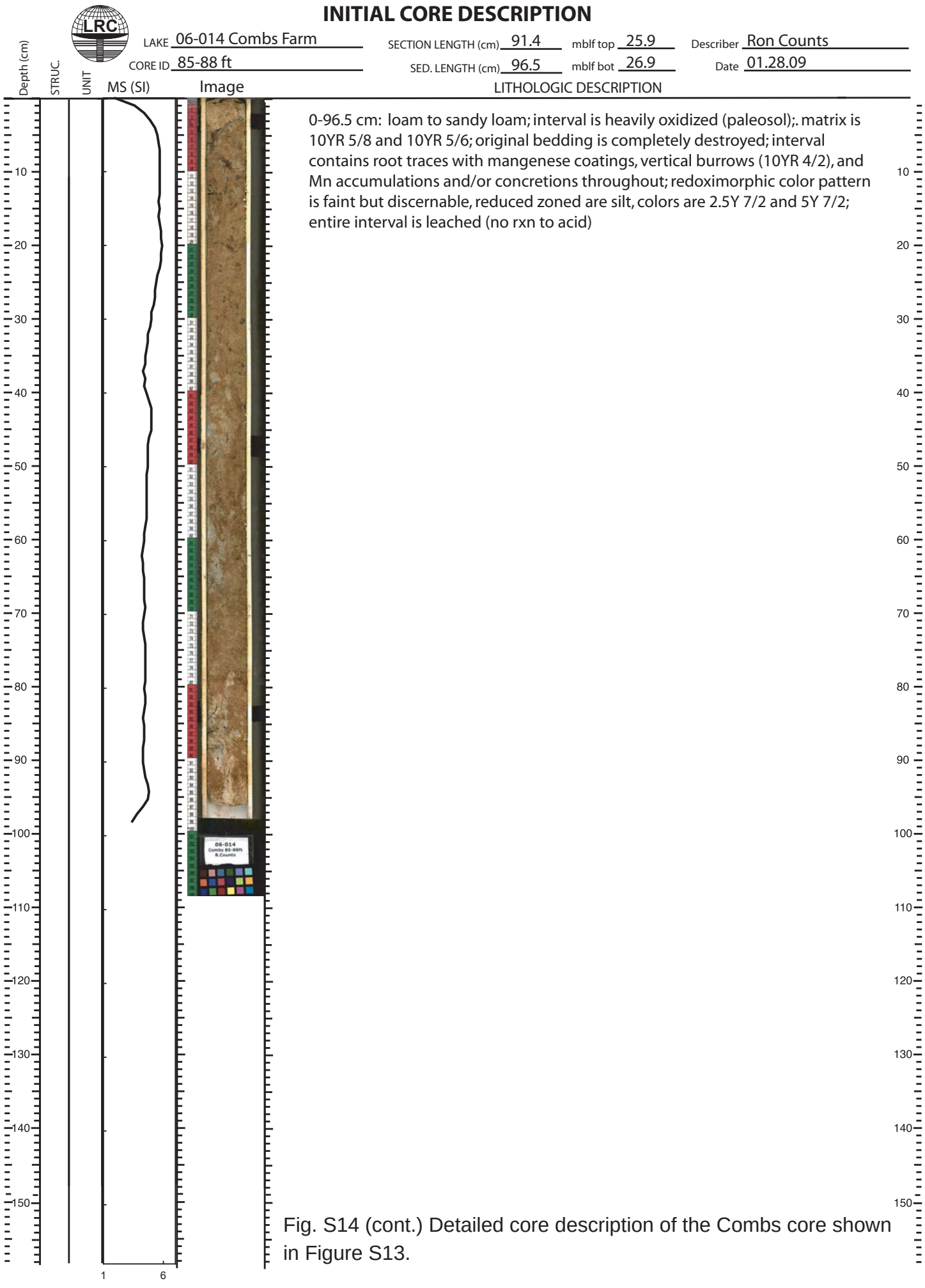

Fig. S14 (cont.) Detailed core description of the Combs core shown in Figure S13.

INITIAL CORE DESCRIPTION

LAKE 06-014 Combs Farm | SECTION LENGTH (cm) 61 | mblf top 26.8 | Describer Ron Counts

CORE ID 88-91 ft | SED. LENGTH (cm) 70 | mblf bot 27.5 | Date 01.28.09

Depth (cm) | STRUC. | UNIT | MS (SI) | Image | LITHOLOGIC DESCRIPTION

0-42 cm: loamy sand; interval is heavily oxidized; original bedding is completely destroyed by bioturbation; matrix has many small areas of variable color (clasts of clay beds or chemical precipitates?); matrix is 10YR 5/8, 10YR 6/8, and 10YR 6/6; clats or colored zones in matrix are 2.5Y 7/3, 2.5Y 6/4, and 2.5Y 7/3; interval has a large vertical root cast or burrow (2.5Y 7/3) from 0-21 cm that has 2 wood fragments that have been converted to Mn; interval from 29-38 cm appears to be a horizontal burrow (2.5Y 7/3); totally leached (no rxn to acid)

42-51 cm: loamy sand; 10YR 6/8; appears to have originally had clay laminae; bedding is disrupted by bioturbation but relict bedding is visible; totally leached (no rxn to acid)

51-70 cm: very fine, well sorted sand , interval from 51-65 is oxidized or iron stained (2.5Y 7/4) with a sharp contact at 65.5 cm (groundwater?); 65.5-70 cm is 2.5Y 7.5/1; interval is totally leached (looks like a dune sand or weathered Pennsylvanian sandsone)

Fig. S14 (cont.) Detailed core description of the Combs core shown in Figure S13.

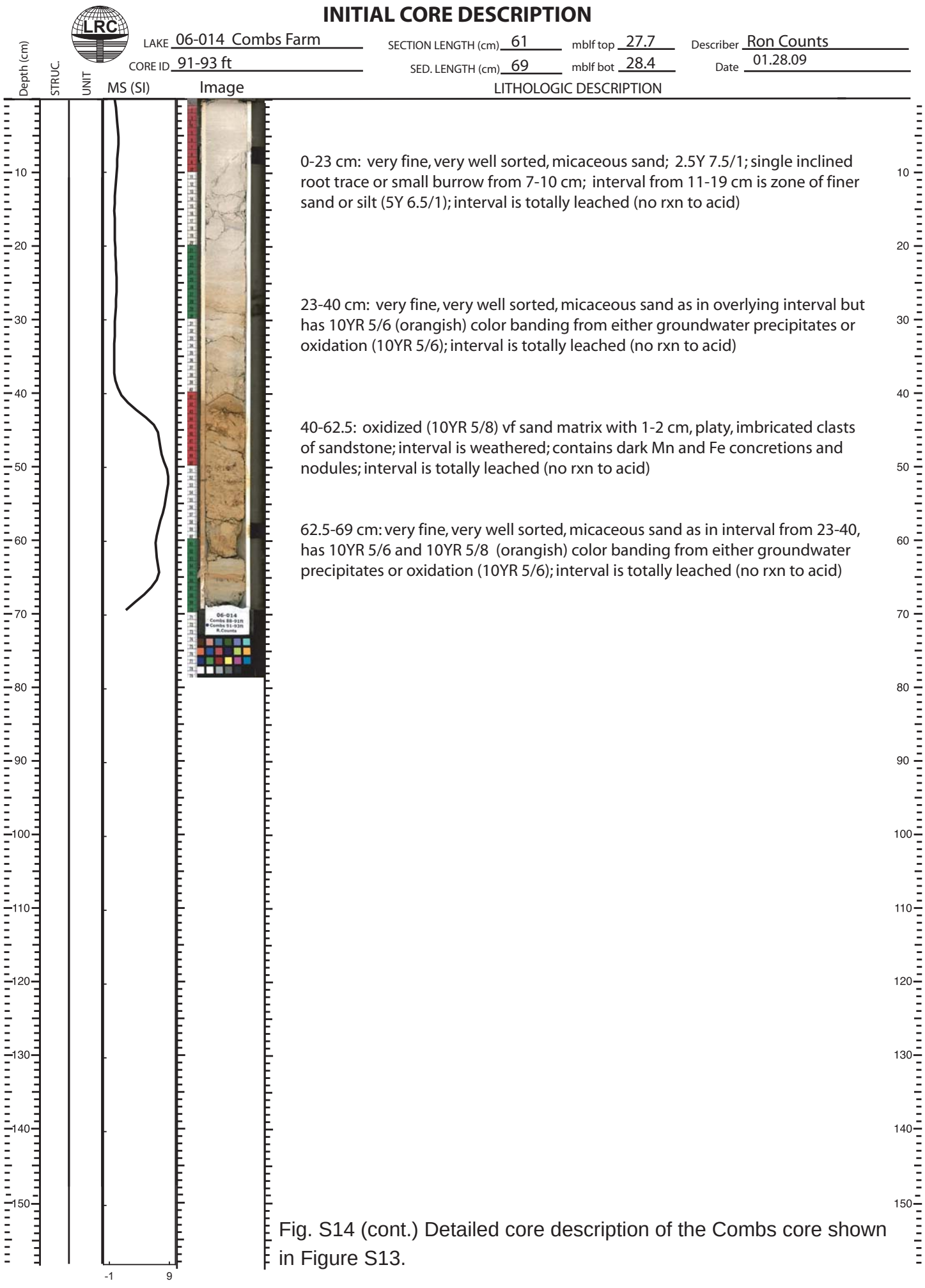

Fig. S14 (cont.) Detailed core description of the Combs core shown in Figure S13.

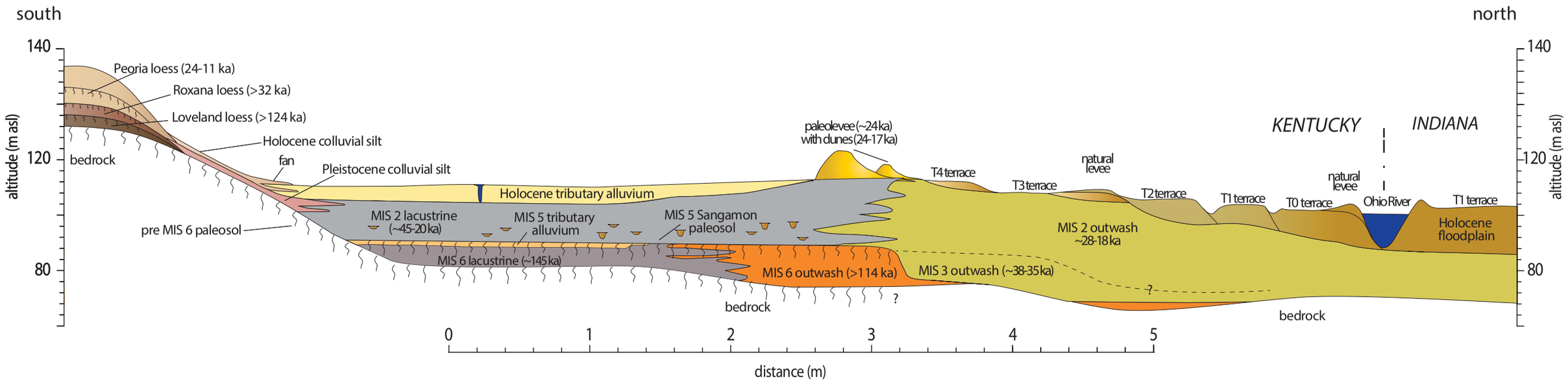

Fig. S15. Composite cross section of the lower Ohio River valley, southwestern Indiana and Western Kentucky .

Rapid field descriptions done while coring, described by Ron Counts, Matt McCauley (USDA-NRCS), and Steve Neyhouse (USDA-NRCS)

Site	Interval	Description
LORV 01	0-5 ft	silty clay and clay; 7.5 YR 4/6
	5-7 ft	medium sand with clay lamella; 10YR 5/6
	7.5-11.5 ft	medium sand with fine organic fragments; could be coal; 7.5 YR 4/3; OSL sample 8.0-9.0 ft
LORV 02	0-90 cm	silt loam to silty clay loam; mottled; 10YR 5/6 and 7.5 YR 4/6
	90-140 cm	fine sand; 7.5YR 5/6 or 5/8, color is between
		OSL sample 122-152 cm, sand from 155-183 ft is black and smells like crude oil, suspect pipeline from one of the nearby pumpjacks is leaking
LORV 03	0-20 cm	silt loam, 10YR 4/3 to 3/3 (nearly mollic)
	20-80 cm	silty clay loam; 10YR 4/4
	80-160 cm	silt loam to loam; redoxomorphic colors; 10YR 4/4 and 10YR 5/2
	160-400	stratified medium sand and silt layers; predominantly 10YR 4/3
		OSL sample 244-274 cm
LORV 04	0-20 cm	Silt loam; 10YR 4/3
	20-65 cm	silty clay loam; 10YR 4/4
	65-95 cm	loamy medium sand to loam, 7.5 YR 4/6
	95-243 cm	medium to coarse sand; 10YR 6/3
		OSL sample 213-244 cm
LORV05	0-20 cm	silt loam; 10YR 3/3 (eroded Mollic epipedon)
	20-36 cm	silt loam; 10YR 4/3
	36-62 cm	silty clay loam; 10YR 4/4
	62-120 cm	silty clay loam; mottled; 10YR 5/6 and 4/2
	120-155 cm	silty clay; mottled; 10YR 4/6 and 5/1
	155-260 cm	silty clay loam; 10YR 4/4(80%) and 10YR 5/2 (20%)
	260-346 cm	lean silty clay loam grading to silt loam; mottled; 10YR 4/3 and 10YR 4/5
	346-?	fine to medium sand; 10YR 4/6
		OSL sample 365-395 cm
LORV 06	0-30 cm	silt loam; 10YR 3/2 to 3/3 (Mollisol)
	30-90 cm	silty clay loam (argillic, 34% clay); 10YR 4/6
	90-125 cm	loam; 10YR 4/6
	125-173 cm	fine to medium sand; 10YR 5/6
	173-198 cm	medium sand; 10YR 6/3
	198-213 cm	sandy loam with lamella; 10YR 4/3
		osl sample 213-243 cm
LORV 07	0-20 cm	silt loam; 10YR 4/3
	20-95 cm	silty clay loam; 10YR 4/6

Site	Interval	Description
LORV 07	95-170 cm	light silty clay loam grading to loam with depth (argillic); 10YR 4/4; silt coats are 10YR 7/2
	170-205 cm	medium sand; 10YR 4/6
	205-245 cm	medium to coarse sand; 10YR 6/3
		OSL sample 213-243 cm
LORV 08	0-55 cm	silty clay (44% clay); 10YR 3/2
	55-83 cm	silty clay; 10YR 4/6
	83-135 cm	silty clay to silty clay loam (40% clay); 10YR 4/2 and 4/4
	135-200 cm	clay loam, (20% clay); 10YR 4/2 and 4/4
	200-245 cm	silt loam; 10YR4/4
	245-265 cm	loam; 10YR 3/2; buried A horizon
	265-293 cm	loam; 10YR 4/6 and 4/2
	293-328 cm	stratified loamy sand to sandy loam; 10YR 4/6
	328-450 cm	laomy sand to sandy loam stratified with fine sand beds; 70% is 10YR 4/3, 30% 10YR 4/2
		OSL sample 457-487 cm
LORV 09	0-20 cm	siloty clay; 10YR 3/2
	20-64 cm	silty clay loam (40% clay); 10YR 5/6
	64-93 cm	clay loam; 10YR 5/6
	93-145 cm	clay loam to loam; 10YR 5/6
	145-190 cm	fine sand; 10YR 4/6
	190-213 cm	medium sand; 10YR 4/4
		OSL sample 213-243 cm
LORV 10	0-24 cm	silty clay; 10YR 3/2
	24-74 cm	silty clay (40% clay) 10YR 4/6
	74-92 cm	silty clay (30% clay) 10YR 4/6
	92-150 cm	silty clay loam; 10YR 4/6
	152-210 cm	LOST CORE
	210-? cm	sandy loam to loamy sand
		OSL sample 213-243 cm
LORV 11	0-18 cm	Ap; silt loaml 10YR 4/3
	18-120 cm	Bt1; silty clay loam (38% clay); 7.5 YR 4/4
	120-135 cm	Bt2; silt loam; 7.5 YR 4/4
	135-165 cm	Bt3; fine sandy loam; 7.5 YR 4/4
	165-174 cm	Bt4; sandy loam to sandy clay loam with lamella; 7/5 YR 4/4
	174-182 cm	BC; fine sand;7.5 YR 4/6
		OSL sample 182-212 cm
LORV 12	0-20 cm	silt loam;10YR 4/3
	20-45 cm	silty clay loam;10YR 4/3 and 3/3
	45-170 cm	silty clay in upper section grading to silty clay loam in lower section; strongly developed soil structure (Alfisol); 10YR 4/4

Site	Interval	Description
LORV 12	170-264 cm	silty clay loam; 7.5YR 4/4 with 7.5 YR 4/3 clay films
	264-330 cm	clay loam grading with depth to sandy clay loam; 7/5 YR 4/4 and 4/2
	330-365 cm	stratified fine sand and sandy clay loam; 10YR 6/4; gleyed lamella in sandy clay loam is 5Y 6/1
		OSL sample 365-395 cm cm
LORV 13	0-25 cm	Ap; silt loam; 10YR 3/3; cumulic Mollisol
	25-120 cm	BA; silty clay loam; 10YR 3/2 with some 10YR 4/4 mottles
	120-225 cm	Bt; silty clay loam grading to clay loam (high sand content for silty clay loam in the lower part); 10YR 4/6
	225-300 cm	Bt; clay loam; 10yr 4/6
	300-305 cm	2C; fine to medium sand; 10YR 4/6
		soil development not as strong as LORV 12
		OSL sample 305-335 cm
LORV14	0-10 cm	AB; silt loam; 10YR 3/2
	10-90 cm	Bw1; silty clay loam; some development, but less development than OSL 13; 10YR 3/2
	90-114 cm	Bw2; silty clay loam; 10YR 4/4
	114-170 cm	Bw3;clay loam grading with depth to loam; 10YR 4/4
	170-204 cm	Bw4;fine sandy loam; 10YR 4/3
	204-260 cm	C1; fine sand; 10YR 4/6
	260-274 cm	C2; saturated fine sand; 10YR 4/6
		OSL sample 274-304 cm
LORV 15	0-22 cm	Ap; silty clay loam; 10YR 3/2
	22-55 cm	BA; silty clay loam; slight development (almost Bw); 10YR 3/2
	55-117 cm	Bt; sandy clay loam;10YR 4/4
	117-152 cm	CB; fine sand; leached; 10YR 6/4
		OSL sample 152-183 cm
LORV 16	0-12 cm	Ap; silt loam; weak fine granular structure; 10YR 5/3
	12-33 cm	Bt1; silt loam; weak fine subangular blocky structure; 10YR 4/4 with 10YR 4/3 silt coats
	33-58 cm	Btx1; fragipan;loam;moderate medium prismatic structure; 10YR 5/3 matrix; mottles are 10YR 6/2 and 7.5 YR 5/8 and are common; Mn stains are 10YR 2/1
	58-80 cm	Btx2; fragipan;loam;moderate coarse prismatic structure; 10YR 6/3 matrix; mottles are 10YR 6/2 and 7.5 YR 5/8 and are common; Mn stains are 10YR 2/1
	80-117 cm	Btx3; fragipan;loam;moderate coarse prismatic structure; 10YR 6/2 matrix; mottles are 10YR 6/2 and 7.5 YR 5/8 and are common; films are 10YR 5/2Mn stains are 10YR 2/1
	117-160 cm	2Btx; clay; matrix is 10YR 5/1, 10YR 6/1 clay films; Mn accumulations
	160-200 cm	2Bt; silty clay; mottled, 50% 2.5Y 5/1, 50% is 7.5 YR 4/4
	200-242 cm	2Bt2; silty clay loam; matrix is 10YR 5/3 with 2.5 YR 5/1 and 7.5 TY 5/6 mottles; few Mn stains; moderate medium prismatic to subangular blocky structure

Site	Interval	Description
LORV 16	242-253 cm	2C; massive silty clay; 10GY 5/1 with 2.5 Y 4/4 mottles
	253-275 cm	2C2; slitly clay; 10Y 4/1
	275-285 cm	2C3; fine sand; 7.5 YR 5/8
		OSL sample 396-426 cm
LORV 17	0-22 cm	Ap; silt loam; 10YR 4/3; waek fine subangular blocky structure
	22-50 cm	Bt; silt loam; 10YR 4/3 matrix with 10YR 4/4 clay films; mottles 10YR 6/2 and 7.5 YR 5/8;moderate medium SBK structure
	50-80 cm	Bt2; silty clay loam; matrix is 10YR 6/2 with 10YR 5.6 mottles and 10YR 5/1 clay films; moderate coarse SNK structure
	80-120 cm	Btx; silty clay loam or heavy silt loam; matrix is 10YR 5/6 with 7.5 YR 58 and 10YR 5/2 mottles and 10YR 4/6 clay films; moderate coarse prismatic structure; few silt coats
	120-148 cm	2Bt; clay loam; matrix is 7.5 YR 5/6 with 7.5 YR 4/6 clay films; moderate medium SBK structure
	148-190 cm	2Bt2; fine sandy loam; matrix is 7.5 YR 5/6 with 7.5 YR 4/6 clay films; moderate medium SBK structure
	190-220 cm	2C; loamy fine sand; massive; matrix is 7.5 YR 5/6
	220-244 cm	NO RECOVERY
	244-518 cm	2C; fine sandm (>90% sand); massive; 10YR 4/4. leached
		OSL sample 366-396 cm
LORV 18	0-30 cm	Ap;sandy loam; 10YR 4/3; weak fine granular structure
	30-75 cm	Bt1; sandy clay loam; 7.5 YR 5/6 matrix with many 7.5 YR 4/4 clay films; small fine SBK structure
	75-100 cm	Bt2; sandy loam; 7.5 YR 5/6 matrix with common 7.5 YR 4/4 clay films; small fine SBK structure
	100-130 cm	Bt3; sandy loam; 7.5 YR 5/6 matrix with few 7.5 YR 4/4 clay films
	130-165 cm	C1;loamy sand; massive;10YR 5/6; few 7.5 YR 4/4 lamella
	165-190 cm	C2; medium to coarse sand; massive; 10YR 5/6 is best average color
		OSL sample 183-213cm
LORV-19	0-20 cm	Ap; loam; 10YR 4/3, weak fine granular structure
	20-50 cm	Bt; clay loam; 7.5 YR 5/6 matrix with many 7.5 YR 4/4 clay films; moderate medium SBK structure
	50-82 cm	Bt2; loam, 7.5 YR 5/6 matrix with many 7.5 YR 4/4 clay films; moderate medium SBK structure
	82-95 cm	Bt3; fine sandy loam; 7.5 YR 5/6 matrix with many 7.5 YR 4/4 clay films; weak fine SBK structure
	95-125 cm	C1;loamy medium sand; 7.5 YR 5/6 matrix, no films or lamella
	125-160 cm	C2; moderately sorted medium sand; massive; 10YR 5/4